THE NUMERICAL MODELLING OF ATOMIC PHYSICS PROCESSES IN LASER-PLASMA INTERACTIONS

By

J. Magill, B.Sc.

A thesis submitted for the degree of Doctor of Philosophy
in the University of Glasgow

Department of Natural Philosophy,
The University,
Glasgow, G12 8QQ.

August 1975

ProQuest LLC.
789 East Eisenhower Parkway
P.O. Box 1346
Ann Arbor, MI 48106 – 1346

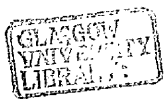

LIST OF CONTENTS

APPENDICES

FOREWORD

This thesis is submitted to the University of Glasgow in support of my application for the degree of Doctor of Philosophy. It contains an account of my own work performed at Culham Laboratory, Abingdon under the supervision of Dr. J.P. Christiansen, and at the Department of Natural Philosophy of the University of Glasgow under the supervision of Dr. E.W. Laing and Dr. J.C. Taylor. The work described in this thesis is the result of my own independent research, except where acknowledged in the text.

ACKNOWLEDGMENTS

The work for the thesis was carried out while the author was a member of the Computational Plasma Physics Group at the University of Glasgow.

I would like to express my gratitude to Dr. K.V. Roberts for permission to work in and use the facilities of the Computational Physics Laboratory at Culham. I wish especially to thank Dr. J.P. Christiansen, for first drawing my attention to the problem, together with Drs. E.W. Laing and J.C. Taylor, and I would like to acknowledge the assistance and co-operation they provided during my three year research period.

During this period of research the author was supported by the Science Research Council.

PREFACE

When a solid target, such as carbon or aluminium, is irradiated with a laser beam some of the energy from the laser can be absorbed by the target surface if the intensity of the radiation is high enough. This absorbed energy vaporises and ionises the target in the region of the focal spot, such that near the solid surface there are free electrons and ions produced at very high temperatures. This collection of ions and electrons, whose dimensions are approximately those of the focal spot of the laser radiation, constitutes a small high temperature high density 'plasma' and this area of study is known as Laser Plasma Interactions. The interest in this type of research has emerged through the possibility of producing sources of highly stripped ions, X-rays and the feasibility of X-ray lasing, and the recent importance of laser fusion (the production of thermonuclear fusion by the laser irradiation of light targets).

Because of the complexity of a complete description of the laser target interaction, if dealt with analytically, computer 'codes' (large computer programs) have been written recently to study the detailed interactions of the various processes involved. Many of these codes are based on describing the plasma in the Magnetohydrodynamic (MHD) approximation, which essentially treats the plasma as a conducting fluid and it is for these codes that the present work is intended.

One aspect of the laser target interaction is concerned with the atomic physics processes present in the plasma. This deals with the various ionisation and recombination processes and enables one to calculate such quantities as the plasma (kinetic) pressure, the internal energy (thermal plus ionisation) and the plasma radiation, and constitutes an

atomic physics model of the plasma concerned. In general these models are based on calculating the population densities or the fractional population densities f_z (where f_z is the fraction of z times ionised material) of the various ionisation stages, from which the macroscopic variables described above may then be calculated. The f_z are governed by a 'rate' equation of the following form

$$\frac{\partial f_z}{\partial t} = \alpha_z f_z + g_z \qquad (1)$$

where α_z is known as the rate coefficient and g_z is a function of the other fractions present. This thesis describes a method of solving the above type of equation, from which we develop a complete atomic physics model intended to supplement an MHD description of the plasma in computer codes.

The main features of the model, to be developed, can be summarised as follows. First of all, we include the explicit time dependence of the ionisation fractions as in the left hand side of equation (1). We thus allow for the finite rates at which the atomic physics processes occur in the plasma. We solve only for the ground state population densities of the ionisation stages thus neglecting completely the populations of the excited states. Secondly, we consider only three adjacent ionisation fractions, such that at any one time we have only three coupled equations of the type (1) to solve. The rate coefficients for these various ionisation and recombination processes are assumed known and accurate for the interactions concerned. Finally, the method of solving the coupled equations of type (1) is based on taking locally analytic solutions to the rate equations, from which we then construct a complete atomic physics model to supplement an MHD description of the laser target in computer codes.

CHAPTER 1

Exposition of the problem

An outline of the basic atomic physics theory will be presented together with a discussion of the contemporary atomic physics models for a plasma undergoing ionisation and recombination.

1.1 On the role of Computational Physics

It is now about 15 years since scientists first started solving problems with the aid of computers.[1,2,3] During this time, the resources of Theoretical Physics, Numerical Analysis, Computer Science and Experimental Physics were being called upon continually and it soon became apparent that the subject of 'Computational Physics' was emerging to form an academic discipline in its own right.

The importance of the subject cannot be underestimated. In previous years, throughout the science student's university training, he was confined to problems of a rather special nature. In general, they resulted from a study of idealised physical systems and are called 'linear' problems.[4,5,6] These linear (or idealised) problems have been studied for hundreds of years and as a result, they are very well understood and form an important part of the science student's education. After University, however, if the student went into industry or into research in general, he found that the 'tools' with which he had been equipped for the study of linear problems very little use in tackling real situations. The methods of Computational Physics now provide the student with an immediate and powerful tool for studying these real systems.

This is not to say that the study of linear systems should be abandoned with all effort devoted to the field of computational physics. Indeed, since computer solutions can never be exact, their credibility relies heavily on how well they compare with the few exact solutions that are known from studying idealised systems. Rather, computational physics should be seen in some ways as bridging the gap between the linear theory and experiment. In order to gain an understanding of the physical system, the strategy must be to approach the problem on a united front, with a knowledge of linear problems, computational physics and experimental physics at our disposal. The tactics will then be

to continually reinforce the individual strengths of each of these methods by their mutual interactions as seen in fig. 1.1

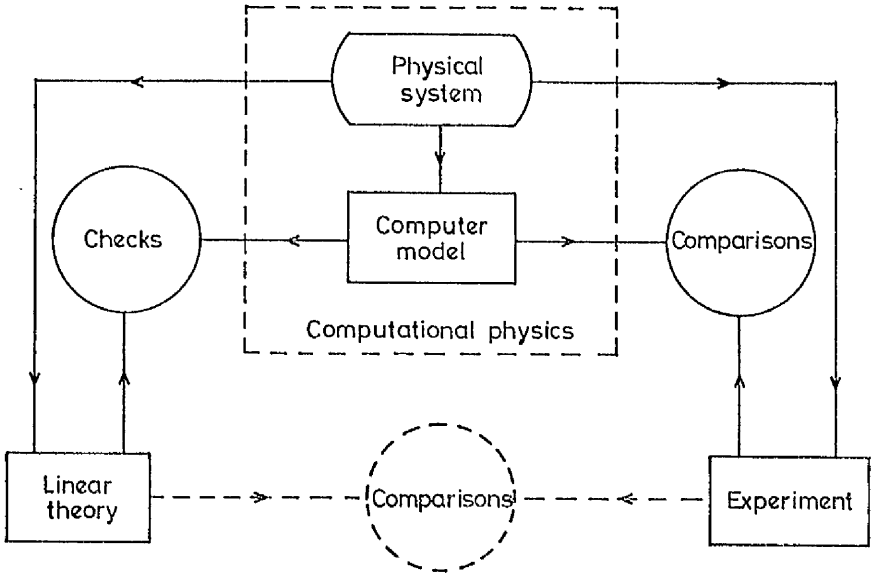

Fig. 1.1 Strategy for the scientific understanding of physical systems

From the physical system we can construct the linear theory governing the system, the computer model representing the system, and the experiment to study the system. The linear theory can be used to provide checks for the computer model in a restricted set of circumstances. The computer model can then be tested against the experimental results and can indicate what the experimentalist should be looking for. This being done, the computer model may have to be modified (e.g. to improve the underlying physics in the model). We then can recheck with linear theory and the cycle starts again. In a few cases the linear theory can be compared directly to the experimental results. In this way we hope to make progress. It is hoped that the philosophy of fig. 1.1 is made apparent throughout this work.

This thesis is concerned with the development of a computer model for studying the time-dependent atomic physics processes which occur when a solid target is irradiated with high intensity laser radiation.[7,8,9] This chapter describes the 'state of the art' at the present time. Contemporary models for the same physical processes, i.e. ionisation and recombination in a plasma, are discussed together with their weaknesses and advantages. In Chapter 2 we present the basic theory upon which the present model is based. It describes the method by which we follow the time evolution of the ionisation fractions. In Chapter 3 we show how the equation of state for the plasma can be found from a knowledge of the ionisation fractions (i.e. we derive such things as internal energy, pressure, specific heat and radiation loss). Chapter 4 describes the computational details of the algorithm and the questions of accuracy, stability etc. are examined. In Chapter 5 we give details of how the model was implemented into the two dimensional laser target code CASTOR[10] together with some results.

1.2 Introduction and Motivation

With the development of high powered lasers and the current interest in laser fusion[11, 12] and laser plasma interactions[13, 14] it is of great interest to be able to estimate reliably the degree of ionisation or the effective ion change $< z >$ of the plasma. The ionisation may not always be assumed instantaneous and complete - especially if some of the heavier elements are being used as targets for the laser radiation. In this case, the ionisation energy may form an important part of the equation of state. Additionally, to estimate the radiation loss accurately, we must know the density of free electrons and the distribution of the ionic states[15]. Once $< z >$ is known, the thermodynamic properties (eg. the internal energy, pressure etc.) of the plasma can be determined.

In general, however, the calculation of the effective charge involves the solution of a fairly large system of coupled, non-linear, partial differential equations. The method of solving the system of equations, in this thesis, will be the subject of Chapter 2. To avoid this procedure, many workers have made basic assumptions in the physics involved in order to obtain a simpler and hence solvable system of equations. These assumptions together with some models for the atomic physics processes in the plasma will be discussed in section 1.5.

Recently a comprehensive list of the ionisation and recombination rate coefficients as a function of electron density and temperature has been published in tabular form, for the elemants in the periodic table up to argon.[16] Fig. 1.2 shows the variation of the ionisation and recombination rate coefficients for the different ion stages, as a function of the electron temperature in carbon, and it is these coefficients which will be used here. The details involved in the calculation of these coefficients will not be mentioned as they are discussed in the previous reference. It will be assumed in the thesis that the rate coefficients for the various atomic processes are known, and accurate, for the materials we are interested in.

Throughout this work most of the emphasis will be placed upon the computational physics rather than the atomic physics aspects of the problem, this reflecting the author's interest. The model was developed concurrently with a two dimensional Eulerian laser-target code which required a rate equation solver package. The code was required to help investigate experiments in progress at Culham Laboratory.[14,17,18] Because the model was to be developed for use in a computer code, this imposed very severe restrictions on its design. It meant that the algorithm had to be very fast since the rate equations had to be solved at each space-time point on a two-dimensional mesh. The problems of speed of the calculation and the storage of the ionisation stage 'vector' are discussed in Chapter 4.

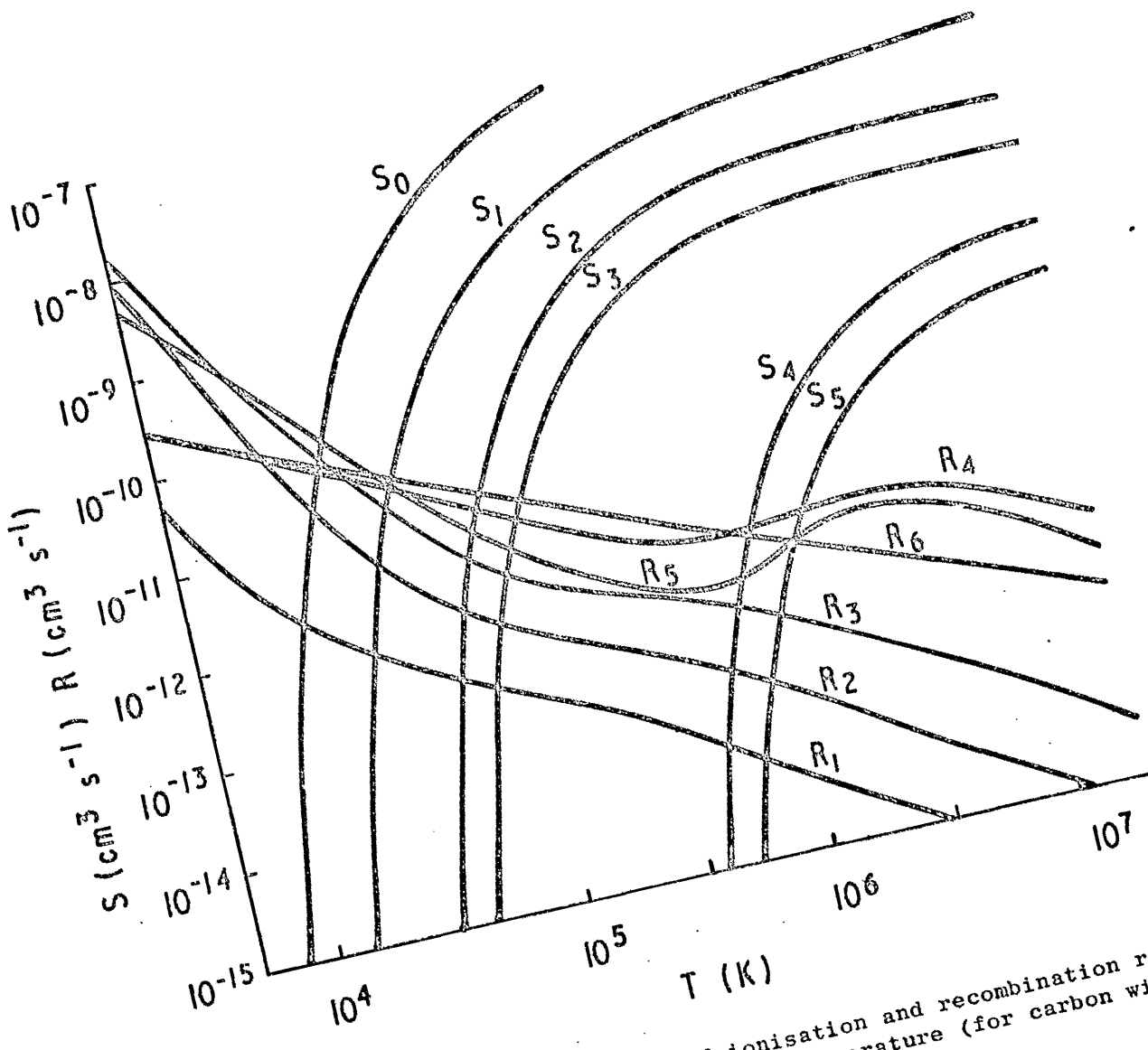

Fig. 1.2 The variation of ionisation and recombination rate coefficients against temperature (for carbon with $n_e = 10^{21}$ cm^{-3})

Finally, it will be shown in Chapter 5 how the model, developed in Chapter 2, can be used as a module or package for insertion into computer codes in general. It can then form the basis of a model for looking at the excited state population within each ionisation stage.

1.3 Atomic Physics Theory for Hydrogen[19]

We begin our discussion of atomic physics theory by its application to a very simple system. The discussion will be confined to the excitation, ionisation, and the recombination of Hydrogen H with electrons e. We denote neutral hydrogen by H and ionised hydrogen by H^+ (hydrogen in its neutral state consists only of one proton and one electron).

We denote the principal quantum numbers of the discrete levels in the hydrogen system by p, q, ... and c for the continuum. n(p), n(q) will then represent the number densities of atoms in the levels indicated and n(c) for the number of free electrons. Also, $n(H^+)$ will represent the number of bare nuclei. We now define

a. S(p,c)* to be the rate coefficient for the process:-

$$H(p) + e \rightarrow H^+ + e + e \qquad (1.3.1)$$

i.e. the collisional ionisation of a hydrogen atom, in state p, to produce a hydrogen ion plus an electron, by a free electron

b. S(p,q) to be the rate coefficient for the process:-

$$H(p) + e \rightarrow H(q) + e \qquad (1.3.2)$$

i.e. the collisional excitation of an electron in state p, in a hydrogen atom to one in state q, by a free electron

c. $\beta(c,p)$ to be the rate coefficient for the process:-

$$H^+ + e + e \rightarrow H(p) + e \qquad (1.3.3)$$

i.e. the recombination of a free electron, by the above three body process, with an ionised hydrogen atom to form a hydrogen atom with its electron in the excited state p. It should be noted that the three bodies are necessary in order to conserve momentum and energy.

*The rate coefficient is defined such that n(c) n(p) S(p,c) is the number of collisions of this type which occur per cm^3 per sec.

d. $\alpha(p)$ to be the rate coefficient for the process:-

$$H^+ + e \rightarrow H(p) + h\nu \qquad (1.3.4)$$

i.e. the recombination of a free electron, by the above process, with an ionised hydrogen atom to form a hydrogen atom with its electron in the excited state p and the emission of a photon ($h\nu$)

All of the rate coefficients in the above processes are functions of electron temperature and density. The above processes hold for hydrogen systems and have been the subject of much research. No more will be said about these systems and we will now go on to study more complex processes.

1.4 Atomic Physics Theory for Many Electron Atoms[20]

For non-hydrogenlike species, the problem becomes extremely complicated. For many electron atoms there is more than one stage of ionisation possible and the processes of section 1.3 must be considered in and between the various ionisation stages. In addition, they should be extended to include multiply excited levels, autoionisation, dielectronic recombination etc.

It should now be noted that the rate coefficients are additionally functions of the particular stage of ionisation we are concerned with. The use of the superscript on S, i.e. $S^z(p,q)$ will indicate the level of ionisation concerned. The letter A will be used instead of H to denote the material concerned and $A^z(p)$ should be interpreted as the z-times ionised atom of element A whose outer electron is in the excited state p. Thus we define

a. $S^z(p,c)$ to be the rate coefficient for the process:-

$$A^z(p) + e \rightarrow A^{z+1}(q) + e + e \qquad (1.4.1)$$

i.e. the collisional ionisation of a z-times ionised atom of element A to produce a (z+1) times ionised atom of the same element plus an electron, outer electrons in state p and q.

b. $\beta^z(p,q)$ to be the rate coefficient for the process:-

$$A^z(p) + e + e \rightarrow A^{z-1}(q) + e \qquad (1.4.2)$$

i.e. the recombination of a free electron with a z-times ionised atom of A whose outer electron is in the state p, to the (z-1) times ionised atom of A whose outer electron is in state q.

c. $\alpha^z(p,q)$ to be the rate coefficient for the process:-

$$A^z(p) + e \rightarrow A^{z-1}(q) + h\nu \qquad (1.4.3)$$

i.e. the recombination of a free electron with a z-times ionised atom of A whose outer electron is in state (p) to produce a (z-1) times ionised atom of A plus a photon ($h\nu$).

It should be noticed that the processes of collisional excitation and de-excitation as discussed in section 1.3 have been omitted in this section. The reason for this is that we will be concerned only with processes which change the population densities of the given ionisation stages and the above processes only effect the internal structure within each given ionisation stage.

Using the above notation, we now examine how these different rate processes can cause changes in the population density of a given ion stage n_z ($= \sum_p n_z(p)$ where p indicates an excited state). Considering all the various processes in and around the ion stage z we are led to the differential equation[15]

$$\frac{\partial n_z}{\partial t} + \underline{\nabla}.(n_z \underline{v}) = -\sum_p n_e n_z(p)\, S^z(p,c) + \sum_p n_e n_{z-1}(p)\, S^{z-1}(p,c)$$

$$-\sum_q \sum_p n_e^2\, n_z(p)\, \beta^z(p,q) + \sum_q \sum_p n_e^2 n_{z+1}(p)\, \beta^{z+1}(p,q)$$

$$-\sum_q \sum_p n_e\, n_z(p)\, \alpha^z(p,q) + \sum_q \sum_p n_e n_{z+1}(p)\, \alpha^{z+1}(p,q) \qquad (1.4.4)$$

Notice that the term $\underline{\nabla}.(n_z \underline{v})$ is included to account for changes in n_z due to compression and advection of the fluid. The first two terms on the right hand side of equation (1.4.4) represent collisional ionisation from levels z and z-1; the next two terms represent three-body recombinations with levels z and z+1, and the last two terms represent radiative recombination with the levels z and z+1. Each of the above terms can be written in the more general form

$$\sum_p \sum_q n_e n_z(p)\, A^z(p,q) \qquad (1.4.5)$$

which in turn can be expressed as

$$n_e \sum_p n_z(p) \sum_q A^z(p,q) = n_e \sum_p n_z(p) \left[A^z(p)\right]_T \qquad (1.4.6)$$

where $\left[A^z(p)\right]_T$ gives the coefficient for the rate process described by A, between the levels p and any of q. Now since

$$n_z \langle\psi(p)\rangle = \sum_p n_z(p)\, \psi(p) \qquad (1.4.7)$$

where $\langle\psi(p)\rangle$ represents the averaged value of $\psi(p)$ over all the states p, we can rewrite equation (1.4.5) as

$$n_e n_z \langle [A^z(p)] \rangle_T \tag{1.4.8}$$

$$\text{where} \quad n_z = \sum_z n_z(p) \tag{1.4.9}$$

or more simply as

$$n_e n_z \langle A^z \rangle \tag{1.4.10}$$

where $\langle A^z \rangle$ gives the rate coefficient summed over the levels p and q.

Using this notation, equation (1.4.4) can be rewritten as

$$\begin{aligned} \frac{\partial n_z}{\partial t} + \nabla.(n_z \underline{v}) = & -n_e n_z \langle S^z \rangle + n_e n_{z-1} \langle S^{z-1} \rangle \\ & -n_e^2 n_z \langle \beta^z \rangle + n_e^2 n_{z+1} \langle \beta^{z+1} \rangle \\ & -n_e n_z \langle \alpha^z \rangle + n_e n_{z+1} \langle \alpha^{z+1} \rangle \end{aligned} \tag{1.4.11}$$

where the quantities in parenthesis are now averaged rate coefficients over the excited states. Although strictly speaking it is these averaged rate coefficients we should use in our calculations, in many cases they are not available and one can only approximate their value. However, we shall assume that these quantities have been determined accurately by some means and proceed from there. In what follows we replace $\langle A^z \rangle$ by A_z for convenience.

1.5 Some Contemporary Atomic Physics Models

In this section a brief survey of the better known atomic physics models will be given together with their limitations as far as application to the laser produced plasma is concerned. The models can be divided basically into two groups - steady state and time dependent models - and it is in this order they will be presented here. It will be shown later that, in general, time dependent models must be used for studying laser-plasma interactions.

a. The Local Thermodynamic Equilibrium (LTE) model[15]

This model assumes that the population density distribution of the electrons is completely determined by particle collisions and that these occur so rapidly that the distribution responds instantaneously to any change in the plasma conditions. Thus each particle collision process is accompanied by its inverse and these pairs of processes occur at equal rates by the principle of detailed balancing. The electron distribution is thus that of a system in thermodynamic equilibrium and is determined by the law of equipartition among the various energy levels, thus needing no knowledge of the atomic cross sections of the various processes. Hence if free electrons are distributed among the energy levels, according to statistical mechanics, their velocities have a Maxwellian distribution. The number of electrons with speeds between v and v + δv is

$$\delta n_v = n_e \, 4\pi \left(\frac{m_e}{2\pi k T_e}\right)^{3/2} \exp\left(-\frac{mv^2}{2kT_e}\right) v^2 \, \delta v \qquad (1.5.1)$$

where n_e is the total density of free electrons, T_e is the electron temperature, m_e is the electron mass and k is Boltzmann's constant. For the bound levels the distribution of the population densities is given by the Boltzmann and Saha equations, i.e.

$$\frac{n(p)}{n(q)} = \frac{\omega(p)}{\omega(q)} \exp\left(\frac{\chi(p,q)}{kT_e}\right) \qquad (1.5.2)$$

$$\frac{n(z+1,g)n_e}{n(z,g)} = \frac{\omega(z+1,g)}{\omega(z,g)} \; 2\left(\frac{2\pi m k T_e}{h^2}\right)^{3/2} \exp\left(\frac{\chi(z,g)}{kT_e}\right) \qquad (1.5.3)$$

where n(p), n(q), n(z+1,g) and n(z,g) are the population densities of the various levels designated by their quantum numbers p, q and g(the ground level) and ionic charge z+1 and z. The term $\omega(z,p)$ is the statistical weight of the designated level, $\chi(p,q)$ is the energy difference between the levels p and q and $\chi(z,g)$ is the ionisation potential of the ion of charge z in its ground level g. Thus the equations (1.5.1) - (1.5.3) summarise the state of the electrons and completely define the LTE model.

The LTE model can be shown to be valid provided the electron density satisfies the relation

$$n_e \geq 1.6 \times 10^{12} \; T_e^{\frac{1}{2}} \; \chi(p,q)^3 \qquad cm^{-3}$$

where T_e is expressed in eV. Thus we see that at low density or high temperatures or a mixture of both low density and high temperature the LTE model breaks down. It is therefore apparent that the LTE model is of very limited use in the study of laser plasma interactions.

b. The Steady-State Corona Model[21]

This model has been in use for some time in the study of laser produced plasmas. Instead of each collision process being balanced by its inverse collision process, this model assumes that the balance is between collisional ionisation (and excitation) and radiative recombination. Consider the processes of collisional ionisation and three-body recombination which, because they are inverse processes, must take place at equal rates in LTE (here N(z) is used instead of N_z), i.e.

$$e + N(z) \leftrightarrow N(z+1) + e + e \qquad (1.5.4)$$

Thus we see that the ionisation rate is proportional to n_e and the recombination rate (three-body) is proportional to n_e^2. Positive ions may also recombine with electrons by a radiative process thus

$$e + A(z+1) \rightarrow A(z) + h\nu \qquad (1.5.5)$$

where $h\nu$ represents the radiated photon. The rate of this process is proportional to n_e, so that at sufficiently low densities this radiative recombination process is more important than the three-body recombination. Then the ionisation balance is between radiative recombination and collisional ionisation. Such a plasma is called a Corona Model Plasma and clearly it refers to plasmas of much lower densities than those encountered in LTE plasmas. The question of relaxation times for the atomic processes is discussed later and for the moment we assume that any change in the plasma parameters takes place sufficiently slowly that the plasma effectively remains in steady state. Again, as in the LTE model,

it is assumed that the electrons have a Maxwellian distribution such that equation (1.5.1) applies to the free electrons. It is not necessary to make any specific assumptions about the velocity distribution of the ions except that their mean energy should be of the same order or less than that of the electrons otherwise ion-ion collisions may be important. It is also assumed that most of the ions are in their ground states and hence we can write down an equation expressing the ionisation and recombination balance, i.e.

$$n_e n(z,g)\ S(T_e,z,g) = n_e n(z+1,g)\ \alpha(T_e,z+1,g) \qquad (1.5.6)$$

$$\text{or} \qquad \frac{n(z,g)}{n(z+1,g)} = \frac{\alpha(T_e,z+1,g)}{S(T_e,z,g)} \qquad (1.5.7)$$

where $S(T_e,z,g)$ is the collisional ionisation coefficient and $\alpha(T_e,z,g)$ is the radiative recombination coefficient. The population densities of the excited levels are determined by a balance between the rate of collisional excitation from the ground level$^{(g)}$ balanced by the rate of spontaneous radiative decay thus

$$n_e n(z,g)\ X(T_e,g,p) = n(z,p) \sum_{q>p} A(p,q) \qquad (1.5.8)$$

The corona model was developed for plasmas of very low electron density and for atom densities sufficiently low to ensure that atom-atom collisions are negligible. To meet this requirement it can be shown$^{(q)}$ that the electron temperature must be greater than about 10^4K and that the electron density must satisfy the inequality

$$n_e < 5.6 \times 10^8\ (z+1)^6\ T_e^{\frac{1}{2}}\ \exp\left(\frac{1.162 \times 10^3\ (z+1)^2}{T_e}\right) \text{cm}^{-3} \qquad (1.5.9)$$

where $z+1$ is the nuclear charge of a hydrogen-like ion and T_e is measured in eV. Thus we see that the steady state corona model is basically a high temperature-low density model for plasmas and again, as such, is of limited use for the laser produced plasma.

c. The Hyman-Raizer Model[22]

A particularly simple method of evaluating the degree of ionisation of a high temperature, high Z plasma has been developed by Hyman on the basis of earlier work by Raizer. There he uses the standard corona-like equations

$$\frac{n_{z+1}}{n_z} = \frac{S(T_e)}{\alpha(T_e,n_e)} \qquad (1.5.10)$$

where n_{z+1}, n_z and S have previously been defined and $\alpha(T_e,n_e)$ is the total recombination coefficient. It may be written more explicitly as

$$\alpha(T_e,n_e) = \alpha^r(T_e) + n_e\,\beta(T_e) \qquad (1.5.11)$$

where α^r is the radiative recombination coefficient and β is the collisional three body coefficient. It is then assumed that n_z and χ_z (the ionisation potential) are continuous functions of the charge z. Hence

$$n(z+1) = n(z) + \frac{dn}{dz} \quad (\Delta z = 1) \qquad (1.5.12)$$

Now substituting (1.5.12) into (1.5.10) gives

$$1 + \frac{d}{dz}(\ln n) = \frac{S}{\alpha} \qquad (1.5.13)$$

In general, n(z) is a fairly sharped peaked function, i.e. only a few ionisation stages are significantly populated for a given electron temperature and density. At the peak of the distribution dn/dz = 0 so that

$$S(T_e, \bar{\chi}) = \alpha(T_e,n_e,\bar{\chi}) \qquad (1.5.14)$$

where $\bar{\chi}$ is an 'effective ionisation potential' at the peak. This expression can then be solved for $\bar{\chi}$ which in turn specifies $< z >$.

This model is very simple indeed, and would be computationally quite efficient, but it is a steady-state model and as such is not of much interest in laser plasma calculations.

d. The Time Dependent Corona Model[15]

This is the first of the time dependent atomic physics models we mention. The only difference between the steady-state and the time-dependent corona models is that we allow the population density of the ground state of an ion to have a time dependence which can be written thus

$$\frac{dn(z,g)}{dt} = n_e n(z-1,g)\ S(T_e,z-1,g) - n_e n(z,g)\ S(T_e,z,g)$$

$$- n_e n(z,g)\ \alpha(T_e,z,g) + n_e n(z+1,g)\ \alpha(T_e,z+1,g) \qquad (1.5.15)$$

And a set of such equations represents the rates of change of the populations of all the ions from z = 0 (neutral atoms) to z = Z (fully stripped). It can also be shown that for any corona model plasma, the atomic relaxation time τ is given, to an order of magnitude, by the equation

$$\tau \simeq \frac{10^{12}}{n_e} \qquad (1.5.16)$$

where n_e must be expressed in cm^{-3} and τ is given in seconds. If we apply this equation to the laser produced plasma, although strictly speaking the density is too high ($n_e \sim 10^{21}\ cm^{-3}$), we see that only for timescales greater than about 1 nanosecond can we apply the steady-state corona model.

e. The Collisional-Radiative Model[15]

Because of the restrictions in the corona model, in the sense that it cannot account for stepwise collision processes, the Collisional-Radiative (CR) model was developed. The basic differences between the CR and the corona models is that in the CR model, account is taken of electron collision processes causing transitions between upper levels (including three body recombination). Thus ionisation is by electron collision from any bound level and is partially balanced by three body recombination into any level, i.e.

$$N(z,p) + e \rightarrow N(z+1,g) + e + e \qquad (1.5.17)$$

where N(z,p) represents an atom or ion of charge z whose outer electron is in the excited state p. Again the coefficients S and β are defined such that the rate of the different processes are

$$\begin{aligned} &\text{a.} \quad \text{ionisation} \qquad n_e n(z,p)\, S(T_e,z,p) \\ &\text{b.} \quad \text{recombination} \qquad n_e n(z+1,g)\, \beta(T_e,z+1,p) \end{aligned} \qquad (1.5.18)$$

Transitions between any pair of bound levels are induced by electron collision and can be represented by

$$N(z,p) + e \rightarrow N(z,q) + e \qquad (1.5.19)$$

where the rate coefficient for the forward process is $n_e n(z,p)\, X(T_e,z,p,q)$. Radiation is emitted when an electron in an upper bound level makes a spontaneous transition to a lower level and when a free electron makes a collisionless transition into a bound level i.e.

$$\begin{aligned} &N(z,p) \rightarrow N(z,q) + h\nu \\ &\text{and} \\ &N(z+1,g) + e \rightarrow N(z,p) + h\nu \end{aligned} \qquad (1.5.20)$$

where the rate for spontaneous decay is $n_e n(z,p)\, A(z,p,q)$ and the rate for radiative recombination is $n_e n(z+1,g)\, \alpha(T_e,z+1,p)$. Further details of this model may be found in the literature.

f. The Pert Model[23]

A model proposed by Pert offers a simple analytic solution to the rate equations under the assumption that if we are considering the rate of change of the fractional population density of a particular ion stage f_i then, provided we focus our attention only on the levels i and i+1 we can formulate the rate equation

$$\frac{df_i}{dt} = n_e S_i f_i + n_e^2 \beta f_{i+1} \qquad (1.5.21)$$

notice here that collisional ionisation from level i-1 and recombination with level i are neglected. The basic assumption in the model is that the population density of the ion stages is spread over only two ionisation stages. Thus together with equation (1.5.21) we have the constraint that

$$f_i + f_{i+1} \sim f_{total} \sim 1 \qquad (1.5.22)$$

and substituting for f_{i+1} in equation (1.5.21) leads to the linear ordinary differential equation

$$\frac{df_i}{dt} = \left(S_i - \beta_{i+1} n_e\right) n_e f_i + \beta_{i+1} n_e^2 \qquad (1.5.23)$$

which for constant coefficients has the solution

$$f_i = \left(f_i^o + \frac{\beta_{i+1} n_e}{S_i - \beta_{i+1} n_e} \right) e^{n_e (S_i - \beta_{i+1} n_e) t} - \frac{\beta_{i+1} n_e}{S_i - \beta_{i+1} n_e} \qquad (1.5.24)$$

and again from the knowledge of the f_i's we can construct our macroscopic variables, such as the mean ionisation level etc. It is clear from this approach that we must have the electron density and the rate coefficients sensibly constant over the duration we are applying equation (1.5.24).

1.6 Some Aspects of Computational Solutions[24]

The standard approach to solving the coupled atomic physics MHD problem numerically has been by using explicit or implicit algorithms[1, 2] Both of these methods have severe drawbacks under certain conditions encountered in the laser produced plasma situation. Using an explicit algorithm, it is necessary to restrict the timestep by the Courant-Freidrichs-Levy (C-F-L) condition to avoid numerical instability. Our timestep is then given by

$$\Delta t = \min(\tau_{atomic}, \tau_{MHD}) \qquad (1.6.1)$$

where τ_{atomic} and τ_{MHD} represents the atomic physics timescales and MHD timescales, characteristics of the problem concerned. However it can easily happen that $\tau_{atomic} \sim 10^{-3}\ \tau_{MHD}$ and thus we would have to follow the evolution of the system on an atomic physics timescale whereas the interesting aspects occur on an MHD timescale. Hence we must look for alternative algorithms.

The implicit algorithm on the other hand imposes no such restriction on the timestep (other than that set by accuracy). It does, however, have its own limitations. Consider the following simple rate equation

$$\frac{\partial f}{\partial t} = -Sf \qquad (1.6.2)$$

In finite difference form this becomes

$$\frac{f^{n+1} - f^{n}}{\Delta t} = -S\ (\theta f^{n+1} + (1-\theta) f^{n}) \qquad (1.6.3)$$

where θ measure the degree of implicitness. We take S constant for simplicity and express (1.6.3) as

$$\frac{f^{n+1}}{f^{n}} = \frac{1 - \Delta t\ S\ (1-\theta)}{1 + \Delta t\ S\ (\theta)} \qquad (1.6.4)$$

From this equation we can now make various observations on the ratio of f^{n+1}/f^{n} for various values of θ and S.

It is clear that if S is large (i.e. the rates are large) f^{n+1} can become zero or negative. In the latter case some cut-off would be introduced (since one cannot have negative fractions) such that the fraction would be replaced by zero as in Fig. 1.6.

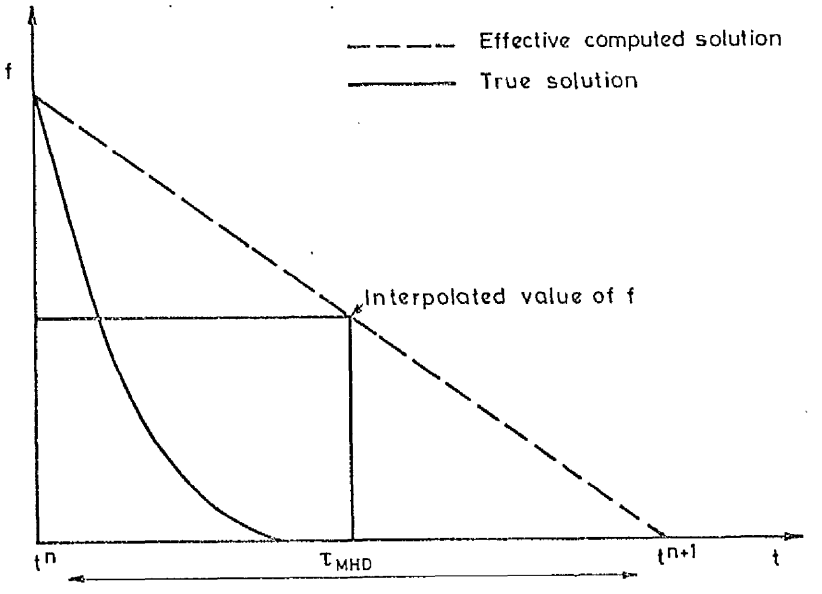

Fig. 1.6 Inaccuracies in f arising from choosing too large a timestep

If, for example, we now wish to know the average charge $\langle z \rangle$ over the timestep we would interpolate between the two time levels n and n+1 at which the quantities are known and we would then use this interpolated value of density to obtain $\langle z \rangle$. From Fig. 1.6 this is obviously a very poor evaluation of f at time $n + \frac{1}{2}$ (c.f. true solution).

The method used in this work will be to fit exponentials to the solution. We can then average the exponential variation over the timestep to obtain the average value of f. Thus since

$$f^{n\to n+1} = f^n e^{-St} \qquad (1.6.5)$$

hence
$$\langle f^{n\to n+1} \rangle = f^n \langle e^{-St} \rangle \qquad (1.6.6)$$

and
$$\langle e^{-St} \rangle = \frac{1}{\tau_{MHD}} \int_0^{\tau_{MHD}} e^{-St}\, dt$$

$$= (S\,\tau_{MHD})^{-1} (1-e^{-S\tau_{MHD}}) \qquad (1.6.7)$$

CHAPTER 2

The Mathematical Model

The underlying theory forming the basis of the thesis is developed in this chapter. It centres around finding 'locally' analytic solutions to the rate equations (1.4.11) in terms of eigenvalues and eigenvectors (section 2.3) and the method of obtaining these eigenvalues and eigenvectors efficiently, is discussed in detail.

2.1 Basic assumptions

In section 1.4 it was stated that we would be using averaged rate coefficients (averaged over the excited states). Since these are not readily available, we use the rate coefficients for the ground state only, for each ionisation stage. These coefficients do, however, allow for stepwise collision processes. Thus it is apparent that we are neglecting the calculation of the excited state populations.

We also neglect completely, the problem of radiation transfer within the plasma, thus assuming the plasma to be optically thin. It may be, however, that for certain lines, especially resonance lines, account should be taken of the changes in the populations of the ionisation stages due to the reabsorption of radiation.

Our attention will be confined to subhydrodynamic timescales ($\sim$ 0.1 nanosecond for laser produced plasmas) such that the advection term represented in the rate equation (1.4.4) by $(\underline{v}.\underline{\nabla})$ can be neglected. Later, it will be shown how this term can be included into the model.

2.2 The rate equations

As was pointed out in the previous chapter, for each ionisation stage we have an equation of the following form

$$\frac{\partial n_z}{\partial t} + \underline{\nabla}.(n_{z-z}\underline{v}_z) = + S_{z-1}\, n_e n_{z-1} - (S_z+R_z)\, n_e n_z + R_{z+1}\, n_e n_{z+1} \qquad (2.2.1)$$

where n_z is the density, and v_z is the velocity of the z times ionised atoms at a given point. We can rewrite the above equation in terms of f_z, the fractional population density of the z times ionised atoms where

$$n_z = f_z\, n_i \qquad (2.2.2)$$

and n_i is the total ion density. Now substituting (2.2.2) into the left hand side of equation (2.2.1) we obtain, after some rearranging

$$f_z \left[\frac{\partial n_i}{\partial t} + \underline{\nabla}.(n_i \underline{v}_z)\right] + n_i \left[\frac{\partial f_z}{\partial t} + \underline{v}_z . \underline{\nabla} f_z\right] \qquad (2.2.3)$$

At this point we assume v_z to be equal to the hydrodynamic flow velocity $\underline{v}$ such that the first term of (2.2.3) goes to zero (i.e. equation of continuity) and equation (2.2.1) becomes, after dividing by n_i

$$\frac{\partial f_z}{\partial t} + (\underline{v}.\underline{\nabla}) f_z = + S_{z-1} n_e f_{z-1} - (S_z + R_z) n_e f_z + R_{z+1} n_e f_{z+1} \qquad (2.2.4)$$

It is interesting to notice that in the equation there is no explicit compressibility term, i.e. $f_z \underline{\nabla}.\underline{v}$, this term has been absorbed in the left hand side of (2.2.3).

We now consider the ions of an element having Z electrons in the neutral state. Defining f_z to be the fractional density of z-times ionised atoms, the rate of change of the $\{f_z\}$ due to collisional ionisation and recombination (radiative three-body, etc.) leads to the system of equations (2.2.4) which written explicitly for each ionisation stage gives

$$\begin{aligned}
\partial f_o/\partial t + (\underline{v}.\underline{\nabla})\, f_o &= - S_o n_e f_o + R_1 n_e f_1 \\
\partial f_1/\partial t + (\underline{v}.\underline{\nabla})\, f_1 &= +S_o n_e f_o - (S_1 + R_1) n_e f_1 + R_2 n_e f_2 \\
\text{"} \quad \text{"} \quad &\quad \text{"} \quad \text{"} \quad \text{"} \\
\text{"} \quad \text{"} \quad &\quad \text{"} \quad \text{"} \quad \text{"} \\
\partial f_z/\partial t + (\underline{v}.\underline{\nabla})\, f_z &= +S_{z-1} n_e f_{z-1} - (S_z + R_z) n_e f_j + R_{z+1} n_e f_{z+1} \\
\text{"} \quad \text{"} \quad &\quad \text{"} \quad \text{"} \quad \text{"} \\
\partial f_Z/\partial t + (\underline{v}.\underline{\nabla})\, f_Z &= +S_{Z-1} n_e f_{Z-1} - R_Z n_e f_Z
\end{aligned} \qquad (2.2.5)$$

where S_Z is the collisional ionisation coefficient for state $Z \rightarrow Z+1$ and R_Z is the total recombination coefficient for state $Z \rightarrow Z-1$. The electron density is denoted by n_e and we assume (for simplicity), that all the ion stages have the same flow velocity $\underline{v}$. Hence we see that (2.2.5) represents a system of coupled, non-linear partial differential equations which we have to solve for the ionisations fractions. In general, such a system

of equations cannot be solved for 'analytically' and we must introduce some simplifying assumptions in order to obtain solutions, or else solve the equations numerically. The approach in this work will be to use a combination of these methods.

2.3 General Solution of the Rate Equations

Since we are confining ourselves to sub-hydrodynamic timescales the advection term, represented by $(\underline{v}.\underline{\nabla})f$ can be neglected. Hence, the system of rate equations (2.2.5) reduces to the matrix equation

$$\frac{\partial \underline{f}}{\partial t} = \underline{\underline{A}}\,\underline{f} \qquad (2.3.1)$$

where

$$\underline{f} = \begin{bmatrix} f_0 \\ f_1 \\ f_2 \\ \\ \\ \\ f_z \\ \\ \\ f_{Z-1} \\ f_Z \end{bmatrix} \text{ and } \underline{\underline{A}} = n_e \begin{bmatrix} -S_0 + R_1 & & & & & & & & & \\ +S_0 & -(S_1+R_1) & +R_2 & & & & & & & \\ & +S_1 & -(S_2+R_2) & +R_3 & & & & & & \\ & & & & & & & & & \\ & & & & & & & & & \\ & & & & & & & & & \\ & & & & & +S_{z-1} & -(S_z+R_z) & +R_{z+1} & & \\ & & & & & & & & & \\ & & & & & & & +S_{Z-2} & -(S_{Z-1}+R_{Z-1}) & +R_Z \\ & & & & & & & & +S_{Z-1} & -R_Z \end{bmatrix} \qquad (2.3.2)$$

Notice that the matrix $\underline{\underline{A}}$ is tridiagonal and that equation (2.3.1) is non-linear through the n_e in matrix $\underline{\underline{A}}$ since

$$n_e = \left(\sum_{z=0}^{Z} z f_z \right) n_i = \langle z \rangle n_i \qquad (2.3.3)$$

where n_i is the total ion density and $\langle z \rangle$, the mean ionisation level. Consider, for a moment, the simpler system containing the following pair of coupled linear equations.

$$\begin{aligned} \dot{y}_1 &= a y_1 + b y_2 \\ \dot{y}_2 &= c y_1 + d y_2 \end{aligned} \qquad (2.3.4)$$

These can be written as the matrix equation

$$\dot{\underline{Y}} = \underline{\underline{B}}\underline{Y} \qquad (2.3.5)$$

$$\text{where } \underline{Y} = \begin{bmatrix} y_1 \\ y_2 \end{bmatrix} \quad \text{and} \quad \underline{\underline{B}} = \begin{bmatrix} a & b \\ c & d \end{bmatrix} \qquad (2.3.6)$$

To solve equation (2.3.5) we substitute the trial solution $\underline{Y} = \underline{X} e^{\lambda t}$, which yields [5]

$$\lambda \underline{X}\, e^{\lambda t} = \underline{\underline{B}}\underline{X}\, e^{\lambda t} \qquad (2.3.7)$$

or

$$\underline{\underline{B}}\underline{X} = \lambda \underline{X} \qquad (2.3.8)$$

Thus we see that for $\underline{X} e^{\lambda t}$ to be a solution of equation (2.3.5), λ must be an eigenvalue of $\underline{\underline{B}}$ and $\underline{X}$ the corresponding eigenvector. Providing these conditions are met, $\underline{X}\, e^{\lambda t}$ is a solution to (2.3.5) and the general solution is given by a linear combination of the different solutions, i.e.

$$\underline{Y} = a_1 \underline{X}_1 e^{\lambda_1 t} + a_2 \underline{X}_2 e^{\lambda_2 t} \qquad (2.3.9)$$

since we have a system of linear equations of order two. In general, for an N^{th} order system, the formal solution is given by [5]

$$\underline{Y} = \sum_{i=1}^{N} a_i \underline{X}_i e^{\lambda_i t} \qquad (2.3.10)$$

where the a_1 ..... a_N are arbitrary constants determined by the initial conditions, since at t = 0 we have

$$\underline{Y}^{(0)} = \sum_{i=1}^{N} a_i \underline{X}_i \qquad (2.3.11)$$

and this provides a system of algebraic equations which can be solved for the a_i. If the $\underline{X}_i$ are orthogonal then the a_i may be written down immediately as

$$a_i = \underline{X}_i^T \cdot \underline{Y}^{(0)} \qquad (2.3.12)$$

where $\underline{X}_i^T$ is the transpose of the vector $\underline{X}_i$.

Returning now to the solution of (2.3.1) we see that provided our macroscopic variables (i.e. <z>, T, n_i) do not change by too much (in the computational solution we will choose a timestep which ensures this condition) the matrix equation (2.3.1) becomes linear for the duration of the timestep, and by analogy with the solution to equation (2.3.5) the solution to (2.3.1) can be written as

$$\underline{f} = \sum_{i=0}^{Z} a_i \underline{X}_i e^{\lambda_i t} \qquad (2.3.13)$$

Notice that in (2.3.2) the matrix $\underline{\underline{A}}$ is square and of order Z+1, but since we have the constraint

$$\sum_{z=0}^{Z} f_z = 1 \qquad (2.3.14)$$

we can eliminate one of the equations of (2.3.1) such that the matrix $\underline{\underline{A}}$ becomes square and of order Z. The λ_i and the $\underline{X}_i$ are the eigenvalues and eigenvectors respectively of the matrix $\underline{\underline{A}}$ and the a_i's are constants depending on the initial conditions. These constants can be obtained by knowing the fractional ionisation stage vector at time zero, i.e. $\underline{f}^{(0)}$ such that

$$\underline{f}^{(0)} = \sum_{i=1}^{i=Z} a_i \underline{X}_i \qquad (2.3.15)$$

Thus knowing $\underline{f}^{(0)}$ and the $\underline{X}_i$'s, the a_i's can be obtained quite simply and by knowing in addition the λ_i's we can solve for $\underline{f}$ in (2.3.13).

The problem remains, however, to find efficient methods to evaluate the eigenvalues and eigenvectors of the matrix $\underline{\underline{A}}$. It can be seen from (2.3.2) that the matrix $\underline{\underline{A}}$ is tridiagonal and 'quasi-symmetric' (i.e. the diagonal elements are real and the product of the off-diagonal elements is greater than zero).[25] Because of this property the matrix $\underline{\underline{A}}$ may be transformed by means of a similarity transform to a symmetric tridiagonal matrix. Thus if the elements of the tridiagonal matrix are

$$a_{ii} = \alpha_i \qquad a_{i,i+1} = \beta_{i+1} \qquad a_{i+1,i} = \gamma_{i+1} \;, \quad a_{i,j} = 0 \text{ otherwise,}$$

then provided $\beta_i \gamma_i > 0 \quad i = 2, N$ $\underline{\underline{A}}$ may be transformed into a real symmetric matrix by means of the similarity transformation with diagonal matrix $\underline{\underline{D}}$. If we define $\underline{\underline{D}}$ by the relations

$$d_{1,1} = 1 \qquad d_{i,i} = (\gamma_2 \gamma_3 \ldots \gamma_i / \beta_2 \beta_3 \ldots \beta_i)^{\frac{1}{2}}$$

then $D^{-1} CD = T$ where T is tridiagonal and

$$t_{ii} = \alpha_i \qquad t_{i,i+1} = t_{i+1,i} = (\beta_{i+1} \gamma_{i+1})^{\frac{1}{2}}$$

Since the eigenvalues of a real symmetric matrix are real, and since the eigenvalues of a matrix are unchanged under a similarity transformation, we see that the eigenvalues of $\underline{\underline{A}}$ in (2.3.2) are all real. Thus, solving the time-dependent matrix rate equation (2.3.1) reduces to finding the real eigenvalues and eigenvectors of the matrix $\underline{\underline{A}}$. Fast algorithms for the type of system are well known and they could be implemented into a general rate equation solver package.[26] The author has tried this and found

that these algorithms are not fast enough for use in computer codes. We have to find a much quicker way to evaluate the eigenvalues, eigenvectors and initial value constants.

2.4 In the Limit of No Recombination

Consider the case where recombination can be neglected (e.g. for very early times in the ionisation of a plasma). This leads to replacing all the Rs in the matrix $\underline{\underline{A}}$ by zero and at this point we see that the Z+1 equations (2.3.1) are not linearly independent (since DET($\underline{\underline{A}}$) = 0). However, since we have the constraint $\sum f_z = 1$ we can neglect the equation for the last ion stage and the solution to equation (2.3.1) can now be written as

$$\underline{f} = \sum_{i=0}^{Z-1} a_i \underline{X}_i e^{\lambda_i t} \tag{2.4.1}$$

and

$$f_z = 1 - \sum_{i=0}^{Z-1} f_i \tag{2.4.2}$$

where

$$\underline{f} = \begin{bmatrix} f_o \\ f_1 \\ f_2 \\ \\ \\ \\ f_j \\ \\ \\ f_{Z-1} \end{bmatrix} \text{ and } \underline{\underline{A}} = n_e \begin{bmatrix} -S_o & & & & & \\ +S_o & -S_1 & & & & \\ & +S_1 & -S_2 & & & \\ & & & & & \\ & & & & & \\ & & & & & \\ & & & +S_{j-1} & -S_j & \\ & & & & & \\ & & & & & \\ & & & & -S_{Z-2} & -S_{Z-1} \end{bmatrix} \tag{2.4.3}$$

We now observe that the matrix $\underline{\underline{A}}$ has many symmetry properties and by inspection that the eigenvalues of $\underline{\underline{A}}$ are now just its diagonal elements and the components of the eigenvectors are just simple combinations of these eigenvalues, i.e. the eigenvalues λ_i of the matrix $\underline{\underline{A}}$ are

$$\lambda_o = -n_e S_o, \quad \lambda_1 = -n_e S_1, \ \ldots\ldots\ldots, \quad \lambda_i = -n_e S_i, \ \ldots\ldots\ldots \lambda_{z-1} = -n_e S_{z-1} \tag{2.4.4}$$

and the eigenvectors $\underline{X}_i$ are given by

$$\underline{X}_o = \begin{bmatrix} 1 \\ \dfrac{\lambda_0}{\lambda_1-\lambda_0} \\ \dfrac{\lambda_0\lambda_1}{(\lambda_1-\lambda_0)(\lambda_2-\lambda_0)} \\ \cdot \\ \cdot \\ \cdot \\ \cdot \\ \cdot \\ \cdot \\ \cdot \end{bmatrix} \quad \underline{X}_1 = \begin{bmatrix} 0 \\ 1 \\ \dfrac{\lambda_1}{\lambda_2-\lambda_1} \\ \dfrac{\lambda_1\lambda_2}{(\lambda_2-\lambda_1)(\lambda_3-\lambda_1)} \\ \cdot \\ \cdot \\ \cdot \end{bmatrix} \quad \underline{X}_2 = \begin{bmatrix} 0 \\ 0 \\ 1 \\ \dfrac{\lambda_2}{\lambda_3-\lambda_2} \\ \cdot \\ \cdot \\ \cdot \end{bmatrix} \quad \ldots\ldots\ldots \tag{2.4.5}$$

Enough elements have been included in the eigenvectors to enable one to see their general pattern. The complete set of eigenvectors is given in Appendix 1. From equation (2.3.15) the general formula for the a_i is shown in Appendix 2 to be

$$a_i = f_i^{(0)} - \sum_{k=0}^{i-1} \frac{a_k \lambda_k \lambda_{k+1} \lambda_{k+2} \ldots\ldots \lambda_{i-1}}{(\lambda_k-\lambda_k)(\lambda_{i-1}-\lambda_k)\ldots(\lambda_{k+1}-\lambda_k)} \qquad i = 1,Z \tag{2.4.6}$$

Hence we see that for sub-hydrodynamic timescales and in the limit of no recombination, we can avoid the time-consuming numerical evaluation of the eigenvalues and eigenvectors which are now provided by expressions (2.4.4) and (2.4.5).

Computer results

Using the eigenvalues (2.4.4), the eigenvectors (2.4.5) and the initial value constants (2.4.6), we are now in a position to do a calculation for the ionisation fractions. One question of interest which arises is how many ionisation stages must one follow in order to obtain reasonably accurate evaluations of the mean ionisation level and mean square ionisation level. One might expect that instead of following all seven ionisation stages of carbon, for example, some small subset of this number may be sufficient.

Fig. 2.4.1 shows the results of a calculation based on all seven ionisation stages of carbon being present. The temperature of the electrons is allowed to vary linearly with time from $T_0 = 10^4$ K at a density of $n_i = 10^{21}$ cm^{-3}. We neglect fractions whose presence is less than about one per cent of largest fraction present and consider the number of fractions present as a function of time. The results indicate that, as far as ionisation is concerned, it should be quite sufficient to follow only three ionisation fractions at any one time, instead of all seven for carbon. The results also show that as the temperature variation rises more steeply, instead of more ionisation fractions appearing, the time axis just undergoes a 'translation'.

Allowing only three ionisation stages present at any one time, another calculation was carried out on carbon which was heated instantaneously to 5×10^5 K. Under the assumptions of constant density and temperature we can compare our results with the theoretical results. Figure 2.4.2 shows the burn through of the ionisation stages to steady state, as a function of time. The continuous curves represent the exact solutions whereas the asterisks denote the results of the present model, and as is seen we have very close agreement. The discrepancy at around

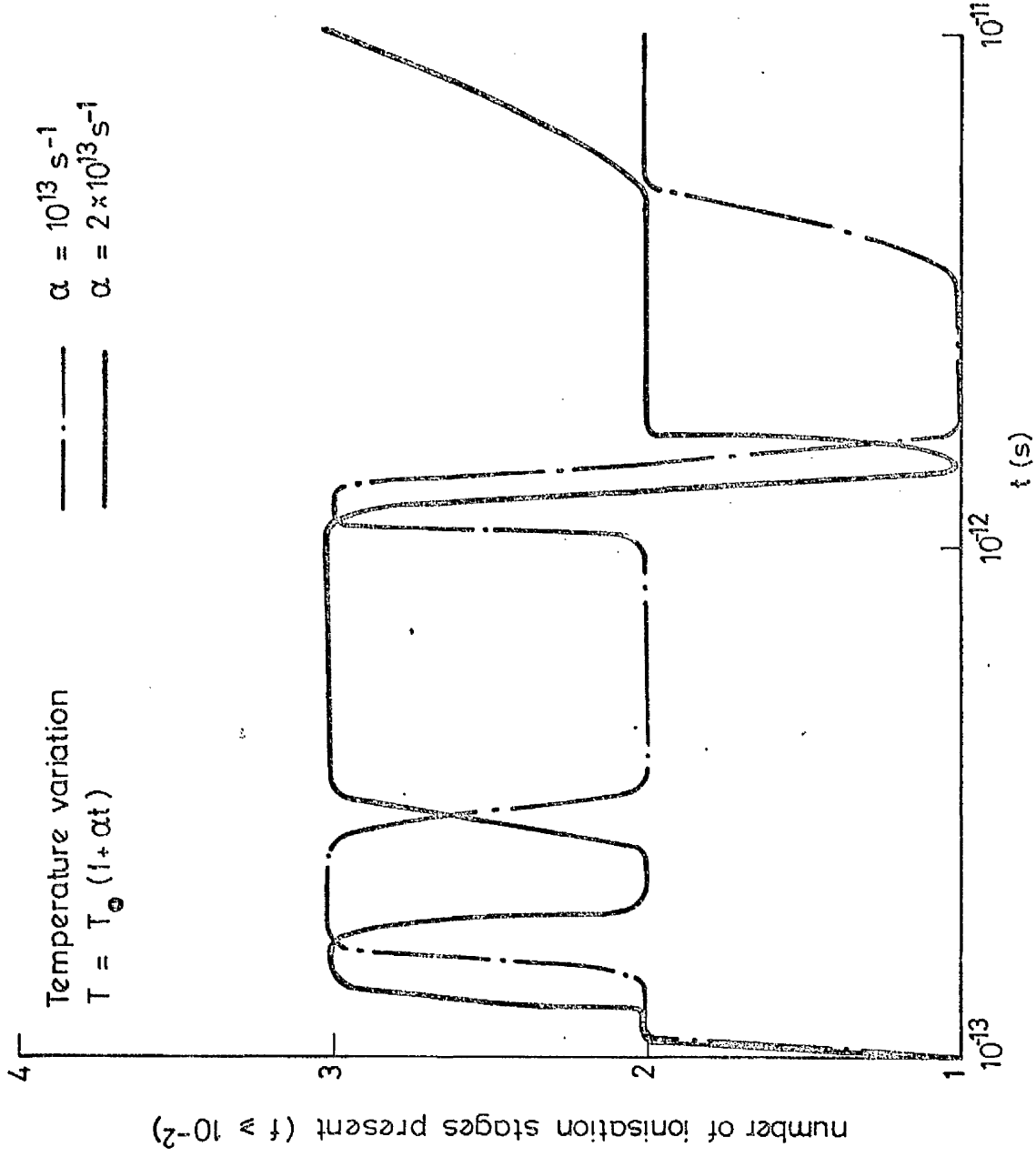

Fig. 2.4.1 The number of ionisation stages present in carbon ($n_i = 10^{21}$ cm^{-3}, $T_o = 10^4$K) as a function of time

2×10^{-13}s arises due to the fact that the exact solutions show we have four ionisation stages present, whereas our computer model only allows for three at any one time. Thus we overestimate f_3 since we cannot allow for f_4 until f_1 dies away. It is interesting to note here that in this extreme case in which an instantaneous temperature pulse is applied to the plasma, it takes 10 picoseconds to reach the steady state value of $f_4 = 1.0$. For a less severe temperature pulse and a higher degree of ionisation, it would take longer to reach equilibrium thus showing that on a picosecond timescale the fractional population densities of the ionisation stages are strongly time-dependent.

In fig. 2.4.3 we show the complete burn through of the ionisation stages in carbon using a temperature pulse rising linearly in time, from 10^4 K to 10^6 K in 100 picoseconds. The curves represent a typical burn through profile and in fig. 2.4.4 we plot the mean ionisation level $\langle Z \rangle$ as a function of time for this situation. The results are shown by the continuous curve. The broken curve gives the values of $\langle z \rangle$ as predicted by the steady-state corona model (where $\langle z \rangle$ is a function of temperature only) and we notice a significant decrease in the estimate of the mean ionisation level when using a time-dependent model.

2.5 An Example

Consider the expression for the solution vector $\underline{f}$, i.e.

$$\underline{f} = \sum_i a_i \underline{X}_i e^{\lambda_i t} \qquad (2.5.1)$$

Now in the limit of no recombination, the λ_i and X_i are the eigenvalues and eigenvectors of the matrix $\underline{\underline{A}}$ of (2.4.3). We see that the eigenvalues of $\underline{\underline{A}}$ are all negative and hence equation (2.5.1) is a sum of decaying terms. It is interesting to consider a simple example to enable us to see the meaning of (2.5.1) more clearly.

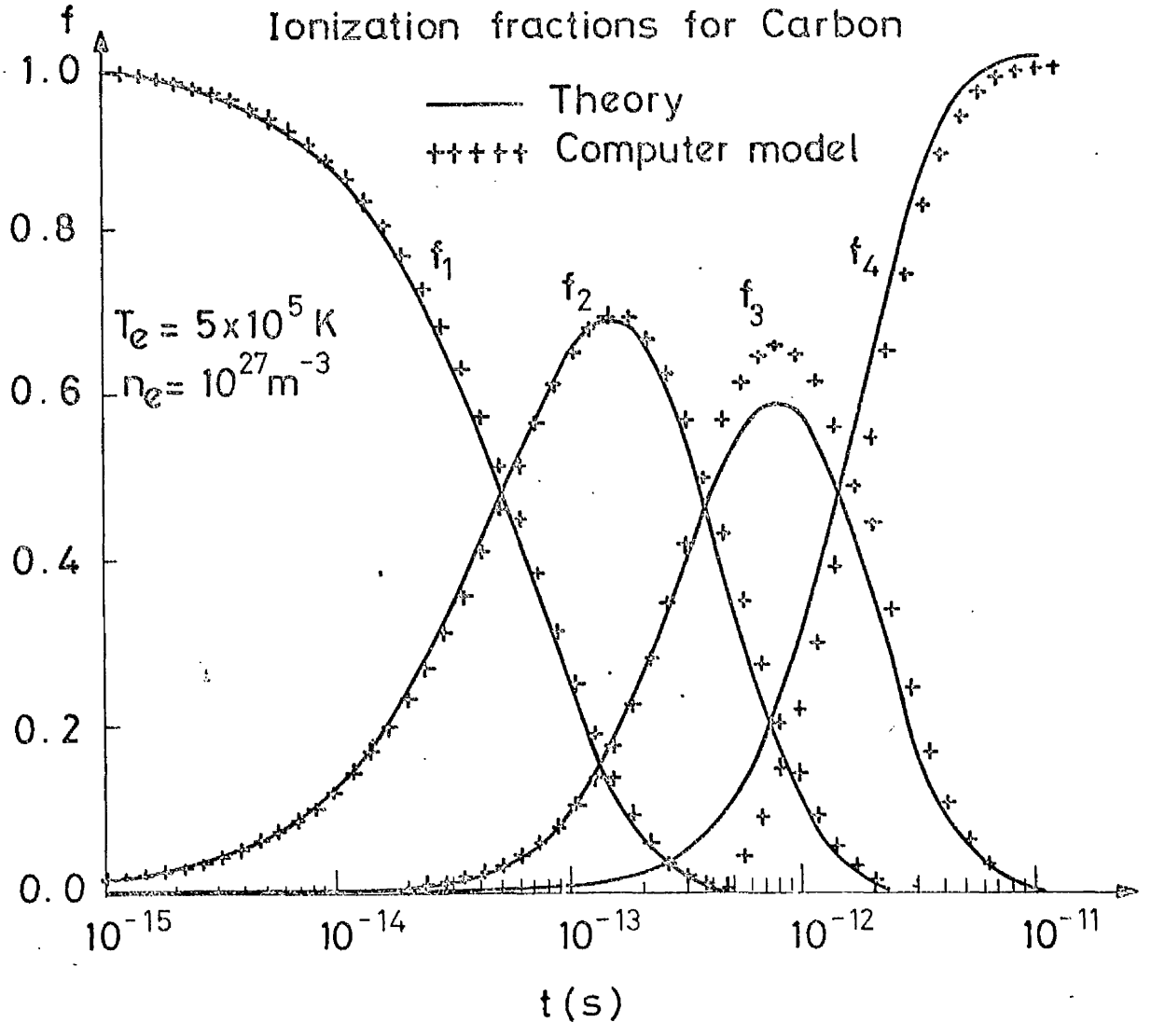

Fig. 2.4.2 The burn through of ionisation stages in carbon held at constant density and temperature

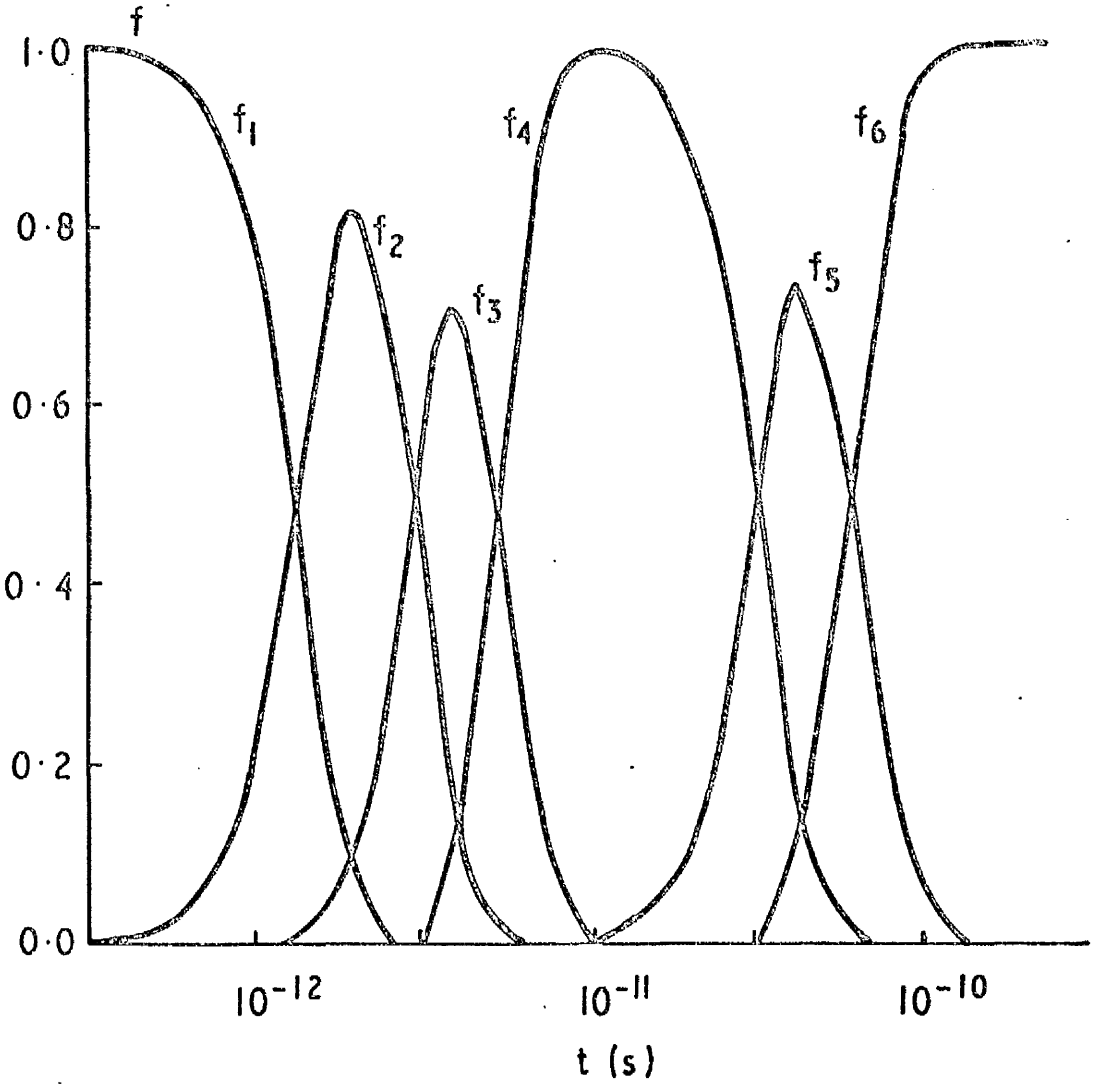

Fig. 2.4.3 The burn through of the ionisation fractions for a linear temperature rise from 10^4K to 10^6K in 0.1 nanosecond

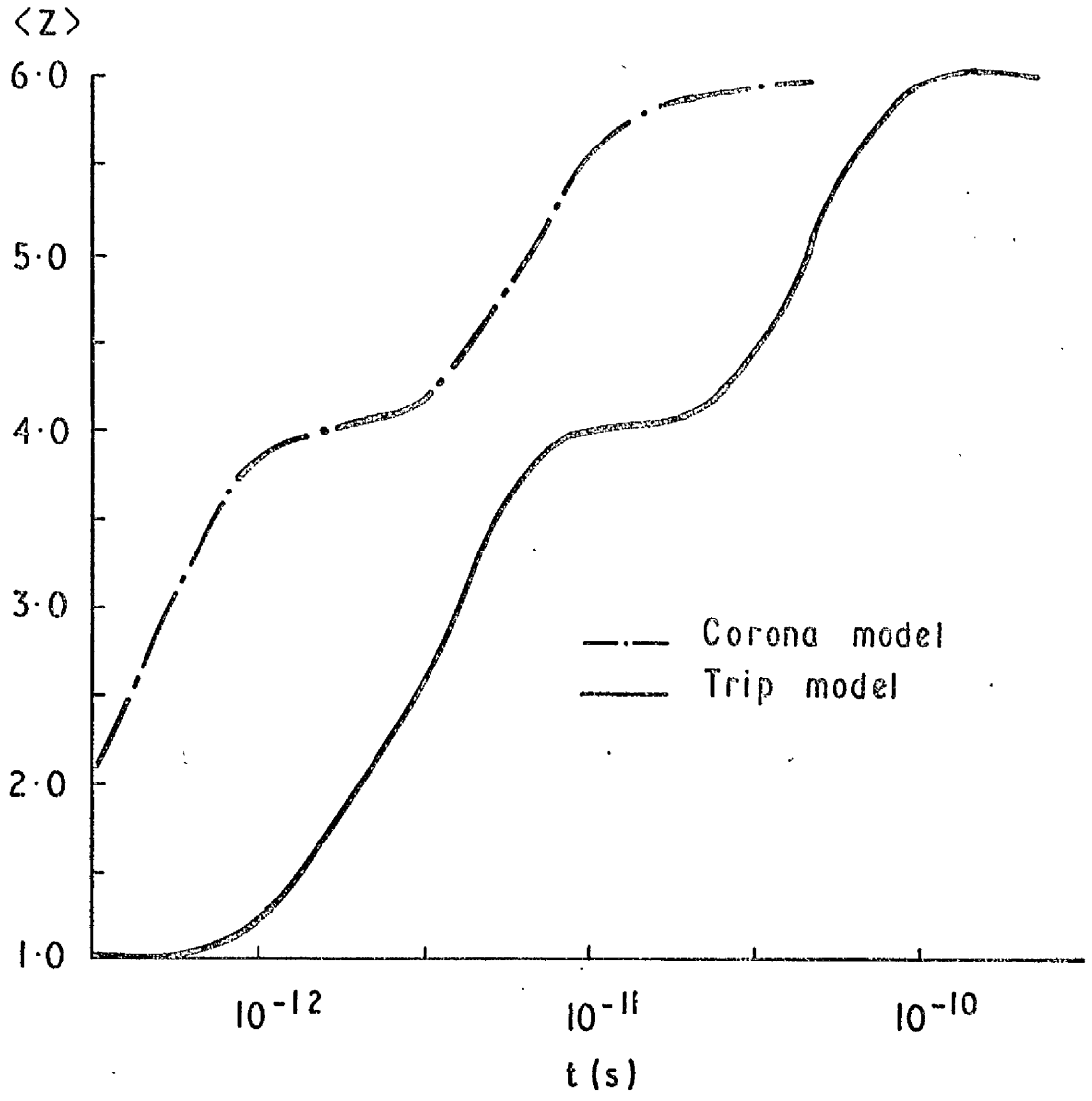

Fig. 2.4.4 The mean ionisation level as a function of time for the temperature pulse of fig. 2.4.3. Predictions using a steady state and time dependent atomic physics models are shown

Consider a system with only three ionisation stages and let f_0, f_1, f_2 be the fractional population densities of these levels. The matrix equation for the system is

$$\begin{bmatrix} \dot{f}_0 \\ \dot{f}_1 \\ \dot{f}_2 \end{bmatrix} = \begin{bmatrix} -S_0 & & \\ +S_0 & -S_1 & \\ & +S_1 & -S_2 \end{bmatrix} \begin{bmatrix} f_0 \\ f_1 \\ f_2 \end{bmatrix} \tag{2.5.1}$$

where $\dot{f}$ is the derivative of f with respect to time and n_e (as in (2.4.3)) has been dropped for clarity. Again, since we have the constraint $\sum f_z = 1$, the system can be reduced to

$$\begin{bmatrix} \dot{f}_0 \\ \dot{f}_1 \end{bmatrix} = \begin{bmatrix} -S_0 & \\ +S_0 & -S_1 \end{bmatrix} \begin{bmatrix} f_0 \\ f_1 \end{bmatrix} \tag{2.5.2}$$

and

$$f_2 = 1 - f_0 - f_1 \tag{2.5.3}$$

By inspection, the eigenvalues, eigenvectors and initial value constants of the ionisation matrix are given by

$$\begin{aligned} \lambda_0 &= -S_0, & \lambda_1 &= -S_1 \\ \underline{X}_0 &= \begin{bmatrix} 1 \\ \dfrac{-S_0}{(S_0-S_1)} \end{bmatrix} & \underline{X}_1 &= \begin{bmatrix} 0 \\ 1 \end{bmatrix} \\ a_0 &= 1 & a_1 &= S_0/(S_0-S_1) \end{aligned} \tag{2.5.4}$$

where the initial value constants are calculated using the initial conditions $f_0 = 1$ and $f_1 = f_2 = 0$.

Substituting expressions (2.5.4) into (2.5.1) yields

$$\begin{aligned} f_0 &= e^{-S_0 t} \\ f_1 &= \frac{-S_0}{(S_0-S_1)} e^{-S_0 t} + \frac{S_0}{(S_0-S_1)} e^{-S_1 t} \\ f_2 &= 1 - f_0 - f_1 \end{aligned} \tag{2.5.5}$$

We will now consider the solutions for very short times such that $\exp(-\delta t) \sim 1 - \delta t$, i.e.

$$\begin{aligned} f_0 &= 1 - S_0 t \\ f_1 &= +S_0 t \\ f_2 &= 0 \end{aligned} \tag{2.5.6}$$

Thus we see that as f_0 decreases initially, f_1 increases to exactly counterbalance the decrease in f_0, and this is what we should expect physically.

2.6 In the Limit of No Innisation

We can also consider the case where ionisation can be neglected (e.g. in an ionised plasma which is rapidly cooled). We then put the S_z in the matrix $\underline{\underline{A}}$ of (2.3.2) to zero and in this case, using the constraint $\sum f_z = 1$, we neglect the equation for the ground state population density. The solution to equation (2.3.1) can now be written as

$$\underline{f} = \sum_{i=1}^{Z} a_i \underline{X}_i e^{\lambda_i t} . \tag{2.6.1}$$

and

$$f_0 = 1 - \sum_{i=1}^{Z} f_i \tag{2.6.2}$$

where the λ_i and $\underline{X}_i$ are the eigenvalues and eigenvectors of the matrix $\underline{\underline{A}}$ where

$$\underline{f} = \begin{bmatrix} f_1 \\ f_2 \\ f_3 \\ \\ \\ f_j \\ \\ f_Z \end{bmatrix} \quad \text{and} \quad \underline{\underline{A}} = n_e \begin{bmatrix} -R_1 & +R_2 & & & & & \\ & -R_2 & +R_3 & & & & \\ & & -R_3 & +R_4 & & & \\ & & & & & & \\ & & & & & & \\ & & & & -R_j & +R_{j+1} & \\ & & & & & & -R_Z \end{bmatrix} \tag{2.6.3}$$

Again, because of the many symmetry properties which the matrix $\underline{\underline{A}}$ now has, we see that by inspection the eigenvalues of $\underline{\underline{A}}$ are just its diagonal elements and the components of the eigenvectors are simple combinations of these eigenvalues, i.e. the eigenvalues λ_i of the matrix $\underline{\underline{A}}$ are now given by

$$\lambda_1 = -n_e R_1, \quad \lambda_2 = -n_e R_2, \ \ldots\ldots, \quad \lambda_i = -n_e R_i, \ \ldots\ldots, \quad \lambda_{\mathbb{Z}} = -n_e R_{\mathbb{Z}} \tag{2.6.4}$$

and the eigenvectors $\underline{X}_i$ are given by

$$\underline{X}_i = \begin{bmatrix} 1 \\ 0 \\ 0 \\ " \\ " \end{bmatrix} \quad \underline{X}_2 = \begin{bmatrix} \frac{\lambda_2}{\lambda_1 - \lambda_2} \\ 1 \\ 0 \\ " \\ " \end{bmatrix} \quad \underline{X}_3 = \begin{bmatrix} \frac{\lambda_2 \lambda_3}{(\lambda_1 - \lambda_3)(\lambda_2 - \lambda_3)} \\ \frac{\lambda_3}{\lambda_2 - \lambda_3} \\ 1 \\ 0 \\ " \end{bmatrix} \ \ldots\ldots \tag{2.6.5}$$

Where enough elements have been included to enable one to see the general pattern of the eigenvectors. The complete set of eigenvectors for the 'no ionisation' case are shown in Appendix 3, and the general formula for the a_i is shown in Appendix 4 to be

$$a_i = f_i^{(0)} - \sum_{K=i+1}^{z_{max}} \frac{a_K \lambda_K \lambda_{K-1} \ldots \lambda_{i+1}}{(\lambda_i - \lambda_K)(\lambda_{i+1} - \lambda_K) \ldots\ldots (\lambda_{K-1} - \lambda_K)} \tag{2.6.6}$$

$$i = z_{max} - 1, \ 0.$$

Computer Results

In section 2.4 we compared the burn through of the ionisation stages in carbon as given by our computer model, against the exact solutions which took into account all the ionisation stages. In those results, the recombination terms were put to zero. In this section we wish again to compare the computer model results against the exact results, but this time in the case where the ionisation coefficients are put to zero.

Using the expressions (2.6.4) - (2.6.6) we obtain the results of figs. 2.6.1 and 2.6.2. Fig. 2.6.1 shows the exact results using all the ionisation stages for a recombination only plasma. The temperature and density were held constant at 10^4 K and 10^{21} cm^{-3} respectively and the initial condition used was that $f_6 = 1$. Fig. 2.6.2 shows the results of the computer model for this case and we notice some significant differences. One thing we notice immediately from fig. 2.6.1 is that at around 10^{-11}s we have six ionisation stages present and so we cannot expect our computer model to represent this situation accurately since there, account is taken of only three ionisation stages. The computer model results are shown in fig. 2.6.2 and we immediately notice the presence of a 'computational' ionisation fraction denoted f_c. The reason for this is as follows. In section 2.7 it will be pointed out that in a recombination plasma, we solve for f_{z+1} and f_z from which we can construct $f_{z-1} = 1 - f_z - f_{z+1}$. Thus we see that knowing f_6 and f_5 we can obtain f_4. However as is seen from fig. 2.6.1 this 'f_4' is actually $f_1 + f_2 + f_3 + f_4$ and we denote this by f_c in fig. 2.6.2. Thus we observe that when a plasma is undergoing rapid recombination, the assumption of there being only three ionisation stages present in the plasma at any one time can lead to wrong results and so care must be taken as to how one interprets these results.

2.7 Ionisation and Recombination I

Previously we have considered situations in which either ionisation or recombination could be neglected. This led to extremely simple and computationally efficient solutions. Is it possible that the ideas developed in the previous sections can be applied to the more general problem where neither ionisation nor recombination can be neglected?

It has been shown in section 2.4 that although there are many ionisation levels in medium and high-Z materials, it is sufficient to

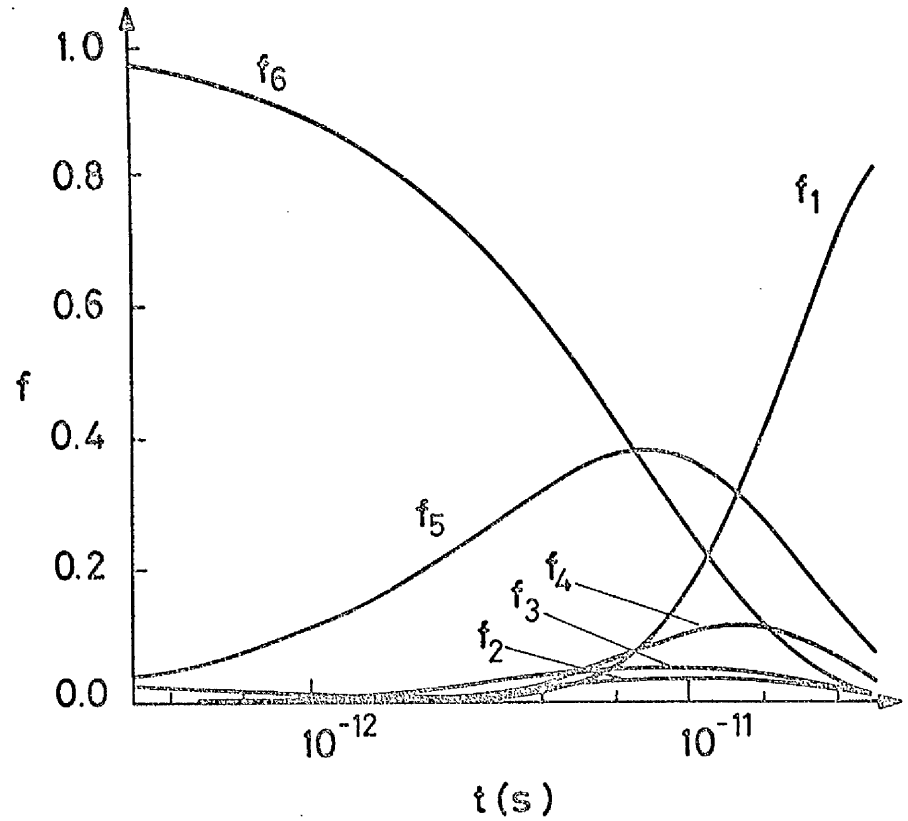

Fig. 2.6.1 The exact solutions for the recombining plasma

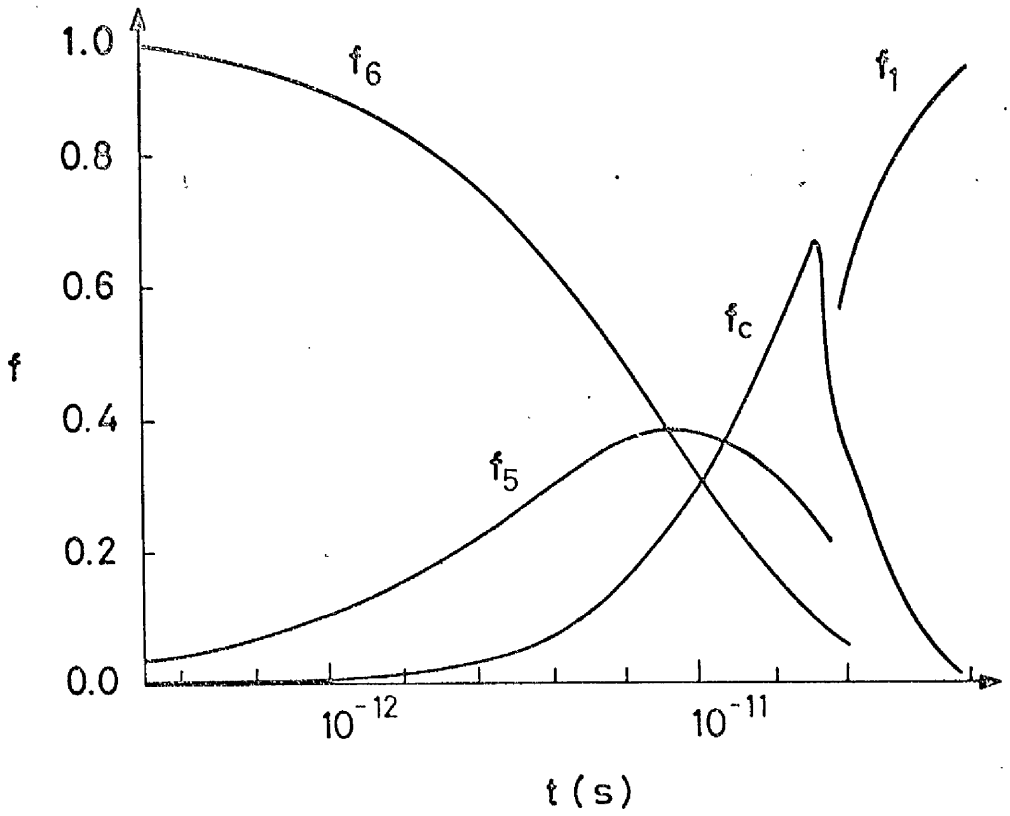

Fig. 2.6.2 The computed solutions for the recombining plasma

consider three ionisation levels only, at any one time. Hence if we know that the mean ionisation level at a point in the plasma is z, then it is sufficient to consider only the ionisation fractions f_{z-1}, f_z, f_{z+1}. The three levels z-1, z, z+1 together with the various ionisation and recombination processes and the governing matrix rate equation are shown in fig. 2.7. 1.

Thus the various atomic physics processes we allow for in and between the three levels shown are ionisation from levels z-1 and z and recombination from level z+1 and z. Notice that in order to have the constraint $\sum f_z = 1$ we must neglect recombination from level z-1 and ionisation from level z+1. The governing rate equations for these processes is shown also in fig. 2.7.1, where the rate coefficients have been put in matrix form and the ionisation fractions have been expressed in terms of an ionisation stage vector. It should be noticed that since we have the constraint $\sum f_z = 1$ we need solve for only two of the ionisation fractions, the third being given immediately by this condition.

Consider now the matrix rate equation of fig. 2.7 written in explicit differential form, i.e.

$$\begin{aligned}
\frac{\partial f_{z-1}}{\partial t} &= -S_{z-1} f_{z-1} + R_z f_z \\
\frac{\partial f_z}{\partial t} &= +S_{z-1} f_{z-1} - (S_z + R_z) f_z + R_{z+1} f_{z+1} \qquad (2.7.1) \\
\frac{\partial f_{z+1}}{\partial t} &= +S_z f_z - R_{z+1} f_{z+1}
\end{aligned}$$

We now invoke the constraint $\sum f_z = 1$, which in this case means

$$f_{z-1} + f_z + f_{z+1} = 1 \qquad (2.7.2)$$

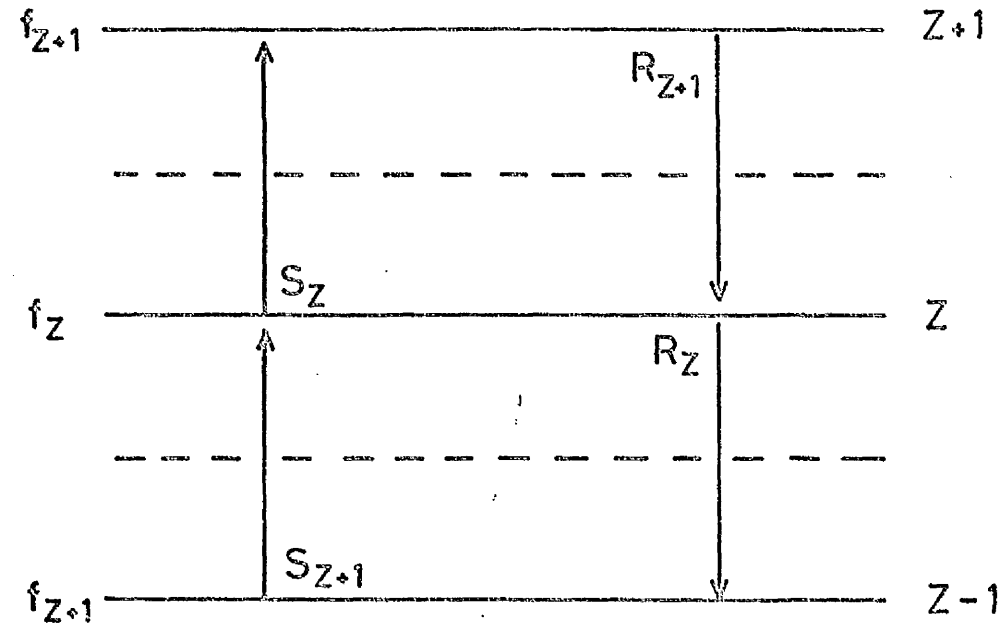

$$\begin{bmatrix} \dot{f}_{Z-1} \\ \dot{f}_Z \\ \dot{f}_{Z+1} \end{bmatrix} = n_e \begin{bmatrix} -S_{Z-1} & +R_Z & \\ +S_{Z-1} & -(S_Z+R_Z) & +R_{Z+1} \\ & +S_Z & -R_{Z+1} \end{bmatrix} \begin{bmatrix} f_{Z-1} \\ f_Z \\ f_{Z+1} \end{bmatrix}$$

Fig. 2.7.1 The ionisation recombination processes between the levels z-1, z and z+1, and the accompanying matrix rate equation.

At this point we substitute for f_{z+1}, from equation (2.7.2) into the equation for f_z in equations (2.7.1), which then becomes

$$\frac{\partial f_z}{\partial t} = +S_{z-1}f_{z-1} \quad -(S_z+R_z)f_z \quad +R_{z+1}(1-f_z-f_{z-1})$$

or

$$\frac{\partial f_z}{\partial t} = (S_{z-1}-R_{z+1})f_{z-1} \quad -(S_z+R_z+R_{z+1})f_z \quad +R_{z+1}$$

And the system of equations (2.7.1) is replaced by

$$\begin{aligned}
\frac{\partial f_{z-1}}{\partial t} &= -S_{z-1}f_{z-1} \quad +R_z f_z \\
\frac{\partial f_z}{\partial t} &= (S_{z-1}-R_{z+1})f_{z-1} \quad -(S_z+R_{z+1}+R_z)f_z \quad +R_{z+1} \\
\frac{\partial f_{z+1}}{\partial t} &= +S_z f_z \quad -R_{z+1}f_{z+1}
\end{aligned} \tag{2.7.3}$$

Again since we have the constraint (2.7.2) we need solve only two of the equation (2.7.3). We choose to solve for f_{z-1} and f_z and rewrite the equations in the following form

$$\frac{\partial \underline{f}}{\partial t} = \underline{\underline{A}}\underline{f} + \underline{g}$$

and (2.7.4)

$$f_{z+1} = 1 - f_z - f_{z-1}$$

where

$$\underline{f} = \begin{bmatrix} f_{z-1} \\ f_z \end{bmatrix} \quad \underline{\underline{A}} = n_e \begin{bmatrix} -S_{z-1} & 0 \\ (S_{z-1}-R_{z+1}) & -(S_z+R_z+R_{z+1}) \end{bmatrix} \quad \underline{g} = n_e \begin{bmatrix} R_z f_z \\ R_{z+1} \end{bmatrix} \tag{2.7.5}$$

We notice here that $\underline{g}$ (since f_z) is time-dependent and that together, the equations of (2.7.4) are exactly equivalent to the matrix rate equation of fig.2.7.1subject to the constraint of (2.7.2).

We now assume that the term $R_z f_z$ in the vector $\underline{g}$ is constant or unimportant, over the timestep we are considering, such that g is now constant. The matrix equation of (2.7.4) can then be solved in the following manner. Substituting the trial solution

$$\underline{f} = \underline{X}\, e^{\lambda t} + \underline{b} \tag{2.7.6}$$

into the matrix equation of (2.7.4) gives

$$\lambda \underline{X} e^{\lambda t} = \underline{\underline{A}}(\underline{X} e^{\lambda t} + \underline{b}) + \underline{g} \tag{2.7.7}$$

and hence we see that (2.7.6) is a solution to (2.7.4) provided $\underline{\underline{A}}\,\underline{b} = -\underline{g}$ and λ and $\underline{X}$ are the eigenvalues and eigenvectors respectively, of the matrix $\underline{\underline{A}}$. The general solution to (2.7.4) is then given by

$$\underline{f} = -\underline{\underline{A}}^{-1}\,\underline{g} + \sum_{i=1}^{2} a_i\, \underline{X}_i\, e^{\lambda_i t} \tag{2.7.8}$$

where the a_i are constants depending on the initial conditions, i.e.

$$\underline{f}^{(0)} = -\underline{\underline{A}}^{-1}\,\underline{g} + \sum_{i=1}^{2} a_i\, \underline{X}_i \tag{2.7.9}$$

The terms in equation (2.7.8) written explicitly are

$$\lambda_1 = -n_e S_{z-1} \qquad \lambda_2 = -n_e (S_z + R_z + R_{z+1})$$

$$\underline{X}_1 = \begin{bmatrix} 1 \\ \dfrac{S_{z-1} - R_{z+1}}{\lambda'_1 - \lambda'_2} \end{bmatrix} \qquad \underline{X}_2 = \begin{bmatrix} 0 \\ 1 \end{bmatrix}$$

$$a_1 = f^{(0)}_{z-1} + \frac{R_z f^{(0)}_z}{\lambda'_1} \qquad a_2 = f^{(0)}_z - a_1 \left(\frac{S_{z-1} - R_{z+1}}{\lambda'_1 - \lambda'_2} \right)$$

$$+ \frac{1}{\lambda'_2} \left[R_{z+1} - \frac{R_z f^{(0)}_z}{\lambda'_1} \left(S_{z-1} - R_{z+1} \right) \right]$$

$$\underline{\underline{A}}^{-1}\underline{g} = \begin{bmatrix} \dfrac{R_z f_z^{(0)}}{\lambda_1'} \\ \dfrac{1}{\lambda_2'}\left[R_{z+1} - \dfrac{R_z f_z^{(0)}}{\lambda_1'}\quad (S_{z-1}-R_{z+1})\right] \end{bmatrix} \text{ and } \lambda' = \frac{\lambda}{n_e} \qquad (2.7.10)$$

These terms are evaluated in Appendix 5.

We will now apply some simple checks for which we already know the results,

Check 1 Neglect the recombination coefficients

Putting the Rs in expression (2.7.10) to zero we see that

$$\lambda_1 = -n_e S_{z-1} \qquad \lambda_2 = -n_e S_z$$

$$\underline{X}_1 = \begin{bmatrix} 1 \\ \dfrac{S_{z-1}}{\lambda_1'-\lambda_2'} \end{bmatrix} \qquad \underline{X}_2 = \begin{bmatrix} 0 \\ 1 \end{bmatrix}$$

$$a_1 = f_{z-1}^{(0)} = 1 \qquad a_2 = \frac{-S_{z-1}}{\lambda_1'-\lambda_2'} \text{ since } \underline{f}^{(0)} = \begin{bmatrix} 1 \\ 0 \end{bmatrix}$$

$$\text{and } \underline{\underline{A}}^{-1}\underline{g} = \underline{0} \qquad (2.7.11)$$

$$\text{hence } \begin{bmatrix} f_{z-1} \\ f_z \end{bmatrix} = \begin{bmatrix} 1 \\ \dfrac{S_{z-1}}{S_z-S_{z-1}} \end{bmatrix} \exp(-n_e S_{z-1} t)$$

$$- \frac{S_{z-1}}{S_z-S_{z-1}} \begin{bmatrix} 0 \\ 1 \end{bmatrix} \exp(-n_e S_z t) \qquad (2.7.12)$$

which is precisely the same result as in section 2.5.

Check 2 The full solution for early times

In this case we use the terms of (2.7.10) but with the initial conditions

$$\underline{f}^{(0)} = \begin{bmatrix} 1 \\ 0 \end{bmatrix}$$

hence $a_1 = 1$ and $a_2 = -\left(\frac{S_{z-1}-R_{z+1}}{\lambda_1'-\lambda_2'}\right) + \frac{R_{z+1}}{\lambda_2'}$

and $\underline{\underline{A}}^{-1}\underline{g} = \begin{bmatrix} 0 \\ \frac{R_{z+1}}{\lambda_2'} \end{bmatrix}$ (2.7.13)

and since the solution is

$$\underline{f} = -\underline{\underline{A}}^{-1}\underline{g} + \sum_{i=1}^{2} a_i \underline{X}_i e^{\lambda_i t} \quad (2.7.14)$$

we have

$$\begin{bmatrix} f_{z-1} \\ f_z \end{bmatrix} = \begin{bmatrix} 1 \\ \frac{S_{z-1}-R_{z+1}}{\lambda_1'-\lambda_2'} \end{bmatrix} e^{-n_e S_{z-1} t} + \left(\frac{R_{z+1}}{\lambda_2'} - \left(\frac{S_{z-1}-R_{z+1}}{\lambda_1'-\lambda_2'}\right)\right)\begin{bmatrix} 0 \\ 1 \end{bmatrix} e^{-n_e(S_z+R_z+R_{z+1})t}$$

$$- \begin{bmatrix} 0 \\ \frac{R_{z+1}}{\lambda_2'} \end{bmatrix} \quad (2.7.15)$$

or $f_{z-1} = e^{-n_e S_{z-1} t}$

and

$$f_z = \left(\frac{S_{z-1}-R_{z+1}}{\lambda_1'-\lambda_2'}\right) e^{-n_e S_{z-1} t} + \left(\frac{R_{z+1}}{\lambda_2'} - \left(\frac{S_{z-1}-R_{z+1}}{\lambda_1'-\lambda_2'}\right)\right) e^{-n_e(S_z+R_z+R_{z+1})t}$$

$$- \frac{R_{z+1}}{\lambda_2'} \quad (2.7.16)$$

We now apply the solution for very small times such that $\exp(-St) \sim 1 - St$ and equate the terms dependent and independent of t.

The terms independent of t can be written as

$$\frac{S_{z-1}-R_{z+1}}{\lambda'_1-\lambda'_2} + \frac{R_{z+1}}{\lambda'_2} - \left(\frac{S_{z-1}-R_{z+1}}{\lambda'_1-\lambda'_2}\right) - \frac{R_{z+1}}{\lambda'_2} = 0 \qquad (2.7.17)$$

as expected, and the terms dependent on to can be written as

$$\left(\frac{S_{z-1}-R_{z+1}}{\lambda'_1-\lambda'_2}\right)\lambda'_1 + \left(\frac{R_{z+1}\lambda'_1+\lambda'_2\lambda'_1}{\lambda'_1-\lambda'_2}\right) = \frac{\lambda'_1}{\lambda'_1-\lambda'_2}\left[S_{z-1}-R_{z+1}+R_{z+1}+\lambda'_2\right]$$

$$\text{or} \quad \frac{\lambda'_1}{\lambda'_1-\lambda'_2}(\lambda'_2-\lambda'_1) = -\lambda'_1 = n_e S_{z-1} \qquad (2.7.18)$$

as expected since for very early time no recombination can have taken place from f_z and f_{z+1} and hence there should be no R terms in (2.7.18).

Check 3 Neglect the ionisation coefficients

This can only be done forvery early times (such that $f_z^{(0)} = 0$) since in a few of the terms we have a division by λ'_1 which is now zero.

From (2.7.10) we have

$$\lambda_1 = 0 \qquad \lambda_2 = -n_e(R_z+R_{z+1})$$

$$\underline{X}_1 = \begin{bmatrix} 1 \\ \frac{R_{z+1}}{R_z+R_{z+1}} \end{bmatrix} \qquad \underline{X}_2 = \begin{bmatrix} 0 \\ 1 \end{bmatrix}$$

$$a_1 = 1 \qquad a_2 = 0$$

$$\underline{\underline{A}}^{-1}\underline{g} = \begin{bmatrix} 0 \\ \frac{R_{z+1}}{R_z+R_{z+1}} \end{bmatrix} \qquad (2.7.19)$$

hence

$$\begin{bmatrix} f_{z-1} \\ f_z \end{bmatrix} = \begin{bmatrix} 1 \\ \frac{-R_{z+1}}{R_z+R_{z+1}} \end{bmatrix} - \begin{bmatrix} 0 \\ \frac{R_{z+1}}{R_z+R_{z+1}} \end{bmatrix} e^{-n_e(R_z+R_{z+1})t} \qquad (2.7.20)$$

$$\text{i.e.} \qquad f_{z-1} = 1 \qquad f_z = 0 \qquad (2.7.21)$$

which is correct, since for very early times f_z and $f_{z+1} = 0$ and there can be no recombination from these levels.

Having done these checks, especially the last one, we notice that in a 'recombination only' plasma we cannot use the terms of (2.7.10), since we have the term $1/\lambda'_1$ and $\lambda'_1 = 0$. This can be avoided quite simply by developing another set of terms, equivalent to (2.7.10) but found in the following manner. Previously, in equations (2.7.1), we substituted for the term $R_{z+1}f_{z+1}$ in the equation for f_z using the constraint (2.7.2). It would have been just as easy to substitute for the term $S_{z-1}f_{z-1}$ in the same equation and then proceeded to evaluate an equivalent set of terms to (2.7.10). This is done in Appendix 6.

It should be remembered that the set of expressions (2.7.10) make up the solution of (2.7.4) provided the term $R_z f_z$ remains constant or unimportant over the timestep. Similarly, the alternative solution developed in Appendix 6 is valid provided the term $S_z f_z$ remains constant or unimportant over the timestep. Hence in a plasma undergoing ionisation the former solution is appropriate, and for a plasma undergoing recombination, we should apply the latter solution. For a plasma in which some of the time levels, as in fig. 2.7, are ionising and some recombining we are in an approximate steady-state and either type of solution can be applied.

2.8 Ionisation and Recombination II

In section 2.8 we extended the ideas developed in sections 2.4 and 2.6 to include ionisation and recombination simultaneously. After some manipulation, we showed that the eigenvalues of the matrix $\underline{\underline{A}}$ were again

just its diagonal elements and elements of the eigenvectors, just simple combinations of these eigenvalues. We also introduced the column vector $\underline{g} = (R_z f_z, R_{z+1})$ and under the assumption of $\underline{g}$ being constant over a timestep we obtained simple algebraic solutions to the rate equations. The solutions obtained in this form could be checked a) in the limit of no recombination b) in the limit of no ionisation, and c) in the limit of very short times.

The approach of section 2.7 thus provided an easily understandable picture of what was happening, i.e. one had a feel for the magnitudes of the eigenvalues and the various quantities involved. The only problem with that analysis was the justification of $\underline{g}$ and hence $R_z f_z$ being constant over one timestep. In this section we show that it is unnecessary to make this assumption and we develop a mathematically more exact (though physically less intuitive) set of solutions to the rate equations.

We consider the set of equations (2.7.3) which we write

$$\frac{\partial \underline{f}}{\partial t} = \underline{\underline{A}}\underline{f} + \underline{g}$$

and

$$f_{z+1} = 1 - f_z - f_{z-1} \qquad (2.8.1)$$

where now

$$\underline{f} = \begin{bmatrix} f_{z-1} \\ f_z \end{bmatrix} \quad \underline{\underline{A}} = n_e \begin{bmatrix} -S_{z-1} & +R_z \\ (S_{z-1}-R_{z+1}) & -(S_z+R_z+R_{z+1}) \end{bmatrix} \quad \underline{g} = n_e \begin{bmatrix} 0 \\ R_{z+1} \end{bmatrix} \qquad (2.8.2)$$

It should be noticed that the term $R_z f_z$ has been removed from $\underline{g}$ and reinserted into $\underline{\underline{A}}$. We observe that, in contrast to sections 2.4 and 2.6, instead of the eigenvalues of $\underline{\underline{A}}$ being the elements of its leading diagonal, the eigenvalues are now modified with the inclusion of the term R_z into the matrix.

However, since the determinant of a matrix ie equal to the product of its eigenvalues, i.e.

$$\text{Det } \underline{\underline{A}} = \prod_i \lambda_i \tag{2.8.3}$$

we have from (2.8.2)

$$S_{z-1}(S_z+R_z+R_{z+1}) - R_z(S_{z-1}-R_{z+1}) = \prod_i \lambda_i$$

or

$$S_{z-1}S_z + S_{z-1}R_{z+1} + R_zR_{z+1} = \prod_i \lambda_i \tag{2.8.4}$$

i.e. the product of the eigenvalues is positive always. The eigenvalues may be obtained from solving

$$\text{Det } (\underline{\underline{A}} - \lambda \underline{\underline{I}}) = 0 \tag{2.8.5}$$

which leads to the equation

$$\lambda^2 + \lambda(S_{z-1}+S_z+R_z+R_{z+1}) + \left[S_{z-1}(S_z+R_z+R_{z+1}) - R_z(S_{z-1}-R_{z+1})\right] = 0$$

and from the coefficient of λ in equation (2.8.6) we see that the sum of eigenvalues is negative and using (2.8.4) we are led to the conclusion that the eigenvalues are negative. To obtain these eigenvalues we must solve (2.8.6) which leads to

$$\lambda_{\pm} = \frac{(\lambda_1^o+\lambda_2^o) \pm \sqrt{(\lambda_1^o-\lambda_2^o)^2 + 4R_z(S_{z-1}-R_{z+1})}}{2} \tag{2.8.7}$$

where λ_1^o and λ_2^o are the diagonal elements of the matrix $\underline{\underline{A}}$. By putting R_z to zero in this expression one obtains the results of sections 2.4 and 2.6. Notice that since we have proved the eigenvalues negative definite, the discriminant of (2.8.7) must be greater than or equal to zero, i.e.

$$(\lambda_1^o-\lambda_2^o)^2 + 4R_z(S_{z-1}-R_{z+1}) \geq 0 \tag{2.8.8}$$

which one may find surprising since for low temperatures $R_{z+1} >> S_{z-1}$. Having found the eigenvalues through equation (2.8.7) we now proceed to calculate the eigenvectors of the matrix $\underline{\underline{A}}$ corresponding to these eigenvalues.

To find the eigenvectors we must solve

$$(\underline{\underline{A}} - \lambda \underline{\underline{I}})\ \underline{X} = 0 \qquad (2.8.9)$$

denoting the elements of $\underline{\underline{A}}$ by a_{11}, a_{12}, a_{21}, a_{22} equation (2.8.9) leads to coupled algebraeic equations

$$\begin{aligned} (a_{11}-\lambda)\ x_1 + a_{12}x_2 &= 0 \\ a_{21}x_1 + (a_{22}-\lambda)\ x_2 &= 0 \end{aligned} \qquad (2.8.10)$$

where x_1, x_2 are the components of the eigenvector $\underline{X}$. In direct analogy with the eigenvectors of (2.7.11), we wish only to solve for the elements x_2 of X_1 and x_1 of X_2, the other elements being identically equal to 1. Thus for $\lambda = \lambda_1$

$$\frac{x_2}{x_1} = -\frac{(a_{11} - \lambda_1)}{a_{12}} \quad \text{or} \quad \frac{-a_{21}}{(a_{22} - \lambda_1)} \qquad (2.8.11)$$

and for $\lambda = \lambda_2$

$$\frac{x_1}{x_2} = \frac{a_{12}}{(a_{11} - \lambda_2)} \quad \text{or} \quad \frac{-(a_{22} - \lambda_2)}{a_{21}} \qquad (2.8.12)$$

However, we must be extremely careful which of these formulae we use to evaluate the eigenvector components. When $a_{12} \to 0$ (i.e. $R_z \to 0$) $\lambda_1 \to a_{11}$ and $\lambda_2 \to a_{22}$ and we see that some of the quantities in (2.8.11) and (2.8.12) become indeterminate, which would computationally lead to grossly inaccurate results. Hence we choose for $\lambda = \lambda_1 = \lambda_+$

$$x_2 = -a_{21}/(a_{22} - \lambda_1) \qquad (2.8.13)$$

and for $\lambda = \lambda_2 = \lambda_-$

$$x_1 = -a_{12}/(a_{11} - \lambda_2) \qquad (2.8.14)$$

which in the limit of $a_{12} = 0$ leads to the eigenvectors of (2.7.11).

Written explicitly, the eigenvectors are given by

$$\text{for } \lambda = \lambda_1 \qquad \underline{X}_1 = \begin{bmatrix} 1 \\ \dfrac{S_{z-1}-R_{z+1}}{\lambda_1+S_z+R_z+R_{z+1}} \end{bmatrix}$$

$$\lambda = \lambda_2 \qquad \underline{X}_2 = \begin{bmatrix} \dfrac{+R_z}{\lambda_2+S_{z-1}} \\ 1 \end{bmatrix}$$

To obtain the initial value constants we take the solution to (2.8.1) at $t = 0$, i.e.

$$\underline{f}^{(0)} = -\underline{\underline{A}}^{-1}\underline{g} + \sum_{i=1}^{2} a_i \underline{X}_i \tag{2.8.16}$$

where $\underline{\underline{A}}^{-1}\underline{g} = \dfrac{1}{\text{Det } \underline{\underline{A}}} \cdot \begin{bmatrix} -(S_z+R_z+R_{z+1}) & -R_z \\ -(S_{z-1}-R_{z+1}) & -S_{z-1} \end{bmatrix} \begin{bmatrix} 0 \\ R_{z+1} \end{bmatrix}$

$$= \frac{-R_{z+1}}{\lambda_1' \lambda_2'} \begin{bmatrix} R_z \\ S_{z-1} \end{bmatrix} \tag{2.8.17}$$

from which it can be shown that

$$a_2 = \left\{ f_z^{(0)} - f_{z-1}^{(0)} x_2 + \frac{R_{z+1}}{\lambda_1' \lambda_2'} \left[R_z x_2 - S_{z-1} \right] \right\} \Big/ (1-x_1 x_2) \tag{2.8.18}$$

$$a_1 = f_{z-1}^{(0)} - \frac{R_{z+1} R_z}{\lambda_1' \lambda_2'} - a_2 x_1$$

where $x_2 = \dfrac{S_{z-1}-R_{z+1}}{\lambda_1'+S_z+R_z+R_{z+1}}$ and $x_1 = \dfrac{R_z}{\lambda_2'+S_{z-1}}$

To summarise, we note the advantages of the above analysis:-

1. The above formalism leads to a mathematically more exact set of solutions to the rate equations.
2. Although we now have to solve an equation to determine the eigenvalues, the programming of the above set of results is simpler than the results of sections 2.7 since there we had two separate cases to consider, i.e. $S_z > R_z$ and $S_z < R_z$, whereas now we have only one case.

2.9 An Alternative Description via Laplace Transform Theory

We now present an alternative description of a plasma undergoing ionisation and recombination in terms of Laplace transform theory, as opposed to the eigenvalue-eigenvector approach used in the previous sections. Again we will use the fact, pointed out in section 2.4, that we need consider only three adjacent ionisation fractions around the mean ionisation level. We rewrite the matrix rate equation of fig. 2.7 as

$$\frac{\partial \underline{f}}{\partial t} = (\underline{\underline{L}} + \varepsilon \underline{\underline{U}})\underline{f} \qquad (2.9.1)$$

where

$$\underline{f} = \begin{bmatrix} f_{z-1} \\ f_z \\ f_{z+1} \end{bmatrix} \quad \underline{\underline{L}} = n_e \begin{bmatrix} -S_{z-1} & 0 & 0 \\ +S_{z-1} & -(S_z+R_z) & 0 \\ 0 & +S_z & -R_{z+1} \end{bmatrix} \quad \underline{\underline{U}} = n_e \begin{bmatrix} 0 & +R_z & 0 \\ 0 & 0 & +R_{z+1} \\ 0 & 0 & 0 \end{bmatrix}$$

and ε is some ordering parameter. We now introduce the Laplace transform[5] of $\underline{f}$ defined by $\tilde{\underline{f}}$ where

$$\tilde{\underline{f}} = \int_0^\infty e^{-pt}\, \underline{f}\, dt \qquad (2.9.3)$$

Taking the Laplace transform of both sides of (2.9.1) gives

$$p\tilde{\underline{f}} - \underline{f}^{(0)} = (\underline{\underline{L}} + \varepsilon \underline{\underline{U}})\tilde{\underline{f}}$$

or

$$\tilde{\underline{f}} = (p\underline{\underline{I}} - \underline{\underline{L}} - \varepsilon \underline{\underline{U}})^{-1}\, \underline{f}^{(0)} \qquad (2.9.4)$$

where $\underline{f}^{(0)}$ is the initial value of the vector $\underline{f}$. From equation (2.9.4) we observe that we now have an algebraic equation for $\underline{f}$ and so to obtain $\underline{f}(t)$ we need only find the inverse transformation of the right hand side of (2.9.4).

The expression $\left[p\underline{\underline{I}} - \underline{\underline{L}} - \epsilon\underline{\underline{U}}\right]^{-1}$ can be expanded thus,

$$\left[p\underline{\underline{I}} - \underline{\underline{L}} - \epsilon\underline{\underline{U}}\right]^{-1} = \left[(p\underline{\underline{I}} - \underline{\underline{L}})(\underline{\underline{I}} - (p\underline{\underline{I}} - \underline{\underline{L}})^{-1}\epsilon\underline{\underline{U}})\right]^{-1} \qquad (2.9.5)$$

where ϵ will be dropped for clarity since it is just an ordering parameter. Remembering that $(\underline{\underline{A}}\ \underline{\underline{B}})^{-1} = \underline{\underline{B}}^{-1}\ \underline{\underline{A}}^{-1}$ we can express the right hand side of (2.9.5) as

$$(\underline{\underline{I}} - (p\underline{\underline{I}} - \underline{\underline{L}})^{-1}\ \underline{\underline{U}})^{-1}\ (p\underline{\underline{I}} - \underline{\underline{L}})^{-1} \qquad (2.9.6)$$

which can be expanded as, referring to (2.9.5)

$$(p\underline{\underline{I}}-\underline{\underline{L}}-\ \underline{\underline{U}})^{-1} = (p\underline{\underline{I}}-\underline{\underline{L}})^{-1} + (p\underline{\underline{I}}-\underline{\underline{L}})^{-1}\ \underline{\underline{U}}(p\underline{\underline{I}}-\underline{\underline{L}})^{-1} + (p\underline{\underline{I}}-\underline{\underline{L}})^{-1}\ \underline{\underline{U}}(p\underline{\underline{I}}-\underline{\underline{L}})^{-1}\ \underline{\underline{U}}(p\underline{\underline{I}}-\underline{\underline{L}})^{-1} + \ldots. \qquad (2.9.7)$$

provided that the norm of $(p\underline{\underline{I}}-\underline{\underline{L}})^{-1}\ \underline{\underline{U}}$ is less than one, i.e.

$$\left\| (p\underline{\underline{I}}-\underline{\underline{L}})^{-1}\ \underline{\underline{U}} \right\| < 1 \qquad (2.9.8)$$

Thus from equation (2.9.4) we can write

$$\tilde{\underline{f}} = (p\underline{\underline{I}}-\underline{\underline{L}})^{-1}\ \underline{f}^{(0)} + (p\underline{\underline{I}}-\underline{\underline{L}})^{-1}\ \underline{\underline{U}}\ (p\underline{\underline{I}}-\underline{\underline{L}})^{-1}\ \underline{f}^{(0)} + \ldots. \qquad (2.9.9)$$

which represents a perturbation expansion for $\tilde{\underline{f}}$ and we can include as many terms as may be necessary.[27] One sees that the zeroth order term contains no $\underline{\underline{U}}$ and we should expect to obtain the same result of section 2.5 if we put the R's in the matrix $\underline{\underline{U}}$ to zero. Consider now, the zeroth order term, i.e.

$$\tilde{\underline{f}} = (p\underline{\underline{I}} - \underline{\underline{L}})^{-1}\ \underline{f}^{(0)} \qquad (2.9.10)$$

the matrix $(p\underline{\underline{I}}-\underline{\underline{L}})^{-1}$ is shown in Appendix 7 to be

$$(p\underline{\underline{I}}-\underline{\underline{L}})^{-1} = \begin{bmatrix} \frac{1}{p+S_{z-1}} & 0 & 0 \\ \frac{S_{z-1}}{(p+S_{z-1})(p+S_z+R_z)} & \frac{1}{(p+S_z+R_z)} & 0 \\ \frac{S_{z-1}S_z}{(p+S_{z-1})(p+S_z+R_z)(p+R_{z+1})} & \frac{S_z}{(p+S_z+R_z)(p+R_{z+1})} & \frac{1}{p+R_{z+1}} \end{bmatrix} \qquad (2.9.11)$$

where the n_e has been dropped for clarity.

Now substituting (2.9.11) into equation (2.9.10) and taking the inverse Laplace transform element by element we obtain (see Appendix 7 on partial fractions)

$$\underline{f}(t) = \begin{bmatrix} e^{-n_e S_{z-1} t} & 0 & 0 \\ \dfrac{S_{z-1}\left(e^{-n_e(S_z+R_z)t} - e^{-n_e S_{z-1} t}\right)}{S_{z-1}-S_z-R_z} & e^{-n_e(S_z+R_z)t} & 0 \\ \alpha & \dfrac{S_z\left(e^{-n_e(S_z+R_z)t} - e^{-n_e S_{z-1} t}\right)}{(S_z+R_z-R_{z+1})} & e^{-n_e R_{z+1} t} \end{bmatrix} \underline{f}^{(0)} \qquad (2.9.12)$$

where

$$\alpha = \frac{S_{z-1}S_z}{(S_{z-1}-S_z-R_z)(S_{z-1}-R_{z+1})} e^{-n_e S_{z-1} t} + \frac{S_{z-1}S_z}{(S_z+R_z-S_{z-1})(S_z+R_z+R_{z+1})} e^{-n_e(S_z+R_z)t}$$

$$+ \frac{S_{z-1}S_z}{(R_{z+1}-S_{z-1})(R_{z+1}-S_z-R_z)} e^{-n_e R_{z+1} t} \qquad (2.9.13)$$

and the n_e has been reinserted into the exponentials. Now taking the expressions (2.7.10) and putting R_{z+1} to zero (in the eigenvalue approach, we are solving only for f_{z-1} and f_z) we obtain

$$\underline{f}(t) = \begin{bmatrix} 1 \\ \dfrac{S_{z-1}}{S_z+R_z-S_{z-1}} \end{bmatrix} e^{-n_e S_{z-1} t} + \frac{S_{z-1}}{S_z+E_z-S_{z-1}} \begin{bmatrix} 0 \\ 1 \end{bmatrix} e^{-n_e(S_z+R_z)t} \qquad (2.9.14)$$

since $\underline{\underline{A}}^{-1}\underline{g} = \underline{0}$ in this case.

Now taking the case where $\underline{f}^{(0)} = [1, 0, 0]$ we can compare (2.9.12) and (2.9.14)over the initial timestep and we obtain identical results as expected.

Although the eigenvalue-eigenvector and perturbation expansion methods offer different approaches, it will be seen from the previous work that the latter approach is less amenable for implementation into a computer program.

2.10 Timescale Necessary for Steady-State

In this section, a simple prescription will be given to enable one to determine whether or not steady state conditions have been reached in the plasma. The assumptions on which the prescription is based are such that the results are only valid to within an order of magnitude.

From the simple Bohr theory of the atom, we have that the energy of an electron, whose principal quantum number is n, in a hydrogenic system is given by [28]

$$E_n = \frac{2\pi^2 \mu e^4}{h^2} \frac{Z^2}{n^2} \qquad (2.10.1)$$

where Z is the nuclear charge, h is Planck's constant, e is the electronic charge and μ is the reduced mass of the system given by

$$\mu = \frac{mM}{m+M} \qquad (2.10.2)$$

where m is the electronic mass and M is the nuclear mass. We will now assume that equation (2.10.1) can be applied to many electron systems such that the outer electron is in a ground state with n = 1

Thus equation (2.10.1) reduces to

$$E = 13.6\ Z^2 \text{ (eV)} \qquad (2.10.3)$$

and we now interpret Z as being the charge as seen by the outer electron and E as its binding energy, which is equal to the electron temperature of the plasma, i.e.

$$T_e = 13.6\ Z^2 \text{ (eV)} \qquad (2.10.4)$$

This now provides a simple relationship between the temperature and the mean ionisation level in a hydrogenic system. Thus knowing the electron temperature we can find an approximate steady-state value for the mean ionisation level, i.e.

$$\langle Z \rangle \sim \left(\frac{T_e}{13.6}\right)^{\frac{1}{2}} \tag{2.10.5}$$

Now look at the solution (2.4.1) to the rate equations, i.e.

$$\underline{f} = \sum_{i=0}^{Z-1} a_i \underline{X}_i e^{\lambda_i t} \tag{2.10.6}$$

and from this, we can find the equation for the j^{th} ionisation fraction, i.e.

$$f_j = \sum_{i=0}^{j} a_i X_i(j) e^{\lambda_i t} \tag{2.10.7}$$

where $X_i(j)$ denotes the j^{th} element of the i^{th} eigenvector and j is obtained from the nearest integer to $\langle Z \rangle$ in (2.10.5), i.e.

$$j = \mathrm{INT}(\langle Z \rangle) \tag{2.10.8}$$

Notice that the eigenvalues, eigenvectors and initial values constants are evaluated at the temperature used in equation (2.10.5). By differentiating equation (2.10.7) with respect of time and equating to zero, we can find the time at which f_j is at a maximum. But we also know from (2.10.5) that f_j being maximised corresponds approximately to steady state conditions being reached, and so the time at which f_j is a maximum is also approximately the time it takes to achieve steady state conditions. Denoting this time by τ_{ST} we have

$$\frac{\partial f_j}{\partial t} = \sum_{i=0}^{j} a_i \lambda_i X_i(j) e^{\lambda_i \tau_{ST}} = 0 \tag{2.10.9}$$

It is now assumed that, due to the rapid variation of the exponential terms in (2.10.9), we need only consider the last two terms in the summation, i.e.

$$a_{j-1}\lambda_{j-1}X_{j-1}(j)e^{\lambda_{j-1}\tau_{ST}} + a_j\lambda_j X_j(j)e^{\lambda_j\tau_{ST}} = 0 \qquad (2.10.10)$$

and this can now be solved for τ_{ST} by taking the logarithms of both terms to obtain

$$\tau_{ST} = \frac{1}{(\lambda_{j-1}-\lambda_j)} \ln\left\{\frac{-a_j\lambda_j X_j(j)}{a_{j-1}\lambda_{j-1}X_{j-1}(j)}\right\} \qquad (2.10.11)$$

Equation (2.10.11) can be further simplified by noting that

$$X_j(j) = 1, \qquad S_{j-1}(j) = \frac{\lambda_{j-2}}{\lambda_{j-1}-\lambda_{j-2}}$$

where $a_j/a_{j-1} \sim 1$ always (see appendix 8). Hence equation (2.9.11) becomes

$$\tau_{ST} = \frac{1}{(\lambda_{j-1}-\lambda_j)} \ln\left\{\frac{-\lambda_j(\lambda_{j-1}-\lambda_{j-2})}{\lambda_{j-1}\lambda_{j-2}}\right\} \qquad (2.10.12)$$

Notice that the time τ_{ST} will be considerably shorter than the actual time to reach steady state since, in order to use expression (2.10.12) we have used a constant temperature and density. Thus if we impose some high temperature and high electron density on a plasma, then the burn through time will be considerably faster than in the case where temperature and density increased linearly (say). Notice that instead of using (2.10.5) to obtain an estimate of <z> knowing T, we use the results shown in fig. 2.10.1. These results are based on a steady state coronal equilibrium and provide a much more accurate evaluation of the mean ionisation level.[21]

To summarise, we list the procedure to obtain τ_{ST}:-

1. Taking some temperature of interest, apply fig. 2.10.1 to find the mean ionisation level at that temperature. This assumes, of course, we have a steady state coronal equilibrium.
2. Knowing $<z>$, we then say that the plasma consists mostly of j-times ionised material, i.e. $f_j \sim 1$ where $j = \text{INT}(<z>)$.
3. Knowing j we can then evaluate the eigenvalues in (2.10.12) from knowing the temperature and density. For most cases we can neglect any recombination effects (for laser produced plasmas) and say that $\lambda_{j-1} \sim -n_e S_{j-1}(T_e)$.

example:- We apply the above method to a plasma whose temperature is 50 eV and whose density is 10^{21} cm^{-3}.

1. Using fig. 2.10.1 $<z>$ is found to be ~ 4
2. Using (2.10.8) j is evaluated as 4
3. For these values of temperature and density we have $\lambda_j = 2.179 \times 10^7$, $\lambda_{j-1} = -7.629 \times 10^{11}$ and $\lambda_{j-2} = 2.88 \times 10^{12}$ and from (2.10.12) we evaluate τ_{ST} to be

$$\tau_{ST} \sim 1.4 \times 10^{-11} \text{ s} \qquad (2.10.13)$$

which agrees well with fig. 2.4.2.

2.11 The Incorporation of Advection

In the previous sections we developed a model for solving the rate equations provided the term $(\underline{v}.\underline{\nabla})f$, representing advection, could be neglected. The model was based on finding the eigenvalues, eigenvectors and initial value constants for a given matrix of rate coefficients.

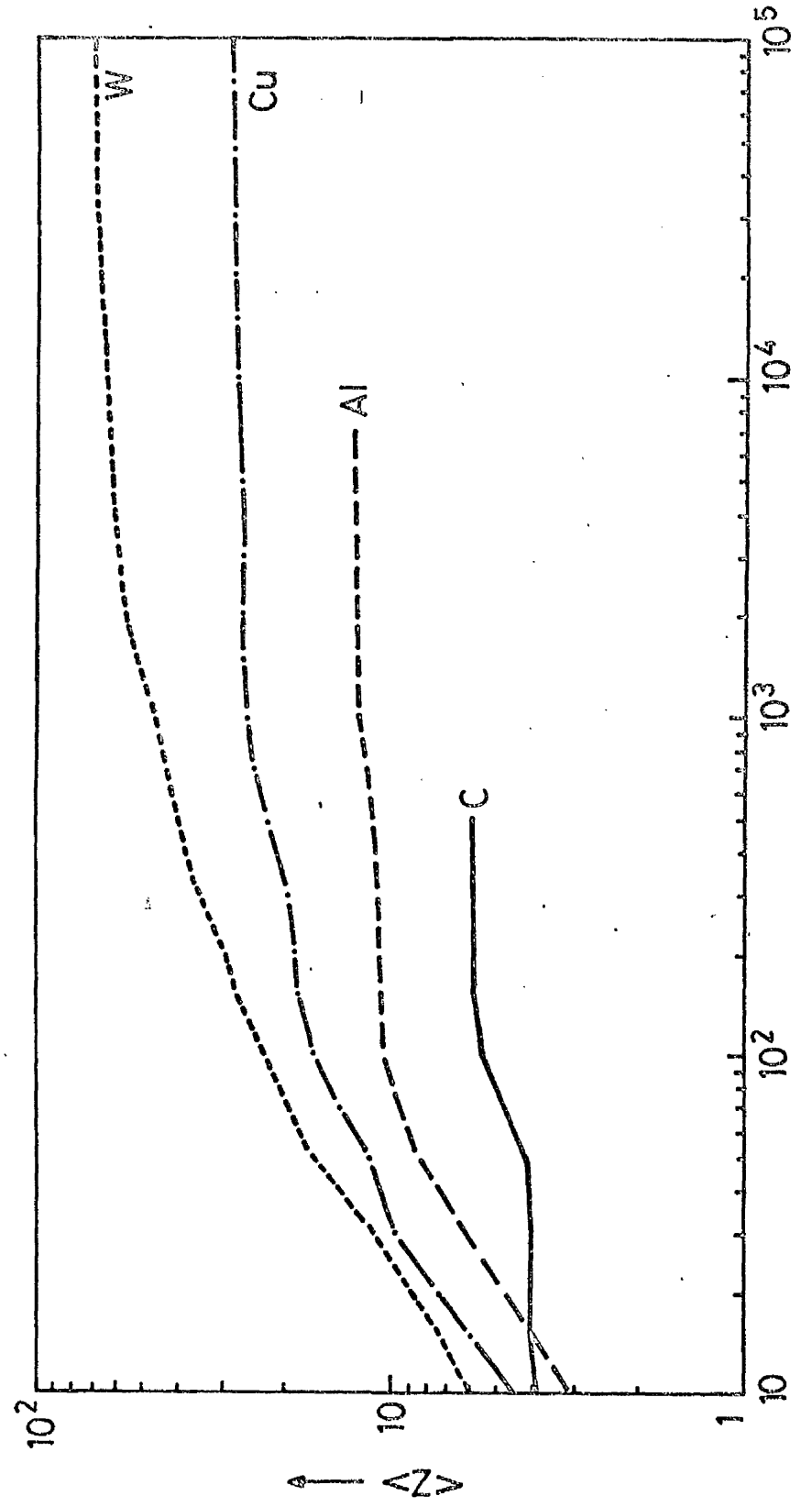

Fig. 2.10.1 The mean ionisation level as a function of temperature given by a corona model

Is it possible that using this formalism we can include the advection term without any loss of efficiency of that model?

We rewrite the system of rate equations (2.2.1) as

$$\frac{\partial \underset{\sim}{f}}{\partial t} + (\underline{v}.\nabla)\underset{\sim}{f} = \underset{\approx}{A}\underset{\sim}{f} \qquad (2.11.1)$$

where, in this notation, $\underset{\sim}{f}$ represents a mathematical column vector with components f_0, f_1, ... f_μ, ... f_Z, $\underline{v}$ is the physical velocity vector and $\underset{\approx}{A}$ denotes a Z x Z square matrix ((2.2.1) is a set of Z+1 equations but we can ignore the equation for the last ion stage since $\sum_Z f_Z = 1$).

We now ask what justification there was in dropping the advection term $\underline{v}.\nabla f$. Strictly speaking we can only do this if we are solving the rate equations in Lagrangian frame of reference, i.e. in a mesh that is moving with the fluid. In that situation, the terms $\partial\underset{\sim}{f}/\partial t$ and $\underline{v}.\nabla\underset{\sim}{f}$ merge into the one term which we will denote by $D\underset{\sim}{f}/Dt$ and we can rewrite (2.11.1) in the Lagrangian formalism,[29] i.e.

$$\frac{D\underset{\sim}{f}}{Dt} = \underset{\approx}{A}\underset{\sim}{f}$$

However, most 'real' codes in more than one dimension are 'Eularian', i.e. the equations are solved on a mesh which is fixed in space, and under this formalism the terms $\partial\underset{\sim}{f}/\partial t$ and $\underline{v}.\nabla\underset{\sim}{f}$ do not merge but remain separate. Also we cannot evaluate the term $\underline{v}.\nabla\underset{\sim}{f}$ directly, since the ionisation stage vector $\underset{\sim}{f}$ is not stored explicitly (cf. Chapter 4). However we can put the term into a more manageable form by making the following observations. Remembering that at any one time we are following only three ionisation fractions evolving in time, it will be shown in Chapter 4 that simple expressions can be obtained for the three fractions in terms of $\langle z \rangle$ and $\langle z^2 \rangle$, the mean ionisational level and mean square ionisational level respectively.

We will denote the three ionisation fractions by f_{j-1}, f_j, f_{j+1} such that

$$f_{j-1} = 0.5j(j+1) - 0.5(2j+1)\langle z\rangle + 0.5\langle z^2\rangle$$

$$f_j = -(j+1)(j-1) + 2j\langle z\rangle - \langle z^2\rangle$$

$$f_{j+1} = 0.5j(j-1) - 0.5(2j-1) + 0.5\langle z^2\rangle$$

$$\text{where } j = \text{INT}\langle z\rangle \qquad (2.11.3)$$

Now taking the gradient of both sides and then the scalar product with $\underline{v}$ gives

$$\underline{v}.\underline{\nabla} f_{j-1} = -0.5(2j+1)\underline{v}.\underline{\nabla}\langle z\rangle + 0.5\,\underline{v}.\underline{\nabla}\langle z^2\rangle$$

$$\underline{v}.\underline{\nabla} f_j = 2j\underline{v}.\underline{\nabla}\langle z\rangle - \underline{v}.\underline{\nabla}\langle z^2\rangle$$

$$\underline{v}.\underline{\nabla} f_{j+1} = -0.5(2j-1)\underline{v}.\underline{\nabla}\langle z\rangle + 0.5\underline{v}.\underline{\nabla}\langle z^2\rangle \qquad (2.11.4)$$

thus we have converted the expression containing a differential operator on $\underset{\sim}{f}$ to an expression containing a differential operator on $\langle z\rangle$ and $\langle z^2\rangle$. Since the terms $\langle z\rangle$ and $\langle z^2\rangle$ are stored explicitly then the right hand side of (2.11.4) can be evaluated quite simply. Denoting the term $\underline{v}.\underline{\nabla}\underset{\sim}{f}$, whose components are shown in (2.11.6), by $\underset{\sim}{h}$ we can now write equation (2.11.1) as

$$\frac{\partial \underset{\sim}{f}}{\partial t} = \underline{\underline{A}}\,\underset{\sim}{f} - \underset{\sim}{h} \qquad (2.11.5)$$

where $\underset{\sim}{f} = \begin{bmatrix} f_{j-1} \\ f_j \\ f_{j+1} \end{bmatrix}$ $\quad \underline{\underline{A}} = \begin{bmatrix} -n_e S_{j-1} & +n_e R_j & \\ +n_e S_{j-1} & -n_e(S_j+R_j) & +n_e R_{j+1} \\ 0 & +n_e S_j & -n_e R_{j+1} \end{bmatrix}$

and we can solve (2.11.5) in the same manner as we solve equation (2.7.4) or by some split step procedure.

CHAPTER 3

The Macroscopic Variables

Once the ionisation fractions present in the plasma are known, the macroscopic variables such as pressure, internal energy, radiation loss etc., may be evaluated. This chapter deals with how these quantities are obtained for a one component plasma.

3.1 Equation of State for a one component plasma

Having obtained the ionisation fractions present in the plasma, as described in chapter 2, it is now possible to evaluate such quantities as the plasma (kinetic) pressure, the internal (thermal plus ionisation) energy, the radiation rates etc. Thus, in this section, we assume the three ionisation fractions known, and proceed to calculate the macroscopic variables described above for a one component (e.g. carbon) plasma. By definition, the mean ionisation level $\langle z \rangle$ is given by

$$\langle z \rangle = \sum_{z=1}^{z_{max}} z f_z \qquad (3.1.1)$$

where f_z is the fractional population density of the z-times ionised material, and z_{max} is the atomic number of the material. Since we consider only three ionisation fractions, this definition reduces to

$$\langle z \rangle = \sum_{z=\alpha-1}^{\alpha+1} z f_z \qquad (3.1.2)$$

where α = Int $\langle z \rangle$ and $\langle z \rangle$ is the mean ionisation level at the previous timestep. Similarly, knowing the population distribution, the mean square ionisation level $\langle z^2 \rangle$ is evaluated as

$$\langle z^2 \rangle = \sum_{z=\alpha-1}^{\alpha+1} z^2 f_z \qquad (3.1.3)$$

Now with this knowledge of $\langle z \rangle$ and $\langle z^2 \rangle$, and using the independent variables n_i, T_i and T_e (the ion density and the ion and electron temperatures respectively) the pressure and internal energy are derived as follows. The electron density is given by

$$n_e = \langle z \rangle n_i \qquad (3.1.4)$$

and the plasma pressure (i.e. ion plus electron kinetic pressures) is given by

$$p = n_i kT_i + n_e kT_e$$

which can be rewritten using (3.1.4) as

$$p = \left(1 + \langle z \rangle \frac{T_e}{T_i}\right) n_i kT_i \qquad (3.1.5)$$

where k is Boltzmann's constant. In the case where $T_e = T_i$, the coefficient of $\langle z \rangle$ i.e. $\frac{T_e}{T_i}$ in expression (3.1.5), is simply put to 1. Similarly, the thermal energy E_{th} is given by

$$E_{th} = \frac{3}{2} n_i kT_i + \frac{3}{2} n_e kT_e$$

which again can be simplified using (3.1.4) to

$$E_{th} = \frac{3}{2} \left(1 + \langle z \rangle \frac{T_e}{T_i}\right) n_i kT_i \qquad (3.1.6)$$

It is important, at this point, to realise that in a partially ionised plasma, the ionisation energy forms an important contribution to the total internal energy. This ionisation energy is evaluated as

$$E_I = n_i \sum_{z=\alpha-1}^{\alpha+1} E_z f_z = \langle E_z \rangle n_i \qquad (3.1.7)$$

where E_z is the energy required to ionise an atom from the neutral state to the z-times ionised state, thus

$$E_z = \sum_{z=0}^{z-1} X_z \qquad (3.1.8)$$

where X_z is the ionisation potential for state z (i.e. the energy required to ionise from state z to z+1). The total internal energy (thermal plus ionisation) of the plasma is now obtained by adding (3.1.6) to (3.1.7) thus

$$E_{tot} = \left[\frac{3}{2}\left(1 + \langle z \rangle \frac{T_e}{T_i}\right) + \frac{\langle E_z \rangle}{kT_i}\right] n_i kT_i \qquad (3.1.9)$$

where E_{tot} represents the total energy of the plasma, as a function of the independent variables n_i, T_i and T_e and the dependent variables $\langle z \rangle$ and $\langle E_z \rangle$. Equations (3.1.4) through to (3.1.9) make up the 'equation' of state for a partially ionised one component plasma. In the foregoing analysis we have allowed for two separate temperatures as is usual in laser plasma interactions, but this can be removed by simply putting $\frac{T_e}{T_i} = 1$ in equations (3.1.5) and (3.1.9).

3.2 The radiation loss from a one component plasma

In an ionised plasma, various radiation processes are present and they constitute an important part in the overall energy balance of the system. The radiation processes we consider in this section are Bremsstrahlung (free-free) radiation, recombination (free-bound) radiation and line (bound-bound) radiation, and the formulae used for these quantities are those developed by previous authors.[30]

Bremsstrahlung radiation:

For photon energies of the order kT, we can obtain an order of magnitude estimate for the power density of Bremsstrahlung radiation P_{ff} due to elastic electron collisions with ions of density n_z and charge ze (where e is the electronic charge) using

$$P_{ff} \approx \frac{64}{3}\left(\frac{\pi}{3}\right)^{\frac{1}{2}} (\beta a_o)^3 \omega_H E_H \left(\frac{kT_e}{E_H}\right)^{\frac{1}{2}} n_e \sum_{z=\alpha-1}^{\alpha+1} z^2 n_z \qquad (3.2.1)$$

where a_o is the Bohr radius, $\omega_H \approx E_H/\hbar$, $\hbar = h/2\pi$ where h is Planck's constant, and E_H is the ionisation energy of hydrogen. Now since $n_e = \langle z \rangle n_i$ and $\sum_z z^2 n_z = \langle z^2 \rangle n_i$ we can write (3.2.1) as

$$P_{ff} \approx \frac{64}{3}\left(\frac{\pi}{3}\right)^{\frac{1}{2}} (\beta a_o)^3 \omega_H E_H \left(\frac{kT_e}{E_H}\right)^{\frac{1}{2}} n_i^2 \langle z \rangle \langle z^2 \rangle \qquad (3.2.2)$$

Recombination Radiation:

To obtain an order of magnitude estimate of the recombination radiation power density, we use the expression

$$P_{fb} \approx \frac{128}{3}\left(\frac{\pi}{3}\right)^{\frac{1}{2}} (\alpha a_o)^3\, \omega_H\, E_H \left(\frac{E_H}{kT_e}\right)^{\frac{1}{2}} n_e \sum_n \sum_z \frac{z^4}{n} n_z \qquad (3.2.3)$$

where n is the quantum number of the level into which the electron is recombining. Now since $\sum_n 1/n^3$ is approximately $\frac{1}{2}n_{min}^2$ where n_{min} is the effective ground state of the atom or ion resulting from the recombination, i.e.

$$n_{min} \approx \left(\frac{z^2\, E_H}{X_{z-1}}\right)^{\frac{1}{2}} \qquad (3.2.4)$$

the above expression for P_{fb} simplifies to

$$P_{fb} \approx \frac{64}{3}\left(\frac{\pi}{3}\right)^{\frac{1}{2}} (\alpha a_o)^3\, \omega_H\, E_H \left(\frac{kT_e}{E_H}\right)^{\frac{1}{2}} n_e \sum_{z=\alpha-1}^{\alpha+1} z^2 \left(\frac{X_{z-1}}{kT_e}\right) n_z \qquad (3.2.5)$$

or

$$P_{fb} \approx \frac{64}{3}\left(\frac{\pi}{3}\right)^{\frac{1}{2}} (\alpha a_o)^3\, \omega_H\, E_H \left(\frac{kT_e}{E_H}\right)^{\frac{1}{2}} \langle z \rangle \left\langle \frac{z^2 X_{z-1}}{kT_e} \right\rangle n_i^2 \qquad (3.2.6)$$

It should be noted that by comparing (3.2.2) with (3.2.6) we see that

$$\frac{P_{fb}}{P_{ff}} \approx \frac{X_{z-1}}{kT_e} \qquad (3.2.7)$$

for a given ion stage z, and the number can be as large as 10, causing recombination radiation to dominate. Only when the temperature is higher than X_{z-1}/k do free-free transitions dominate.

Line Radiation:

The power density from line radiation is estimated from

$$P_L \approx 8\pi^{\frac{1}{2}} \beta a_o^2 \, c \, E_H \left(\frac{E_H}{kT_e}\right)^{\frac{1}{2}} n_e \sum_{z=\alpha-1}^{\alpha+1} n_z^g \sum_n f_{n1}^z \exp\left(\frac{-E_{n1}^z}{kT_e}\right) \qquad (3.2.8)$$

where c is the speed of light, n_z^g is the ground state population density of ions of charge z, f_{n1}^z is the oscillator strength for a ground state transition to level n with associated energy difference E_n^z. Under the assumption that most of the radiation occurs in the resonance line, we can omit the summation over the other excited states, accounting for them by putting $f_{21}^z \, n_z^g \approx 0.5 \, n_z$, thus

$$P_L \approx 4\pi^{\frac{1}{2}} \alpha a_o \, c \, E_H \left(\frac{E_H}{kT_e}\right)^{\frac{1}{2}} n_i \langle z \rangle \left\langle \exp\left(\frac{-E_{21}^z}{kT_e}\right) \right\rangle \qquad (3.2.9)$$

The value of E_{21}^z (the 1 refers to the ground state with quantum number n) may be found in tables under the 'most important transition'. Alternatively, it may be estimated from Bohr theory, i.e.

$$E_{21}^z = (\beta z)^2 \frac{m_e c^2}{2} \left[\frac{1}{N^2} - \frac{1}{(N+1)^2}\right] \qquad (3.2.10)$$

where $m_e c^2$ is the electron rest energy.

It should be noted that for ions with one or more bound electrons, line radiation dominates continuum (Bremsstrahlung plus recombination) radiation and so a more accurate evaluation of continuum radiation than the order of magnitude estimates provided by (3.2.2) and (3.2.6) is unnecessary. When there are no bound electrons, i.e. completely stripped ions present, there is no line radiation emitted and equations (3.2.2) and (3.2.6) are almost exact when one includes the appropriate gaunt factors. The total continuum radiation power density is then given by

$$P_{cont} = P_{ff} + P_{fb} \tag{3.2.11}$$

and substituting expressions (3.2.2) and (3.2.6) using $X_{z-1} = z^2 E_H$ we have, neglecting recombination into excited states,

$$P_{cont} \approx \frac{64}{3}\left(\frac{\pi}{3}\right)^{\frac{1}{2}} (\alpha a_o)^3\, \omega_H E_H \left(\frac{kT_e}{E_H}\right)^{\frac{1}{2}} n_e \sum_{z=\alpha-1}^{\alpha+1} z^2 \left(g_{ff}^2 + \frac{2z^2 E_H}{kT_e} g_{fb}^2\right) n_z$$

or

$$P_{cont} \approx \frac{64}{3}\left(\frac{\pi}{3}\right)^{\frac{1}{2}} (\alpha a_o)^3\, \omega_H E_H \left(\frac{kT_e}{E_H}\right)^{\frac{1}{2}} n_i^2 \langle z\rangle \langle z^2\rangle \left(g_{ff}^2 + \frac{2z^2 E_H}{kT_e} g_{fb}^2\right)$$

where the g_{ff}^z and g_{fb}^z are the averaged free-free and free-bound factors for ions of charge z.

The radiation rates described previously must have an upper limit, namely the black body limit. Thus, whenever the radiation rates exceed the black body radiation rate (as can easily happen in a low temperature high density solid target) we put the radiation rate equal to the black-body rate. This rate is given by the Stefan-Boltzmann law

$$P_B = aT^4 \tag{3.2.14}$$

where $a = 5.67 \times 10^{-8}$ watt/m^2K^4 is the Stefan Boltzmann constant.

It may also be of interest to know the frequency distribution of the energy radiation. This can, for example, tell us how much energy is being radiated in the X- and UV-regimes. The frequency distribution of the energy radiated (continuum radiation) $S(\nu)$ varies as[30]

$$S(\nu)d\nu \simeq n_i^2 \langle z\rangle \left(\langle z^2\rangle \frac{1}{T_e^{\frac{1}{2}}} C_B + \frac{1}{T_e^{3/2}} C_R e^{X_z/kT_e}\right) e^{-h\nu/kT_e}\, d\nu \tag{3.2.15}$$

where C_B and C_R are constants. Defining now a radiation temperature by

$$T_r = h\nu \tag{3.2.16}$$

we can replace (3.2.15) by

$$S(T_r)\, dT_r = P_c \frac{1}{T_e} e^{-T_r/T_e} dT_r \qquad (3.2.17)$$

from which we can construct the spectral energy distribution as a function of the radiation temperature

$$E(T_r) = \int_{t_o}^{} \int_{z_o}^{} \int_{R_o}^{} S(T_r > T_m)\, 2\pi r\, dr\, dz\, dt \qquad (3.2.18)$$

where $T_m = h\omega_p$, $\omega_p^2 = \frac{n_e e^2}{\epsilon_o m_e}$

A summary of the solution to the rate equations, evaluation of the macroscopic parameters and radiation rates is given in fig. 3.2.1.

Time-dependent ionisation and recombination

State of plasma described by ionization stage vector:

$$\underline{f} = (f_o, f_1, f_2, \ldots\ldots f_Z)$$

f_j is the relative population density of the j times ionized stage:

$$\sum_{j=0}^{Z} f_j = 1.$$

Time-dependence : $\frac{\partial \underline{f}}{\partial t} = \underline{\underline{A}} \cdot \underline{f}$ (No hydrodynamics)

$\underline{\underline{A}}$ contains coefficients for ionization and recombination rates.

Solution: $\underline{f} = \sum_{i=0}^{Z-1} a_i \underline{X}_i e^{\lambda_i t}$, $0 \leq t \leq \delta t$ ($\underline{\underline{A}}$ constant)

MHD coefficients: $\langle z \rangle = \sum_{j=0}^{Z} j f_j$

$$\langle z^2 \rangle = \sum_{j=0}^{Z} j^2 f_j$$

Plasma Pressure: $P = (1 + \langle z \rangle) n_i k T_e$

Internal Energy: $E = \frac{3}{2} (1 + \langle z \rangle) n_i k T_e + n_i E_z$

Ionisation Energy: $E_z = \sum_{j=0}^{Z-1} X_j$

Line Radiation: $P_L \simeq \frac{n_i^2 \langle z \rangle}{T_e^{\frac{1}{2}}} \langle \exp(-E_{N1}^z / kT_e) \rangle$

Continuum Radiation: $P_c \simeq n_i^2 \langle z \rangle T_e^{\frac{1}{2}} \left(\langle z^2 \rangle + \left\langle \frac{z^2 \chi_{z-1}}{kT_e} \right\rangle \right)$

Frequency Distribution: $S(\nu)\, d\nu \simeq n_i^2 \langle z \rangle \left(\frac{\langle z^2 \rangle}{T_e^{\frac{1}{2}}} C_B + \frac{e^{\chi_z / kT_e}}{T_e^{3/2}} C_R \right) e^{-h\nu/kT_e} \, d\nu$

Fig. 3.2.1 A summary of the atomic physics model

CHAPTER 4

The Computational Details

The questions of computational stability and accuracy are dealt with in this chapter. The method of storing the ionisation stage vector is discussed also, together with the running times and storage requirements of the computer program.

4.1 The Accuracy of the Algorithm

In computational work, when a differential equation is replaced by a difference equation, the question arises as to how accurate this difference equation is to the original differential equation.[1,2] In this work difference equations are not used to represent the true equation, instead we use locally analytic solutions as described in Chapter 2 but the accuracy of this process can still be examined.

The exact differential equation representing the system is, as shown in Chapter 2,

$$\frac{\partial \underline{f}}{\partial t} = \underline{\underline{A}}\underline{f} \tag{4.1.1}$$

where the quantities have been defined previously. It was also shown that the solution to (4.1.1) is

$$\underline{f} = \sum_i a_i \underline{X}_i e^{\lambda_i t} \tag{4.1.2}$$

again where all the quantities have been defined. Although (4.1.2) is the solution as used in this work, we can formally define a solution to (4.1.1) given by

$$\underline{f} = e^{\underline{\underline{A}}t}\,\underline{f}^{(0)} \tag{4.1.3}$$

in direct analogy to the solution $f = f_o e^{\alpha t}$ of the simple equation

$$\frac{\partial f}{\partial t} = \alpha f \tag{4.1.3}$$

The quantity $e^{\underline{\underline{A}}t}$ used in equation (4.1.3) is defined as

$$e^{\underline{\underline{A}}t} \equiv \underline{\underline{I}} + \underline{\underline{A}}t + \frac{(\underline{\underline{A}}t)^2}{2} + \cdots \tag{4.1.4}$$

and using this definition one can clearly see that equation (4.1.3) is the solution to (4.1.1). Using this solution we can now carry out the accuracy analysis quite simply.

Rewriting the solution to the rate equation (4.1.1) indicating explicitly at what time levels the various quantities are known (4.1.3) becomes

$$\underline{f}^{n} = e^{\underline{\underline{A}}^{n-1}\Delta t}\,\underline{f}^{n-1} \tag{4.1.5}$$

where $\underline{f}^{n}$ indicates the value of $\underline{f}$ at time level n, $\underline{\underline{A}}^{n-1}$ indicates the matrix of rate coefficients which have been evaluated at level n-1 and Δt represents the timestep from level n-1 to level n. $\underline{f}^{n}$ and $e^{\underline{\underline{A}}^{n-1}\Delta t}$ can be expanded thus

$$\underline{f}^{n} = \underline{f}^{n-1} + \Delta t \left.\frac{\partial \underline{f}}{\partial t}\right|^{n-1} + \frac{\Delta t^2}{2} \left.\frac{\partial^2 \underline{f}}{\partial t^2}\right|^{n-1} + \ldots\ldots \tag{4.1.6}$$

and

$$e^{\underline{\underline{A}}^{n-1}\Delta t} \equiv \underline{\underline{I}} + \underline{\underline{A}}^{n-1}\Delta t + \tfrac{1}{2}(\underline{\underline{A}}^{n-1}\Delta t)^2 + \ldots\ldots \tag{4.1.7}$$

Using (4.1.6) and (4.1.7) we have

$$\underline{f}^{n} - e^{\underline{\underline{A}}^{n-1}\Delta t}\,\underline{f}^{n-1} = \left(\underline{f}^{n-1} + \Delta t \left.\frac{\partial \underline{f}}{\partial t}\right|^{n-1} + \frac{\Delta t^2}{2}\frac{\partial^2 \underline{f}}{\partial t^2} + \ldots\right) - \underline{f}^{n-1}\left(\underline{\underline{I}} + \underline{\underline{A}}^{n-1}\Delta t + \tfrac{1}{2}(\underline{\underline{A}}^{n-1}\Delta t)^2 + \ldots\right) \tag{4.1.8}$$

which can be simplified to

$$\underline{f}^{n} - e^{\underline{\underline{A}}^{n-1}\Delta t}\,\underline{f}^{n-1} = \Delta t\left(\frac{\partial \underline{f}}{\partial t} - \underline{\underline{A}}\underline{f}\right)^{n-1} + \frac{\Delta t^2}{2}\left(\frac{\partial^2 \underline{f}}{\partial t} - \underline{\underline{A}}^2\underline{f}\right)^{n-1} + \ldots \tag{4.1.9}$$

or

$$\left(\frac{\partial \underline{f}}{\partial t} - \underline{\underline{A}}\underline{f}\right)^{n-1} = \frac{1}{\Delta t}\left(\underline{f}^{n} - e^{\underline{\underline{A}}^{n-1}\Delta t}\,\underline{f}^{n-1}\right) + \frac{\Delta t}{2}\left(\frac{\partial^2 \underline{f}}{\partial t^2} - \underline{\underline{A}}^2\underline{f}\right)^{n-1} + \ldots \tag{4.1.10}$$

Thus it is apparent that equation (4.1.5) representing the solution to (4.1.1), is first order accurate in time. In section 2.7 the matrix rate equation was of the form

$$\frac{\partial \underline{f}}{\partial t} = \underline{\underline{A}}\underline{f} + \underline{g} \tag{4.1.11}$$

now using the notation of (4.1.4) we can write the solution to this equation as

$$\underline{f} = e^{\underline{\underline{A}}t}\left(\underline{f}^{(0)} + \underline{\underline{A}}^{-1}\underline{g}\right) - \underline{\underline{A}}^{-1}\underline{g} \tag{4.1.12}$$

where the quantities have all been defined previously. Now rewriting

(4.1.12) indicating explicitly at what time levels the various quantities are known, we have by analogy with equation (4.1.5)

$$\underline{f}^n = e^{\underline{\underline{A}}^{n-1} t} (\underline{f}^{(0)} + \underline{\underline{A}}^{-1} \underline{g})^{n-1} - (\underline{\underline{A}}^{-1} \underline{g})^{n-1} \qquad (4.1.13)$$

and carrying out the same accuracy analysis as for equation (4.1.5) we again see that, as expected, equation (4.1.13) is first order accurate in time.

4.2 Stability of the Algorithm

Together with the accuracy, we must also examine the stability of the algorithm. When one uses a numerical algorithm to obtain a solution to a differential equation, it has been found that small errors introduced by round-off etc. can grow without bound and eventually swamp the time solution. This phenomenon is referred to as 'instability' and can be examined in the following way. Starting with the exact differential equation at time level n-1, i.e.

$$\frac{\partial \underline{f}}{\partial t} = n_e \underline{\underline{A}} \underline{f} \qquad (4.2.1)$$

(as described in Chapter 2) we assume the elements of the matrix $n_e \underline{\underline{A}}$ to be constant from time level n-1 to n and we write the solution as

$$\underline{f}^n = \sum_i a_i^{n-1} \underline{X}_i^{n-1} e^{\lambda_i^{n-1} \Delta t} \qquad (4.2.2)$$

for a timestep $\Delta t = t^n - t^{n-1}$. The eigenvalues etc. have all been evaluated at time level n-1 and are held constant at time value to time level n. Formally we can also write the solution (4.2.2) in the following form

$$\underline{f}^n = e^{(\underline{\underline{A}}^{n-1}) \Delta t} \underline{f}^{n-1} \qquad (4.2.3)$$

as discussed in section 4.1, and it is in this form that we carry out the stability analysis. It should be remembered that since

$$n_e = n_i \sum_z z f_z \tag{4.2.4}$$

we can introduce the vector $\underline{z} = (1, 2, \ldots z, \ldots Z)$ such that we can express the electron density n_e as

$$n_e = n_i \, \underline{z}.\underline{f} \tag{4.2.5}$$

Substituting (4.2.5) into (4.2.3) we have

$$\underline{f}^n = e^{\underline{z}.\underline{f}^{n-1}} \, \underline{\underline{A}}^{n-1} \, \underline{f}^{n-1} \tag{4.2.6}$$

where the $n_i \Delta t$ has now been absorbed into the matrix $\underline{\underline{A}}$.

We now ask the question, suppose there is a small error $\underline{\varepsilon}$ in $\underline{f}$ at time level n-1, what error will this produce at time level n through our numerical algorithm (4.2.6)? Denoting $\underline{\varepsilon}^n$ and $\underline{\varepsilon}^{n-1}$ as the errors at time levels n and n-1 respectively, we have

$$(\underline{f}^n + \underline{\varepsilon}^n) = e^{\underline{z}.\,(\underline{f}^{n-1}+\underline{\varepsilon}^{n-1})\underline{\underline{A}}^{n-1}} \, (\underline{f}^{n-1} + \underline{\varepsilon}^{n-1}) \tag{4.2.7}$$

After expanding equation (4.2.7) and using (4.2.6) we can obtain an expression for $\underline{\varepsilon}^n$ in the following form, i.e.

$$\underline{\varepsilon}^n = \left(e^{\underline{z}.\underline{\varepsilon}^{n-1} \, \underline{\underline{A}}^{n-1}} - 1 \right) \underline{f}^n + e^{\underline{z}.\underline{f}^{n-1}} \underline{\underline{A}}^{n-1} \, e^{\underline{z}.\underline{\varepsilon}^{n-1}} \underline{\underline{A}}^{n-1} \, \underline{\varepsilon}^{n-1} \tag{4.2.8}$$

We now expand (4.2.8) retaining only the terms first order in $\underline{\varepsilon}^{n-1}$, i.e.

$$\underline{\varepsilon}^n = \underline{z}.\underline{\varepsilon}^{n-1} \underline{\underline{A}}^{n-1} \, \underline{f}^n + e^{\underline{z}.\underline{f}^{n-1}} \underline{\underline{A}}^{n-1} \, \varepsilon^{n-1} \tag{4.2.9}$$

Now substituting for $\underline{f}^n$ in (4.2.9) using (4.2.6) and using the fact that $\underline{\underline{A}} \, e^{\underline{\underline{A}}} = e^{\underline{\underline{A}}} \, \underline{\underline{A}}$ we obtain

$$\underline{\varepsilon}^n = e^{\underline{z}.\underline{f}^{n-1}} \underline{\underline{A}} \left\{ \underline{\varepsilon}^{n-1} + \underline{z}.\underline{\varepsilon}^{n-1} \, \underline{\underline{A}}^{n-1} \, \underline{f}^{n-1} \right\} \tag{4.2.10}$$

Upon expansion, element by element, it can easily be shown that $\underline{z}.\underline{\underline{\varepsilon}}^{n-1} \, \underline{\underline{A}}^{n-1} \, \underline{f}^{n-1} = \underline{\underline{A}}\underline{z}\underline{f}\underline{\varepsilon}^{n-1}$ where $\underline{z}\underline{f}$ is the outer product defined by

$$\underline{z}\underline{f} = \begin{pmatrix} f_1 & 2f_1 \\ f_2 & 2f_2 \end{pmatrix} \tag{4.2.11}$$

in the case where $\underline{f}$ is the vector with components (f_1, f_2). Thus we can write

$$\underline{\varepsilon}^{n} = \underline{\underline{G}}^{n-1} \underline{\varepsilon}^{n-1} \tag{4.2.12}$$

where

$$\underline{\underline{G}}^{n-1} = e^{\underline{z}.\underline{f}^{n-1}\underline{\underline{A}}} \left(\underline{\underline{I}} + \underline{\underline{A}}^{n-1} \underline{z}\underline{f}^{n-1}\right) \tag{4.2.13}$$

now in the scalar case, equation (4.2.1) can be written as

$$\frac{\partial f}{\partial t} = -\alpha f \tag{4.2.14}$$

(remember the eigenvalues of $\underline{\underline{A}}$ are always negative) and the amplification matrix (4.2.12) becomes an amplification factor given by g where

$$g = e^{-\alpha} (1 - \alpha) \tag{4.2.15}$$

and the condition that the algorithm is stable is $|g| \leq 1$ thus since

$$\left| e^{-\alpha} (1 - \alpha) \right| \leq 1 \text{ for } \alpha \text{ positive} \tag{4.2.16}$$

the algorithm for solving (4.2.13) is unconditionally stable. To extend this result to the vector equivalent of (4.2.13) implies we must show that the modulus of the largest eigenvalue of the matrix $\underline{\underline{G}}^{n-1}$ is less than or equal to 1. The author has been unable to show this, but is satisfied that it must be so since no stability problems have been encountered in the running of the program.

4.3 Storage of the Ionisation Stage Vector

Consider, for a moment, a two dimensional Eulerian mesh containing typically 20 x 40 grid points at each of which the MHD equations are solved. In order to record the ionisation stages of aluminium (say), which has fourteen on each of the grid points it would appear that we would require a three dimensional array of dimensions 20 x 40 x 15 corresponding to 44.8 kilobytes of storage within the computer. In

practice, it is not ncessary to consider all the ionisation stages at any one time and so the storage requirements are not as severe as stated above. It does, however, still remain a problem.

An alternative approach is developed here, where the ionisation stages are not stored explicitly (in the form of an a x b x c matrix) but implicitly through the averaged quantities $\langle z \rangle$ $\langle z^2 \rangle$ etc. The strength of the method lies in the fact that only three ionisation stages are being considered at any one time.

In Chapter 3, when evaluating the macroscopic quantities it was necessary to derive

$$\langle z \rangle,\ \langle z^2 \rangle,\ \langle E_z \rangle,\ \langle z^2 X_{z-1} \rangle \text{ and } \left\langle \exp\left(\frac{-E_{nl}^2}{kT_e}\right) \right\rangle \qquad (4.3.1)$$

where each of the quantities are defined by

$$\sum_{z=0}^{zmax} z f_z = \langle z \rangle$$

$$\sum_{z=0}^{zmax} z^2 f_z = \langle z^2 \rangle$$

$$\sum_{z=0}^{zmax} E_z f_z = \langle E_z \rangle$$

$$\sum_{z=0}^{zmax} z^2 X_{z-1} f_z = \langle z^2 X_{z-1} \rangle$$

$$\sum_{z=0}^{zmax} \exp\left(\frac{-E_{nl}^z}{kT_e}\right) f_2 = \left\langle \exp\left(\frac{-E_{nl}^z}{kT_e}\right) \right\rangle \qquad (4.3.2)$$

and we also have

$$\sum_{z=0}^{zmax} f_z = 1$$

Now in our computer solution, each of the quantities in (4.3.1) have to be stored at each point on the mesh. Since these quantities form the right hand sides of the set of equations (4.3.2) we can write this set of equations in the form

$$\underline{\underline{A}}\underline{f} = \underline{b} \tag{4.3.3}$$

where $\underline{\underline{A}}$ is a square matrix of order 6 whose elements are given by the left hand sides of (4.3.2), and $\underline{f}$ contains any six adjacent fractions from f_o to f_z. At this stage $\underline{\underline{A}}$ and $\underline{b}$ are known and we can solve for $\underline{f}$ i.e.

$$\underline{f} = \underline{\underline{A}}^{-1}\underline{b} \tag{4.3.4}$$

since the quantities (4.3.1) are updated every timestep, we can by applying (4.3.4) find the updated values of any six adjacent ionisation stages. This is what is meant by the implicit storage of the ionisation vector.

As is seen from (4.3.4), the process of updating the ionisation fractions involves a matrix inversion operation and since this is to be done at every space-time point it can be quite time consuming. We really require some fast algorithm for inverting the matrix $\underline{\underline{A}}$ which, because of its lack of symmetry, is not readily available. As it happens, under certain assumptions the matrix $\underline{\underline{A}}$ may be readily inverted. In Chapter 2 it was shown that at any instant it is sufficient to consider only three ionisation stages. Realising this, and using the subset of equations of (4.3.2)

$$\begin{aligned}
&\sum_{z=0}^{zmax} f_z = 1 \\
&\sum_{z=0}^{zmax} z f_z = \langle z \rangle \\
&\sum_{z=0}^{zmax} z^2 f_z = \langle z^2 \rangle
\end{aligned} \tag{4.3.5}$$

where all of the terms on the left hand side have been put to zero except the three terms adjacent to and including the mean ionisation level, we now find that the matrix $\underline{\underline{A}}$ has very special properties. Again we have the equation

$$\underline{\underline{A}}\underline{f} = \underline{b}$$

where

$$\underline{\underline{A}} = \begin{bmatrix} 1 & 1 & 1 \\ z_{j-1} & z_j & z_{j+1} \\ z_{j-1}^2 & z_j^2 & z_{j+1}^2 \end{bmatrix} \quad \underline{f} = \begin{bmatrix} f_{j-1} \\ f_j \\ f_{j+1} \end{bmatrix} \quad \text{and } \underline{b} = \begin{bmatrix} 1 \\ \langle z \rangle \\ \langle z^2 \rangle \end{bmatrix} \qquad (4.3.6)$$

and j is the nearest integer to $\langle z \rangle$.

The important difference now is that since we have restricted ourselves to following three ionisation stages, the matrix $\underline{\underline{A}}$ has many symmetry properties. Since

$$\underline{f} = \underline{\underline{A}}^{-1}\underline{b}$$

and

$$\underline{\underline{A}}^{-1} = \frac{\underline{\underline{A}}^J}{D(\underline{\underline{A}})} \qquad (4.3.7)$$

where $D(\underline{\underline{A}})$ is the determinant of the matrix $\underline{\underline{A}}$ and is known as a Vandermonde determinant because of its properties.[25] One of these is that

$$D(\underline{\underline{A}}) = (z_j - z_{j-1})(z_{j+1} - z_{j-1})(z_{j+1} - z_j) \qquad (4.3.8)$$

which in the present situation is equal to 2 for all cases since $z_j - z_{j-1} = z_{j+1} - z_j = 1$ and $z_{j+1} - z_{j-1} = 2$. The adjoint $\underline{\underline{A}}^J$ of $\underline{\underline{A}}$ is (expressed in terms of z_j)

$$\underline{\underline{A}}^{J} = \begin{bmatrix} z_j(z_j+1) & -(2z_j+1) & 1 \\ -2(z_j+1)(z_j-1) & 4z_j & -2 \\ z_j(z_j-1) & -(2z_j-1) & 1 \end{bmatrix} \qquad (4.3.9)$$

The solution vector $\underline{f}$ can now be expressed using (4.3.7)-(4.3.9)

$$\underline{f} = 0.5 \begin{bmatrix} z_j(z_j+1) & -(2z_j+1) & 1 \\ -2(z_j+1)(z_j-1) & 4z_j & -2 \\ z_j(z_j-1) & -(2z_j-1) & 1 \end{bmatrix} \begin{bmatrix} 1 \\ \langle z \rangle \\ \langle z^2 \rangle \end{bmatrix} \qquad (4.3.10)$$

and it is now apparent that we have produced a general formula for the different ion stages. Thus expanding (4.3.10) we have

$$\begin{aligned} f_{z_{j-1}} &= 0.5\, z_j(z_j+1) - 0.5(2z_j+1)\langle z \rangle + 0.5\langle z^2 \rangle \\ f_{z_j} &= -(z_j+1)(z_j-1) + 2z_j\langle z \rangle - \langle z^2 \rangle \\ f_{z_{j+1}} &= 0.5\, z_j(z_j-1) - 0.5(2z_j-1)\langle z \rangle + 0.5\langle z^2 \rangle \end{aligned} \qquad (4.3.11)$$

We have now completely overcome the problem of inverting the matrix $\underline{\underline{A}}$ by providing the simple expressions (4.3.11).

Consider now a simple example to check the above result. We take fully ionised carbon for which we know there is only one ionisation stage present, i.e. f_6. In this case $\langle z \rangle = 6$ and $\langle z^2 \rangle = 36$. Substituting into (4.3.11) we obtain

$$\begin{aligned} f_5 &= +21 - 39 + 18 = 0 \\ f_6 &= -35 + 72 - 36 = 1 \\ f_7 &= +15 - 33 + 18 = 0 \end{aligned} \qquad (4.3.12)$$

which is correct. Thus we see that the above algorithm provides an extremely efficient procedure for evaluating $\underline{f}$ overcoming completely the problem of storing $\underline{f}$ explicitly. It should also be noticed that the method relies on the determinant of $\underline{\underline{A}}$ being a Vandermonde determinant, and so we can only solve for three ionisation stages. If we wanted four fractions known at any instant then we would have to resort to the matrix inversion procedure described earlier.

It should be noticed from (4.3.12) that since the carbon is fully ionised $z = 6$, and from (4.3.11) we evaluate f_7 although this must always be zero for carbon. It would have been more profitable had we introduced a cut-off once we reached the fractions f_4, f_5, f_6. Thus the set of equations (4.3.11) apply provided we are not near the extremities of z and we now develop an equivalent set of equations which apply in these regions.

Case 1: Almost Fully Ionised Material

Consider some material which is almost fully ionised (such that only the last three ionisation fractions are present). If the atomic number of the material is A then we have

$$f_{A-2} + f_{A-1} + f_A = 1$$

$$(A-2)\, f_{A-2} + (A-1) f_{A-1} + A f_A = \langle z \rangle$$

$$(A-2)^2\, f_{A-2} + (A-1)^2\, f_{A-1} + A^2 f_A = \langle z^2 \rangle$$

or written in matrix notation we have

$$\begin{bmatrix} 1 & 1 & 1 \\ A-2 & A-1 & A \\ (A-2)^2 & (A-1)^2 & A^2 \end{bmatrix} \begin{bmatrix} f_{A-2} \\ f_{A-1} \\ f_A \end{bmatrix} = \begin{bmatrix} 1 \\ \langle z \rangle \\ \langle z^2 \rangle \end{bmatrix} \qquad (4.3.14)$$

which upon inverting gives

$$\begin{bmatrix} f_{A-2} \\ f_{A-1} \\ f_A \end{bmatrix} = 0.5 \begin{bmatrix} A(A-1) & -(2A-1) & 1 \\ -2A(A-2) & 4(A-1) & -2 \\ (A-1))A-2) & -(2A-3) & 1 \end{bmatrix} \begin{bmatrix} 1 \\ \langle z \rangle \\ \langle z^2 \rangle \end{bmatrix} \qquad (4.3.15)$$

or upon expanding (4.3.15)

$$\begin{aligned} f_{A-2} &= 0.5A(A-1) - 0.5(2A-1)\langle z \rangle + 0.5\langle z^2 \rangle \\ f_{A-1} &= -A(A-2) + 2(A-1)\langle z \rangle - \langle z^2 \rangle \\ f_A &= 0.5(A-1)(A-2) - 0.5(2A-3) + 0.5\langle z^2 \rangle \end{aligned} \qquad (4.3.16)$$

Case 2: Almost neutral material

In this case we examine material in the very early stages of ionisation (such that only the first three ionisation stages are present). Due to complications in evaluating the electron density for $\langle z \rangle < 1.0$ we neglect completely the population of the ground state and start with the first ionisation stage, such that the fractions concerned are f_1, f_2, f_3 where from (4.3.6) we have

$$\begin{aligned} f_1 + f_2 + f_3 &= 1 \\ f_1 + 2f_2 + 3f_3 &= \langle z \rangle \\ f_1 + 4f_2 + 9f_3 &= \langle z^2 \rangle \end{aligned} \qquad (4.3.17)$$

which can be expressed as the matrix equation

$$\begin{bmatrix} 1 & 1 & 1 \\ 1 & 2 & 3 \\ 1 & 4 & 9 \end{bmatrix} \begin{bmatrix} f_1 \\ f_2 \\ f_3 \end{bmatrix} = \begin{bmatrix} 1 \\ \langle z \rangle \\ \langle z^2 \rangle \end{bmatrix} \qquad (4.3.18)$$

which, solving for $\underline{f}$ gives

$$\begin{bmatrix} f_1 \\ f_2 \\ f_3 \end{bmatrix} = 0.5 \begin{bmatrix} 6 & -5 & 1 \\ -6 & 8 & -2 \\ 2 & -3 & 1 \end{bmatrix} \begin{bmatrix} 1 \\ \langle z \rangle \\ \langle z^2 \rangle \end{bmatrix} \qquad (4.3.19)$$

and upon expanding gives

$$\begin{aligned} f_1 &= 3 - 2.5 \langle z \rangle + 0.5 \langle z^2 \rangle \\ f_2 &= -3 + 4 \langle z \rangle - \langle z^2 \rangle \\ f_3 &= 1 - 1.5 \langle z \rangle + 0.5 \langle z^2 \rangle \end{aligned} \qquad (4.3.20)$$

Thus the set of equations (4.3.11), (4.3.16) and (4.3.20) provides the expressions for evaluating the fractions once $\langle z \rangle$ and $\langle z^2 \rangle$ are known. Equations (4.3.20) are applied when

$$1 \leqslant \langle z \rangle \leqslant 2.5$$

Equations (4.3.16) are applied where

$$A - 1.5 < \langle z \rangle \leqslant A$$

and equations (4.3.11) are applied for any other values of $\langle z \rangle$.

4.4 The Timestep Control

One of the problems of using packages with computer codes is in setting up a reasonable timestep control. The analysis of Chapter 2 is based on the assumption that the quantities n_e and T_e, the electron density and temperature are approximately constant over the timestep concerned. We must therefore reduce the timestep until these conditions are met.

The timestep used to solve the rate equations of Chapter 2 will be given by the external code. This timestep will be based on MHD considerations and may allow too large a variation in the mean ionisation level $\langle z \rangle$ of the plasma. This difficulty is overcome by using the following technique.

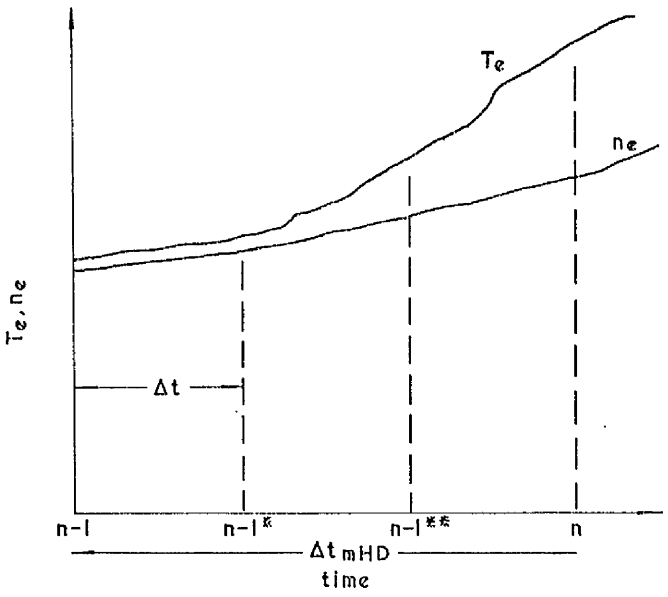

Fig. 4.4 Typical variations of temperature and density as a function of time

Fig. 4.4 shows a typical variation of electron temperature and density against time. In advancing the ionisation fractions from time level n-1 to time level n using the timestep Δt_{MHD} (supplied by external code) it was found (say) the variation in $\langle z \rangle$ was too large. In solving the rate equations over a timestep Δt we must have Δt such that

$$\delta\langle z \rangle = \langle z \rangle^{n} - \langle z \rangle^{n-1} \leq \text{AKT} \qquad (4.4.1)$$

where AKT is ~ 0.2. If this condition is not met, then we reduce the timestep over which we solve the rate equations to

$$\Delta t = \Delta t_{MHD} \cdot \frac{\text{AKT}}{\delta\langle z \rangle} \qquad (4.4.2)$$

and continue to solve using a timestep Δt until we make up the full timestep Δt_{MHD}. After each update of the fractions using timestep Δt, we update the density and temperature (by linear interpolation) to the new time levels n-1*, n-1** etc. where

$$n\text{-}1^{**} - n\text{-}1^{*} = n\text{-}1^{*} - n\text{-}1 = \Delta t \qquad (4.4.3)$$

In the present version of the program only the density n_e is updated after each Δt - the temperature is held constant at T_e^{n-1}. It can happen also that the variations in $\delta\langle z\rangle$ over one timestep are so large that we terminate the program. In this case the only thing to be done, is to reduce the timestep Δt_{MHD}

4.5 The Changeover Philosophy

One of the points concerning the numerical details, which as yet has not been discussed, is when does one stop looking at the fractions f_{j-1}, f_j, f_{j+1} and proceed to evaluate f_{j-2}, f_{j-1}, f_j or f_j, f_{j+1}, f_{j+2}? In the results presented in this thesis, this was determined by the value of $\langle z\rangle$ the mean ionisation level. If, for example, $\langle z\rangle$ was equal to 3.2 the fractions we would concern ourselves with are f_2, f_3 and f_4 and this would be the case until $\langle z\rangle$ reached 3.5 (if ionising) or 2.5 (if recombining) at each of these latter $\langle z\rangle$ values one would switch to the fractions f_3, f_4, f_5 or f_1, f_2, f_3. Although this changeover philosophy works quite well and is very simple to apply, it can be improved upon. In Chapter 2 it was shown that the system of equations we concern ourselves with is

$$\begin{aligned}
\frac{\partial f_{z-1}}{\partial t} &= -S_{z-1}f_{z-1} + R_z f_z \\
\frac{\partial f_z}{\partial t} &= +S_{z-1}f_{z-1} - (S_z+R_z)f_z + R_{z+1}f_{z+1} \\
\frac{\partial f_{z+1}}{\partial t} &= +S_z f_z - R_{z+1}f_{z+1}
\end{aligned} \qquad (4.5.1)$$

where the electron density n_e has been absorbed in the rate coefficients for simplicity. This, then, is the set of equations we choose to 'solve' at any grid point whose mean ionisation level is <z>. It has the properties that

$$\frac{\partial f_{z-1}}{\partial t} + \frac{\partial f_z}{\partial t} + \frac{\partial f_{z+1}}{\partial t} = 0 \qquad (4.5.2)$$

which is consistent with the condition that

$$f_{z-1} + f_z + f_{z+1} = 1 \qquad (4.5.3)$$

However, in equation (4.5.1) a certain amount of physics has been neglected since we neglect recombination from level z-1, i.e. the term $R_{z-1}f_{z-1}$ in the first equation of (4.5.1), and ionisation from level z+1, i.e. the term $S_{z+1}f_{z+1}$ in the last equation of (4.5.1). The important point to notice is that since we are dealing with the level z-1, z, z+1 both of these terms can be evaluated quite simply. Thus together with the set of equations (4.5.1) we can also solve the equations

$$\frac{\partial f_{z-2}}{\partial t} = +R_{z-1}f_{z-1}$$

and (4.5.4)

$$\frac{\partial f_{z+2}}{\partial t} = +S_{z+1}f_{z+1}$$

which have the solutions

$$f_{z-2} = \sum R_{z-1}f_{z-1}\,\Delta t$$

and (4.5.5)

$$f_{z+2} = \sum S_{z+1}f_{z+1}\,\Delta t$$

thus we can now check to see if $f_{z-2} > f_{z-1}$ or if $f_{z+2} > f_{z+1}$ and if this is so we can move on to the next set of fractions. This approach would avoid having to introduce arbitrary crossover points changing from one set of fractions to the next. In equations (4.5.4) no other terms

are introduced on the right hand side since this is quite consistent with assumptions made earlier that only three ionisation stages are involved at any one instant.

4.6 The Computer Program - TRIP

Based on the model developed in Chapters 2, 3 and 4, the computer program TRIP (Time-dependent Recombination Ionisation Package) has been written for use in computer codes to follow the time dependent atomic physics processes in the laser produced plasma.

The structure of TRIP is based on the Olympus system, as are the standards of documentation and the notation.[32,33] This is to enable a fast understanding of the program and to allow for its efficient implementation into computer codes already set up in different computers. Standard fortran is used throughout.

The program TRIP consists of two subroutines, subroutine DATSET and subroutine TRIP. DATSET is an initialisation subroutine which is called only once during the execution of the program. It basically sets the target material, target specifications, reads in the rate coefficients into two dimensional arrays for later access, and evaluates certain other quantities required for the running of TRIP. TRIP is the main calculation subroutine to be called at every space time point on a mesh which updates the fractions (and the macroscopic variables such as $\langle z \rangle$, $\langle z^2 \rangle$ etc.) to the new time level.

In its present form, the program can do 100 timesteps at a single grid point in 1 etu - 3.6 seconds of cpu time on an ICL 4/70 computer. Thus using the program in conjunction with an MHD code on a 20 x 40 mesh it would take about 8 etu's per timestep to update the ionisation fractions at every point on the mesh. This can, however, be reduced considerably by only solving for the ionisation fractions at points of interest (eg. around the critical density in a laser produced

plasma). The storage requirement for the program neglecting data is around 5 kilo bytes.

CHAPTER 5

Implementation of the Model into Computer Codes

The details involved in implementing the program TRIP into computer codes are examined in this chapter with specific reference to the Castor code. The results thus obtained are discussed in detail with specific reference to the macroscopic parameters such as the total radiation loss and the plasma temperature.

5.1 TRIP - A Time-dependent Recombination Ionisation Package

Combining the results of Chapters 2, 3 and 4, a time dependent recombination ionisation package has been constructed. The package is intended for use in computer codes in which a knowledge of time dependent atomic physics processes is required. The package is designed in such a manner that it will be called at every grid point of the region under investigation, to update the ionisation fractions from one time level to the next. It can also be used to evaluate such quantities as the radiation loss, the internal energy, the plasma pressure etc., at the same grid points. The package can be used in the steady state limit and the details of this are discussed briefly in section 5.6.

It is intended that TRIP will be published eventually in Computer Physics Communications. It will be able to handled any target material up to argon in the periodic table (any element can be handle provided the data on the rate coefficients is known, but in the version to be published only data up to argon will be included). The rate coefficients are evaluated at forty different temperatures between 5×10^3K and 5×10^7K and at six densities from 10^{10} m^{-3} to 10^{30} m^{-3}. The rate coefficients used here in tabular form are expected to be more accurate than those obtained using general formulae such as those given by McWhirter.

The present chapter is concerned with the details of how TRIP can be merged with a computer code - in this case CASTOR. We start by giving some of the physics and numerical details of the CASTOR code and then proceed to describe how TRIP can be combined with such a code. We then describe in detail the results obtained and examine the differences between time dependent and steady state atomic physics models for full scale laser target calculations. Finally we give brief details of how the model can be extended to include calculations on the excited state

state population densities and radiation reabsorption of the plasma. The importance of these effects is discussed in connection with the study of X-ray sources and X-ray lasers.

5.2 The Castor Code

Over the past few years workers at Culham Laboratory and at NRL Washington have collaborated in developing a two-dimensional Eulerian, MHD, laser target code CASTOR. This code has been constructed to help investigate and understand the physics involved in laser target experiments in progress at various laboratories.

Fig. 5.2.1 shows a typical laser target set up with the laser radiation incident from the left of the target. The laser pulse is shown as being Gaussian both in space and time but the code can handle any realistically shaped pulse. We restrict our field of interest to an axisymmetric system around the Z axis, and the R-Z cylindrical region around the critical density describes the area covered by the Eulerian mesh. It is assumed initially that there exists a density gradient away from the target surface. This has the advantage of overcoming the problem of how the laser energy is absorbed initially by a solid target, and is quite realistic since this density gradient could be created by a weak laser prepulse. If desired, however, the code can account for evanescent wave absorption.[34] The absorption of the laser energy is mainly by inverse Bremsstrahlung but we can dump a fraction of the remaining energy at the critical density to account for anomalous absorption processes.[11] As the laser energy is absorbed around the critical density, the plasma becomes hotter and expands forming a high temperature low density corona. Behind the critical density energy is transferred from the high temperature region by heat diffusion into the nearly solid target. As this high density material becomes hotter, it too starts to blow off causing a burn through of the target. The

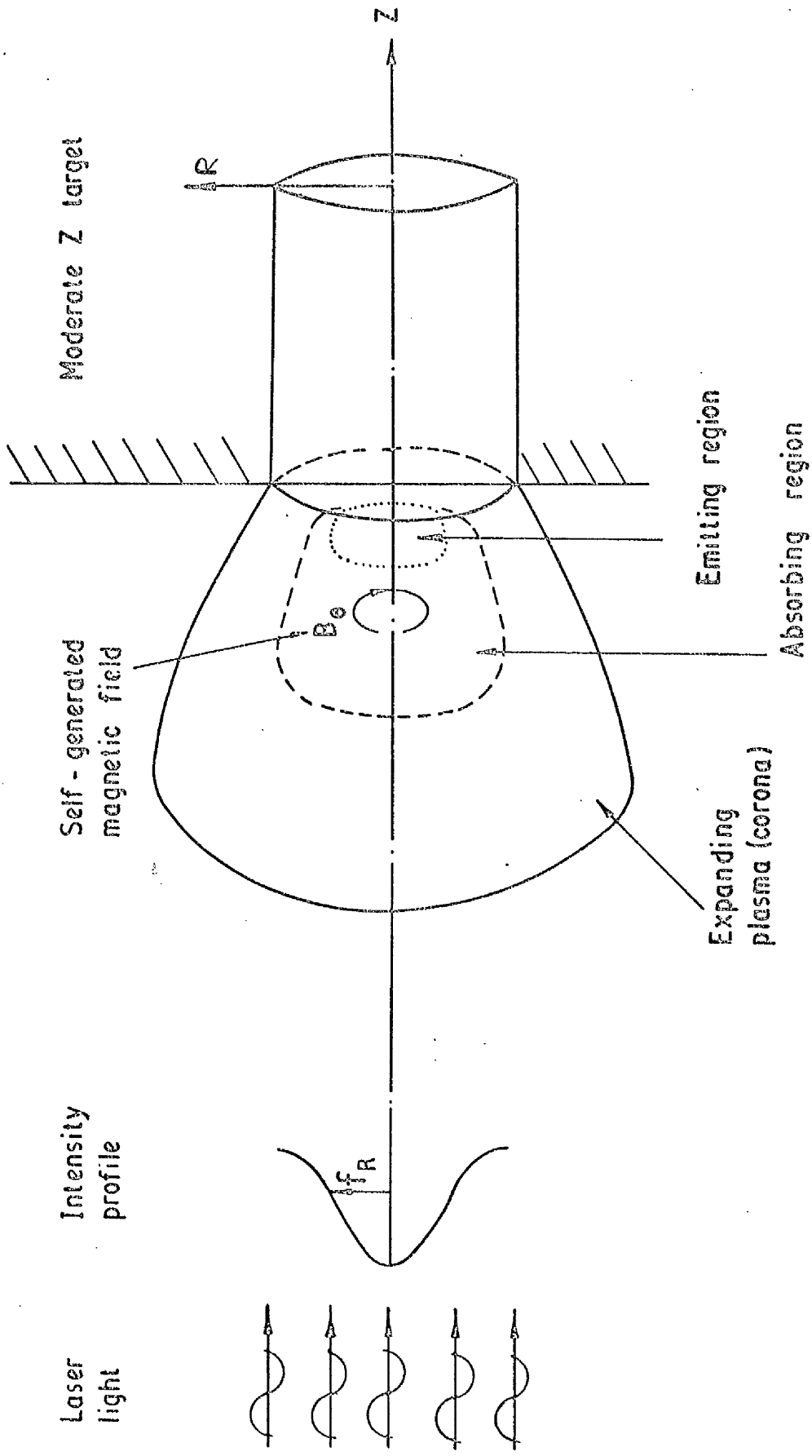

Fig. 5.2.1 Typical laser target arrangement

choice of target is limited by the atomic physics model of the plasma being used. We can use an ideal gas equation of state, a corona model or a time-dependent recombination ionisation model (described in this thesis) and due to limited data we are restricted to moderate Z targets.

Figure 5.2.2 summarises the equations used in the CASTOR code. These equations express conservation of mass, momentum, energy (internal), and magnetic flux and are written in conservative form.[1,2,3] It should be noted that since the system of figure 5.2.1 is axisymmetric, the only magnetic field we can allow is in the θ-direction. For further information on this system of equations and the transport coefficients the reader should consult Braginskii.[35]

We now describe briefly how the equations of fig. 5.2.2 are solved in finite difference from. We split these equations and identify two basic processes, i.e. those of advection and diffusion. The generalised advection processes are carried out by using FCT[36] (Flux Corrected Transport) which has been developed to solve equations of the form

$$\frac{\partial f}{\partial t} + \underline{\nabla}.(f\underline{v}) = \underline{\nabla}.\underline{G} + F\underline{\nabla}H + Q \qquad (5.2.1)$$

When the standard finite difference schemes, such as Lax-Wendroff or Leapfrog schemes, are used to solve equation (5.2.1) in the presence of large gradients in f, it is well known[1] that large errors can arise due to numerical diffusion and dispersion. The FCT algorithm has been developed especially to handle shocks and situations in which large gradients appear. The essence of the algorithm is that it estimates the amount of numerical diffusion which has occurred over each timestep and corrects for this by applying an antidiffusion stage. As for the dispersion, non-physical maxima and minima are suppressed.

MHD - equations in conservation form

Mass : $\frac{\partial \rho}{\partial t} + \nabla.(\rho \underline{v}) = 0$

Momentum: : $\frac{\partial \rho \underline{v}}{\partial t} + \nabla.(\rho \underline{v}\underline{v}) = -\nabla p + \underline{J} \times \underline{B} + \frac{\hat{\underline{z}}}{c} P_{LAS}$

Energy : $\frac{\partial \varepsilon}{\partial t} + \nabla.(\varepsilon \underline{v}) = -p\nabla.\underline{v} - \nabla.\underline{Q} + \underline{E} \cdot \underline{J} + P_{LAS} - P'_L - P_c$

Magnetic field : $\frac{\partial \underline{B}_\theta}{\partial t} = -\nabla \times \underline{E}$

Electric field : $\underline{E} = -\underline{v} \times \underline{B} + \eta \underline{J} + \frac{1}{en_e}(\underline{J} \times \underline{B} - \nabla P_e + \underline{R}_T)$

Thermal flux : $\underline{Q} = -\eta_1 \nabla T_e - \eta_2 \hat{\underline{\theta}} \times \nabla T_e + \frac{Te}{en_e}(\beta_1 \underline{J} + \beta_2 \hat{\underline{\theta}} \times \underline{J})$

Thermoelectric field : $R_T = -\beta_1 \nabla T_e - \beta_2 \hat{\underline{\theta}} \times \nabla T_e$

Fig. 5.2.2 The fluid equations used in Castor

In equation (5.2.1) we can obtain the equation of continuity by putting the right hand side to zero and f equal to ρ(the density). We can obtain the conservation of momentum by putting $f = \rho\underline{v}$, $\underline{G} = 0$, $F = 1$ and $H = p$ (the pressure), and Q equal to the source terms. Similarly we can solve the internal energy and magnetic field equation by adjusting the variables f, $\underline{G}$, H, and Q.

Along with the FCT, we employ a second order accurate predictor-corrector scheme to solve equation (5.2.1).

As far as the magnetic field and heat diffusion are concerned we have to solve a generalised diffusion equation of the form

$$\frac{\partial f}{\partial t} = F^1 \frac{\partial}{\partial x}\left(F^2 \frac{\partial}{\partial x}(F^3 f)\right) + S \qquad (5.2.2)$$

where f represents the variable to be diffused over the spatial dimension x. The true diffusion process occurs through all the space dimensions, but we have used a split step process to break this up into a series of one dimensional diffusion equations.[37]

We space centre the right hand side of equation (5.2.2) at the mesh point j (our algorithm is then second order accurate in space) and rewrite equation (5.2.2) as

$$\left.\frac{\partial f}{\partial t}\right|_j = A_j f_{j-1} + B_j f_j + C_j f_{j+1} + D_j \qquad (5.2.3)$$

The time discretisation is done in the following manner

$$\left(\frac{f^{n+1}-f^n}{\Delta t}\right)_j = \theta\left[A_j f_{j-1}+B_j f_j+C_j f_{j+1}+D_j\right]^{n+1} + (1-\theta)\left[A_j f_{j-1}+B_j f_j+C_j f_{j+1}+D_j\right]^n \qquad (5.2.4)$$

where θ measures the degree of implicitness. For $\theta = \frac{1}{2}$ the algorithm (5.2.4) is also second order accurate in time. However, in the present code we choose the fully implicit case with $\theta = 1$ but with the coefficients A, B, C and D evaluated at level n, i.e. we are using backward substituted coefficients, thus equation (5.2.4) becomes

$$A_j^n f_{j-1}^{n+1} - \left(\frac{1}{\Delta t} - B_j^n\right) f_j^{n+1} + C_j^n f_{j+1}^{n+1} + \left(D_j^n + \frac{f_j^n}{\Delta t}\right) = 0 \qquad (5.2.5)$$

which can be written in the form

$$\underline{\underline{A}}\,\underline{f} = \underline{b} \qquad (5.2.6)$$

and because $\underline{\underline{A}}$ is tridiagonal, fast algorithms are available for evaluating $\underline{f}$.(1)

To solve the equations of fig. 5.2.2 we use a split step method such that all of these equations can be decomposed into the forms of equations (5.2.1) and (5.2.2) and solved as explained in the text.

5.3 Castor with TRIP

Figure 5.3.1 shows the time level diagram of CASTOR with TRIP and describes how the main and auxiliary variables are advanced in time from level n to level n+1. The main variables in the calculation are the temperature, the magnetic field, the internal energy (thermal plus ionisation), the fluid mass density, and the fluid momentum density. We distinguish between the different physical effects in advancing from n to n + 1 and so in the diagram we introduce a diffusion stage, an advection stage, and an ionisation stage. The time level structure could be sub-divided further since the diffusion and advection stages are split into separate one dimensional diffusion and advection problems.

The split-step procedure can be explained by a simple example.(37) Consider the equation

$$\frac{\partial u}{\partial t} = \frac{\partial}{\partial x_1}\left(a_1 \frac{\partial u}{\partial x_1}\right) + \frac{\partial}{\partial x_2}\left(a_2 \frac{\partial u}{\partial x_2}\right) \qquad (5.3.1)$$

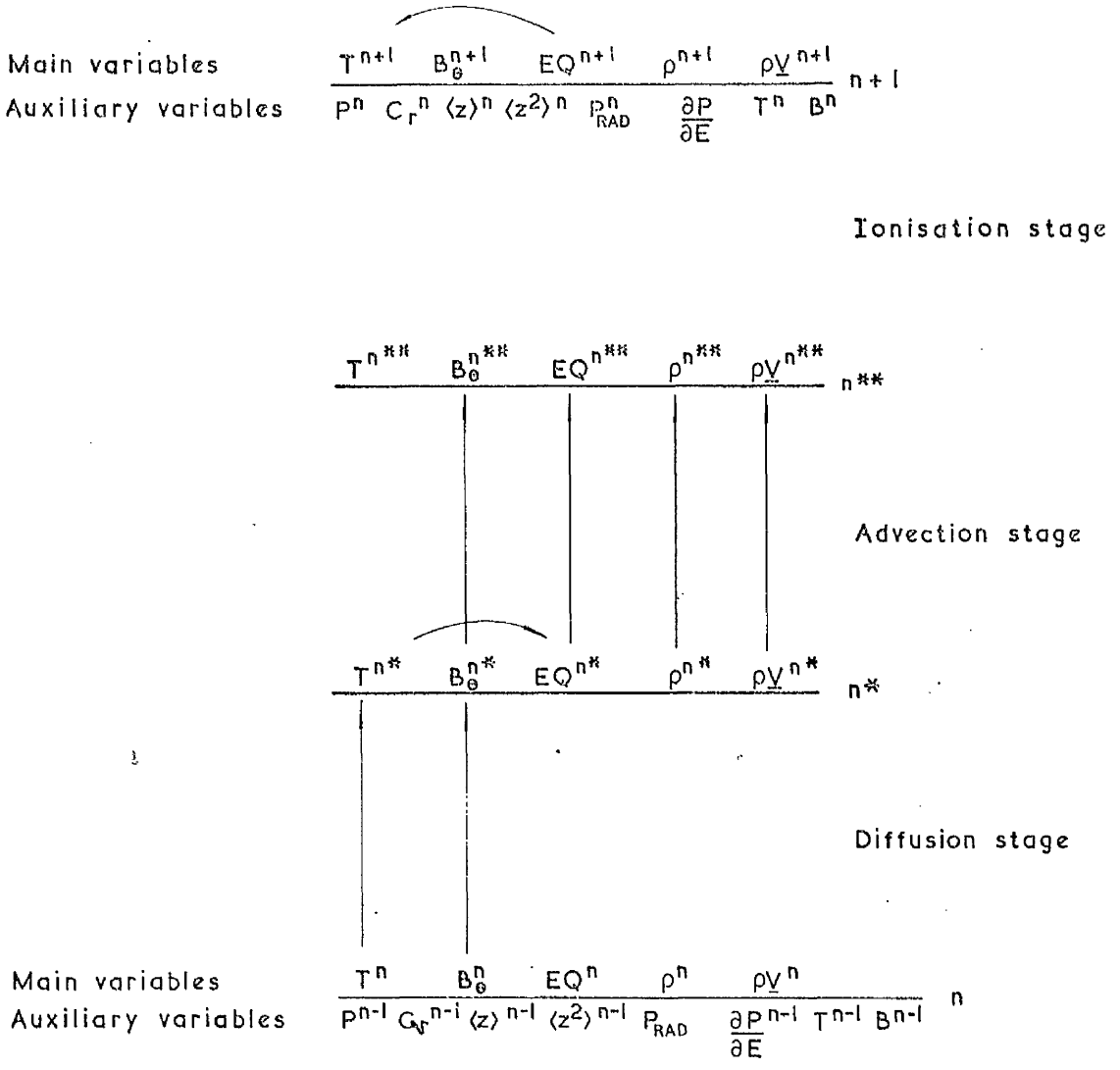

Fig. 5.3.1 Time level diagram of castor with trip.

which we rewrite as the pair of equations

$$\frac{1}{2}\frac{\partial u}{\partial t} = \frac{\partial}{\partial x_1}\left(a_1 \frac{\partial u}{\partial x_1}\right) \qquad (5.3.2)$$

and

$$\frac{1}{2}\frac{\partial u}{\partial t} = \frac{\partial}{\partial x_2}\left(a_2 \frac{\partial u}{\partial x_2}\right) \qquad (5.3.3)$$

And in advancing the calculation from $t = n\Delta t$ to $t = (n+1)\ \Delta t$ it is assumed that equation (5.3.2) holds from $t = n\Delta t$ to $t=(n+\frac{1}{2})\ \Delta t$ and equation (5.3.3) holds from $t = (n+\frac{1}{2})\ \Delta t$ to $t = (n+1)\ \Delta t$. Thus the discretised left hand side of (5.3.2) is written

$$\frac{u^{n+\frac{1}{2}} - u^{n}}{\Delta t} \qquad (5.3.4)$$

and it should be noticed that although when solving (5.3.2) we use the full Δt, we are advancing the variable u only to time $(n+\frac{1}{2})\ \Delta t$. Thus although the timestep between the levels n, n*, n** is Δt the variables are not advanced in time through the full Δt.

5.4 Results

In the first set of results of using TRIP with CASTOR, we compared the radiation losses as a function of the rate coefficients. It was found that the absorbed laser energy profile was almost independent of the value of the rate coefficients and since the reason for this is not obvious we will explain it in more detail near the end of this section. The total energy radiated against time for different sets of rate coefficiants is shown in fig. 5.4.1. The continuous curve shows the radiation loss against time using Summers' rate coefficients whereas the broken curves on either side give the radiation loss by decreasing and increasing the rate coefficients by a factor three. We observe the radiation loss to be not too sensitive to the rates of the atomic processes. It is however rather surprising to see that by increasing the rates the actual radiation loss decreases.

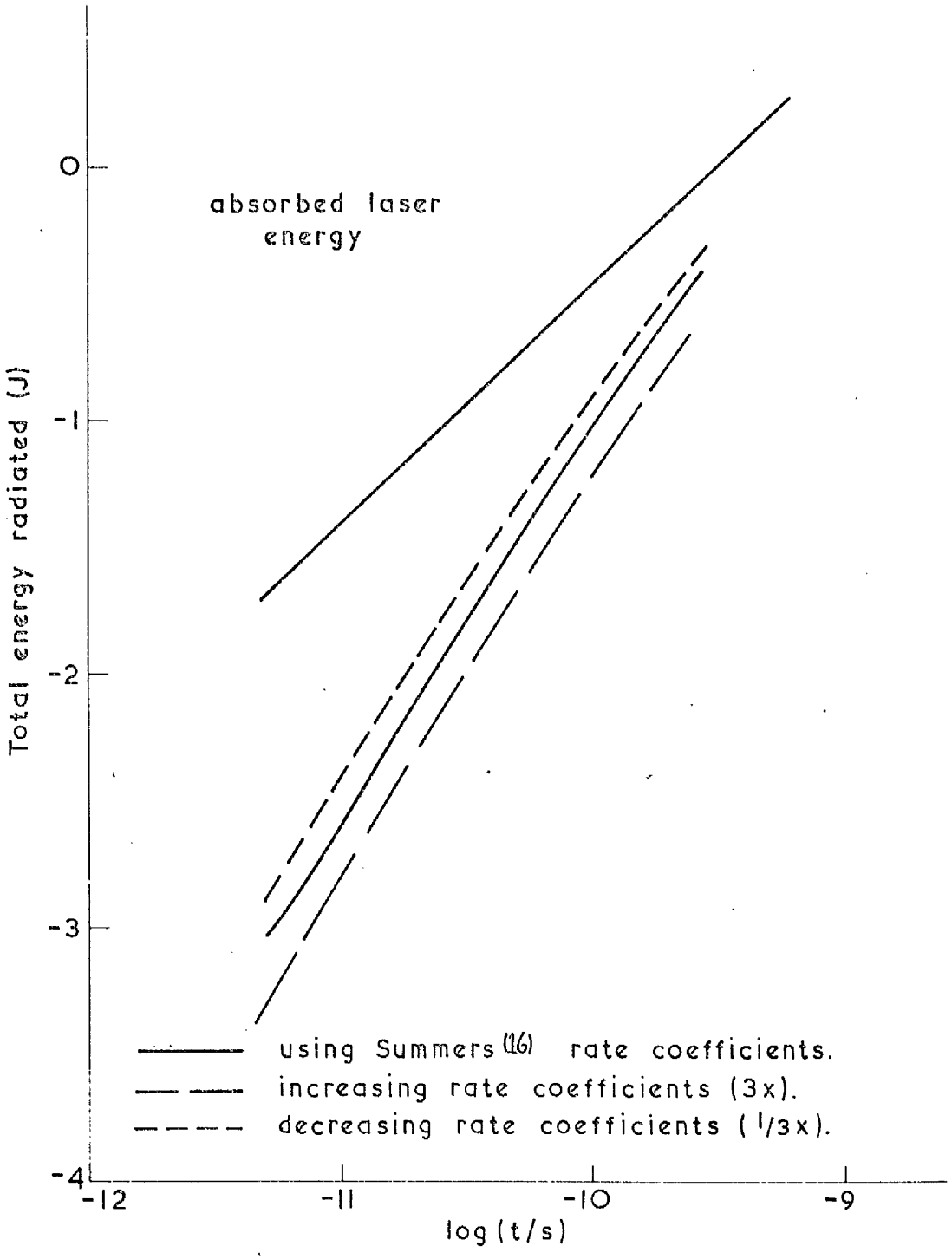

Fig. 5.4.1 Sensitivity of the energy radiated to the values of the rate coefficients[16]

Since the radiation rates of Chapter 3 are all dependent on $< z >$ and $<z^2>$, one would tend to imagine that if the rates increase (i.e. $<z>$, $<z^2>$ increase) the radiation rates would also increase. This situation is made even clearer in fig. 5.4.2 where we compare the radiation loss using a steady-state and the time dependent (TRIP) models.[38] Using the time-dependent model we obtain lower values of $<z>$ and $< z^2>$, at a given time, and one would expect correspondingly lower radiation rates. This however is not the case and the reason for this discrepancy is explained as follows. For a plasma undergoing ionisation, it is well known [30] that the line radiation dominates the continuum radiation. Now the line radiation, as given in Chapter 3, varies as

$$(kT_e)^{-\frac{1}{2}} < z > <\exp\left(\frac{-E^z_{21}}{kT_e}\right)> \qquad (5.4.1)$$

and we now show that the line radiation is not dominated by T_e or $< z >$ but by the exponential term. For a given internal energy the temperature and the mean ionisation level are connected through the relationship

$$E = \frac{3}{2}(1 + <z>)\, n_i kT + E_z n_i \qquad (5.4.2)$$

where all the terms have been defined in Chapter 3. Thus for a given internal energy E a time-dependent model will give a lower value of $<z>$, and hence a higher value of temperature than a steady state model would predict. Thus we see that the term

$$\frac{E^z_{21}}{kT_e}$$

in expression (5.4.1) will become smaller since the term E^z_{21} is a function of $<z>$. The variation of the line radiation factor (the experimental expression in (5.4.1)) as a function of E^z_{21}/kT_e is shown in Table 5.4.1.

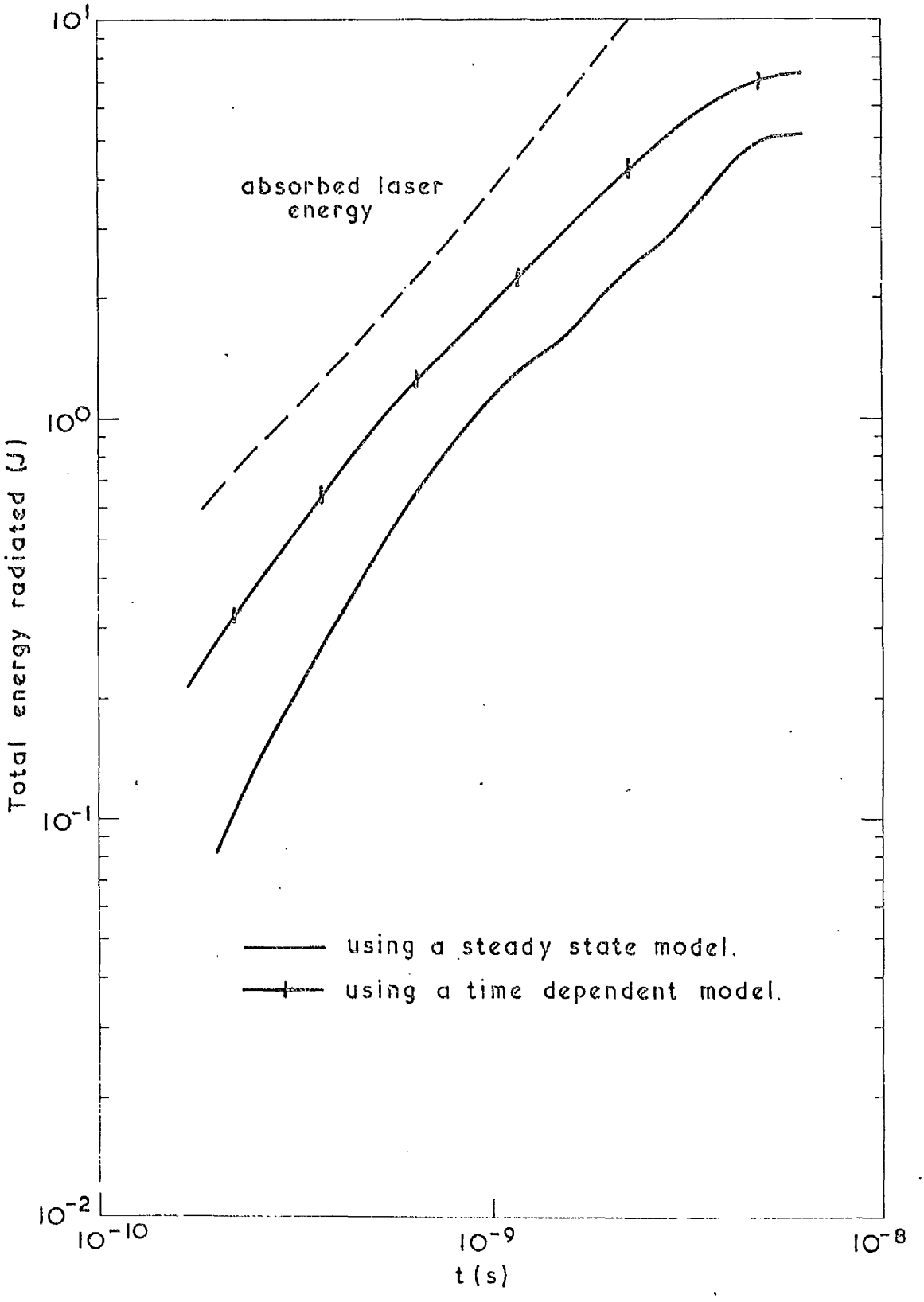

Fig. 5.4.2 Total radiation loss as predicted by time dependent and steady state atomic physics models

E^z_{21}/kT_e	6	4	2
$\exp\left(\frac{-E^z_{21}}{kT_e}\right)$	2.4×10^{-3}	1.8×10^{-2}	1.4×10^{-1}

Table 5.4.1. The strong variation of the line radiation factor against changes in the temperature and mean ionisation level.

Thus we observe that if the quantity E^z_{21}/kT_e changes by a factor three, the line radiation factor changes by about two orders of magnitude. Thus if E^z_{21}/kT_e decreases by a factor 3 (typical when using a time dependent model) the line radiation factor increases vastly thus explaining the results of figs. 5.4.1 and 5.4.2.

In figure 5.4.3 we show the temperature and mean ionisation level profiles, taken at 0.5 nanoseconds, using a steady state and time dependent atomic physics model. Now as stated earlier the total absorbed energy is approximately the same in both cases. Because of this and due to the fact that the mean ionisation levels are considerably lower using the time dependent model, we should expect higher temperatures throughout the entire plasma volume. Fig. 5.4.3 shows that this is the case only beyond about 160 μm along the target axis. The reason the temperatures are not higher in the lower density corona is due to very high line radiation rates, as explained previously, in that region. It should be noted that the absorption coefficient for inverse Bremsstrahlung varies approximately as (39)

$$\frac{z^3}{T_e^{3/2}}$$

where z is the mean ionisation level of the radiating region. By examination of fig. 5.4.3 we observe that the absorption of energy by this process throughout the plasma region is actually lower using a time dependent model. However, it should be remembered that the energy not

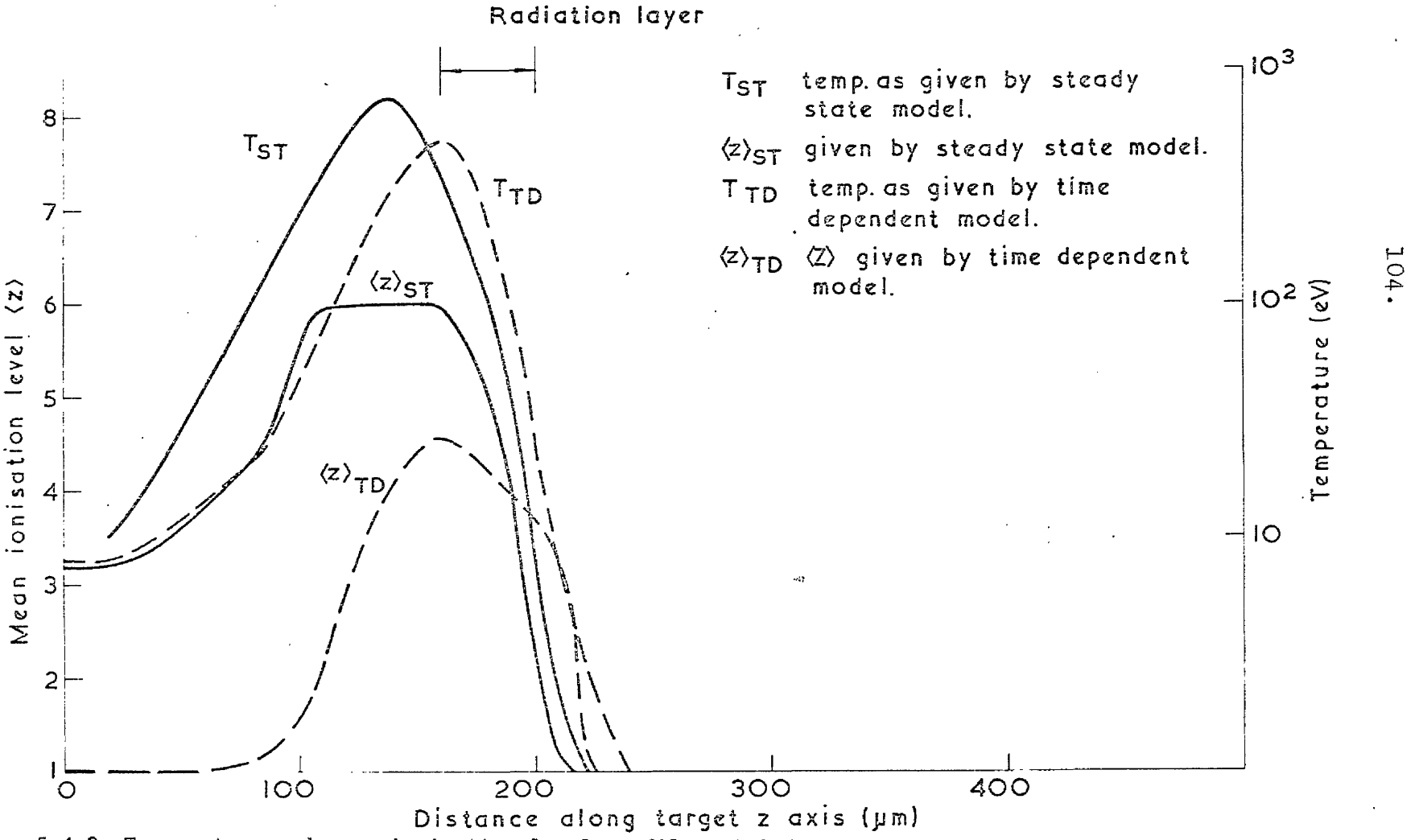

Fig. 5.4.3 Temperature and mean ionisation level profiles at 0.5 nanoseconds as predicted by time dependent and steady state atomic physics models

104.

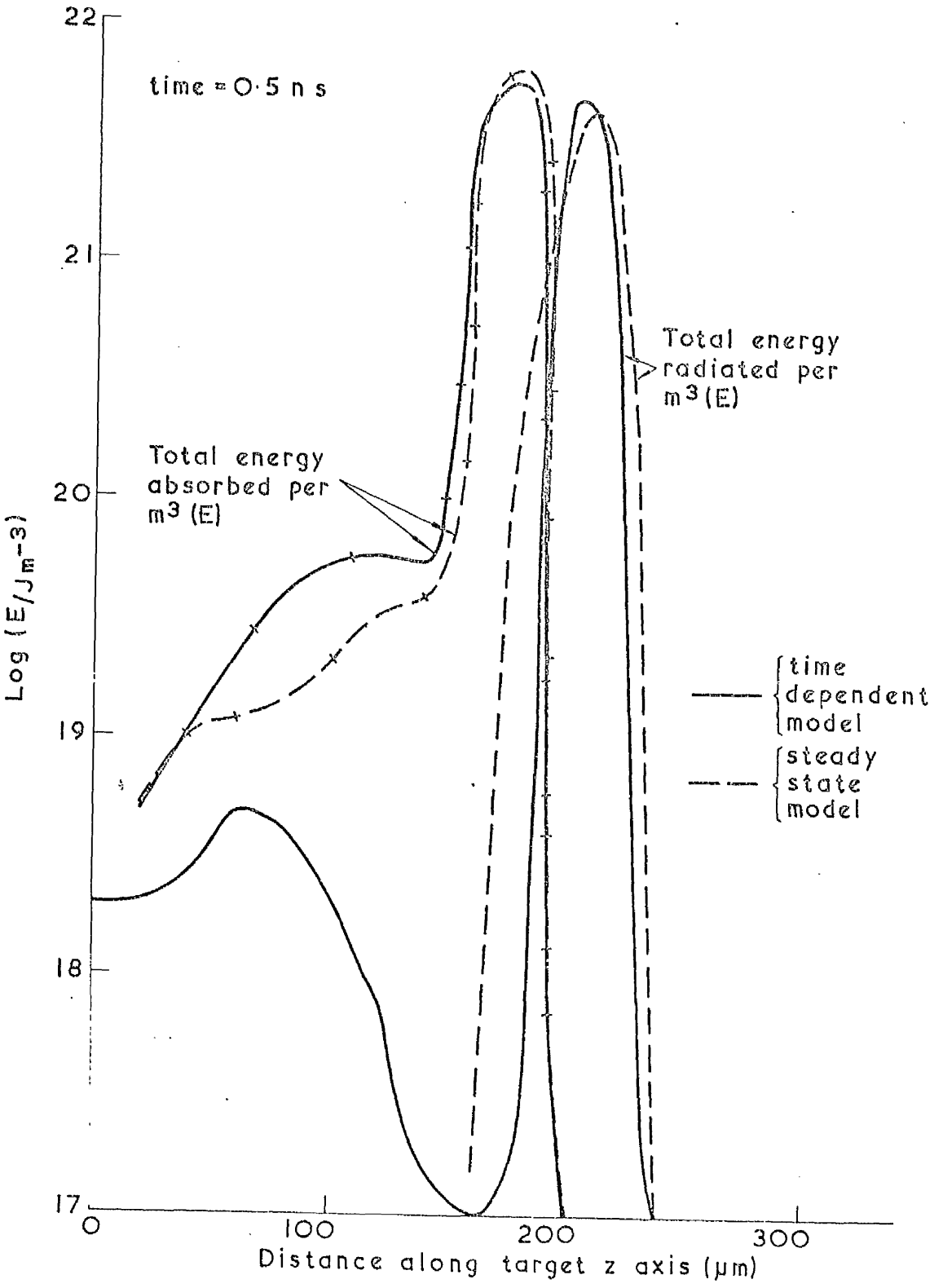

Fig. 5.4.4 Absorbed laser energy against energy radiated using time dependent and steady state atomic physics models

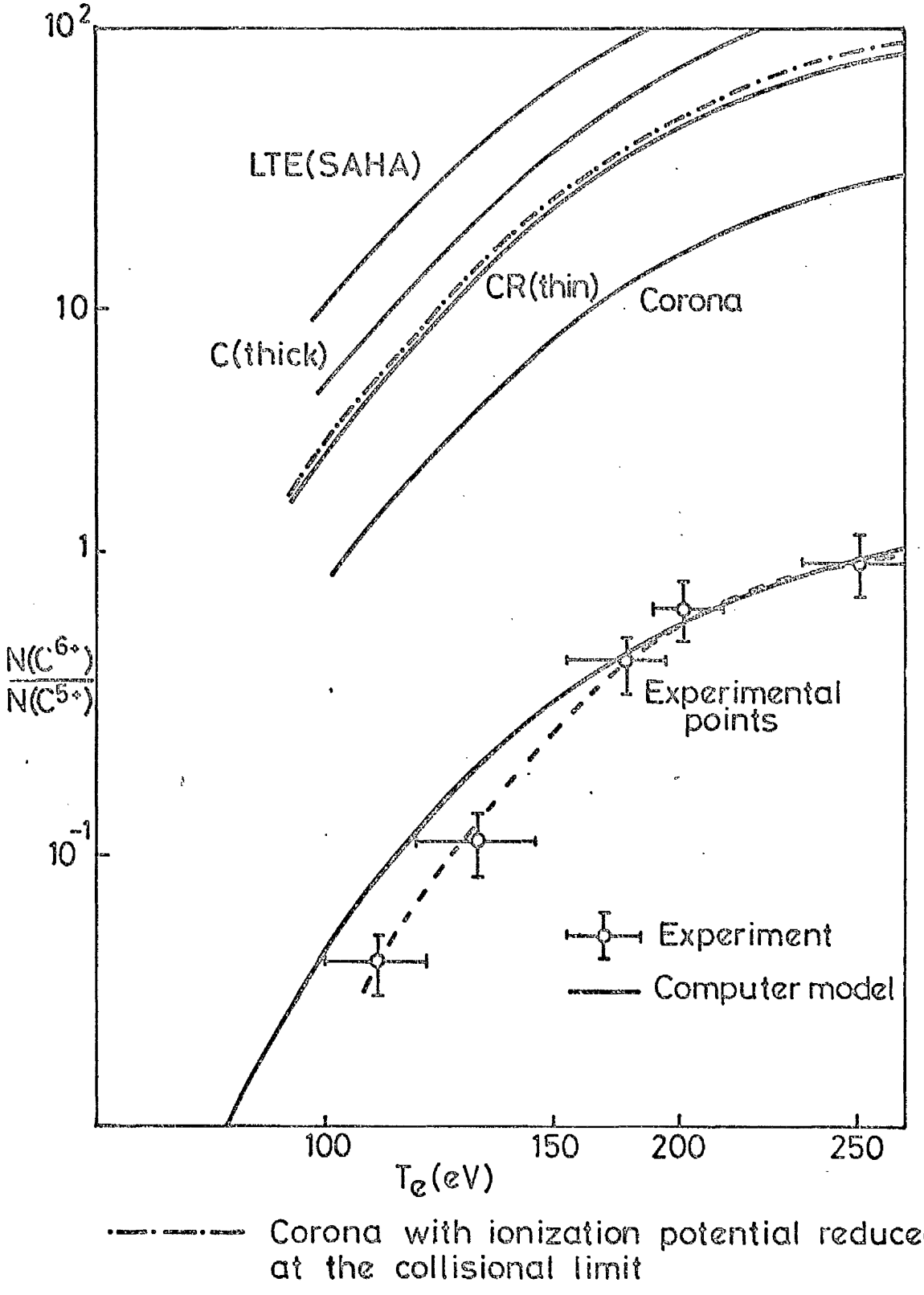

Fig. 5.4.5 The ratio $N(C^{6+})/N(C^{5+})$ against temperature as predicted by time dependent (computer model) and steady state atomic physics processes

absorbed by inverse Bremsstrahlung is, in the calculations presented here, dumped at the critical density. Thus we see that it is due to the dominant energy absorption mechanism being dumping energy at the critical density, which accounts for the absorbed laser energies being approximately constant, as stated earlier.

To conclude, we compare the results of the time dependent atomic physics model against various well known steady state models for a given set of experimental results. The experiment in question [40] measures the ratio of six times ionised to five times ionised carbon at around the critical density of a laser irradiated carbon target for very early times in the plasma history. The actual time at which the calculations were taken was estimated at around 10 picoseconds and experimental details can be found in the literature. To simulate this experiment we switched off the hydrodynamics and heat diffusion and raised the temperature linearly, from 10^4K to various values around 10^6K, in 10 picoseconds. The results shown are in good agreement with experiment and as expected differ greatly from steady state results.

5.5 Conclusions

In Chapter 1 we developed the atomic physics theory for hydrogen and many electron atoms. As far as the many electron systems were concerned we showed that if the excited states were neglected, the problem became considerably simpler.

Next we described briefly various contemporary atomic physics models ranging from the better known steady state LTE and corona models to the less well known time-dependent models. It was shown that the range of applicability for most of the models was outside the parameter range

of importance encountered in the laser produced plasma. It was also demonstrated that when time dependent atomic physics equations were solved by the standard explicit or implicit algorithms, severe problems were encountered, such as the use of very small timesteps, or the loss of accuracy encountered with large timesteps. The method of fitting exponentials, as described in this thesis overcomes both of these difficulties.

Next we showed, in Chapter 2, that the rate equations governing the various ionisation and recombination processes could be written as the matrix equation

$$\frac{\partial \underline{f}}{\partial t} = \underline{\underline{A}}\,\underline{f} \qquad (5.5.1)$$

if hydrodynamic motion is ignored. Because of the nature of the ionisation recombination processes, the matrix $\underline{\underline{A}}$ is tridiagonal with many useful symmetry properties. It was then shown that through the constraint $\sum f_z = 1$ and under the assumption of there being only three ionisation stages present, equation (5.5.1) can be rewritten as

$$\frac{\partial \underline{f}}{\partial t} = \underline{\underline{B}}\,\underline{f} + \underline{g} \qquad (5.5.2)$$

where the matrix $\underline{\underline{B}}$ is now lower triangular. To solve equation (5.5.2) we choose a timestep such that the elements of $\underline{\underline{B}}$ and $\underline{g}$ remain approximately constant. It was shown that this timestep was controlled by variations in $\langle z \rangle$, the mean ionisation level. Equation (5.5.2) then reduces to a linear ordinary differential equation whose solution can be written as

$$\underline{f} = -\underline{\underline{B}}^{-1}\underline{g} + \sum_i a_i \underline{X}_i e^{\lambda_i \Delta t} \qquad (5.5.3)$$

where Δt is the timestep chosen above and the λ_i, $\underline{X}_i$ and a_i are the eigenvalues, eigenvectors and initial constants for the matrix $\underline{\underline{B}}$. Because the matrix $\underline{\underline{B}}$ is lower triangular, its eigenvalues can be written down immediately as being just the diagonal elements and the components of the eigenvectors are just simple combinations of these eigenvalues. Time consuming iterative procedures for the evaluation of the λ_i and $\underline{X}_i$ are thereby avoided. We also developed a simple criterion for establishing whether or not it was necessary to use a time-dependent model.

Having solved for the ionisation fractions in Chapter 3 we proceeded to evaluate some of the macroscopic plasma variables explicitly dependent on the ionisation fractions. These included the mean ionisation level, the mean square ionisation level, the plasma kinetic pressure and the internal energy (thermal plus ionisation). To evaluate the radiation loss from the plasma, we assumed it to be optically thin and divided the radiation loss into three basic types. These were Bremsstrahlung, recombination and line radiation and the formulae for these expressions were obtained from the literature. Due to the assumptions made in the development of these expressions, they provided only order of magnitude estimates for the radiation loss.

In Chapter 4 we looked at some of the computational aspects of the algorithm developed in Chapter 2 for solving the rate equations. We showed that the algorithm was essentially first order accurate in time although the very close agreement obtained in Chapter 2 with known analytic solutions seems to suggest that the coefficient of the Δt must be quite small. We also tried to show the unconditional stability of the algorithm, but could only do this for the scalar equivalent of equation (5.5.1). The results do however tend to indicate that the algorithm is unconditionally stable.

We also developed a method for the implicit storage of the ionisation stage vector, i.e. the ionisation fractions are not stored explicitly. This centres around solving an equation of the form

$$\underline{\underline{V}}\underline{f} = \underline{b} \qquad (5.5.3)$$

for the ionisation fractions $\underline{f}$. The clumsy matrix inversion procedures for solving this equation are avoided when one realises that the determinant of $\underline{\underline{V}}$ is a Vandermonde determinant with very special properties. Because of this, simple expressions can be obtained for the fractions depending on only the mean ionisation level and mean square ionisation level.

In Chapter 5 we described TRIP (the Time-dependent Recombination Ionisation Package) which consisted of the results developed in Chapters 2,3 and 4. To use TRIP we described how the package was implemented into the Castor code - a two dimensional Eulerian laser target MHD code. We described in detail how the various processes of advection, diffusion and ionisation merged with one another to form a complete and consistent model. This being done, we compared the results from CASTOR using a time dependent atomic physics model (TRIP) and a steady state atomic physics model (the CORONA model). Significant differences emerged not only in the degree of ionisation of the plasma but also in the total radiation loss. The radiation loss was found to be substantially higher than that given under steady state Corona equilibrium and this is attributed to a greatly increased amount of line radiation - as explained in detail in section 5.3. It is expected that if account is taken of the reabsorption of the line radiation, the emitted energy would instead go into thermal energy resulting in very much higher temperatures.

We conclude, therefore, by making the observations that for subnanosecond timescales in the laser produced plasma, significant differences in the macroscopic variables do appear when, instead of using equilibrium ionisation recombination models, one takes into account the finite rates at which the atomic physics processes occur.

5.6 Future Work

1. One of the fundamental assumptions in this thesis has been in limiting our interest to only three ionisation fractions at any one instant of time. It was shown that as far as ionisation is concerned the assumption is a good one, but when rapid recombination is taking place one must exert great care in interpreting the results as shown in section 2.6.

To overcome this difficulty one could extend the model to handle more than three ionisation stages. This, however, may prove rather difficult since the essence of the method developed in Chapter 2 relies heavily on the fact that we have only three fractions present. Thus to extend the model in this way would destroy the many symmetry properties realised earlier. It would also be less efficient to evaluate the eigenvalues and eigenvectors and thus increase the timestep per calculation.

Since the difficulty arises only in the final stages of the recombination an alternative would be to use a steady state model in this regime, and assume equilibrium conditions have been reached. Steady state conditions are found simply by putting $\partial \underline{f}/\partial t = 0$ in equation (5.6.1)

$$\frac{\partial \underline{f}}{\partial t} = \underline{\underline{A}}\,\underline{f} = 0 \qquad (5.6.1)$$

and solving for $\underline{f}$. This leads to the set of relations[21]

$$R_z f_z = S_{z-1} f_{z-1} \qquad 1 \leq z \leq z_{max} \tag{5.6.2}$$

which have the solutions

$$f_z = \left(\frac{S_{z-1}}{R_z}\right)\left(\frac{S_{z-2}}{R_{z-1}}\right) \cdots \left(\frac{S_o}{R_1}\right) f_o$$

$$= \prod_{i=1}^{z} \left(\frac{S_{i-1}}{R_i}\right) f_o \tag{5.6.3}$$

Using the normalisation condition $\sum_z f_z = 1$ we can obtain an expression for f_o, i.e.

$$f_o = \left[1 + \sum_{z=1}^{z_{max}} \prod_{i=1}^{z} \left(\frac{S_{i-1}}{R_i}\right)\right]^{-1} \tag{5.6.4}$$

from which we can construct any of the f_z through the relations (5.6.2).

2. In recent years much interest has been concentrated on the production of X-ray lasers and X-ray sources.[41,42] One mechanism for this is as follows: In highly stripped medium z targets such as Aluminium, the recombining electrons can emit photons whose energy is of the order of 1 keV, i.e. these photons constitute X-rays. Under certain conditions, the recombining electrons can cause a population inversion in the plasma which can then lead to X-ray lasing action.[43] To study this effect the model developed in Chapter 2 can be extended to solve for the excited state population densities of one or two highly stripped ions. In this case we have an equation of the form

$$\frac{\partial \underline{g}}{\partial t} = \underline{\underline{X}}\,\underline{g} \tag{5.6.5}$$

where the vector $\underline{g}$ contains the population densities of the excited states and the matrix $\underline{\underline{X}}$ contains rate coefficients for various excitation and de-excitation processes between the excited states. Here the matrix $\underline{\underline{X}}$ is general with no symmetry properties and hence there are no

simple ways of constructing the eigenvalues and eigenvectors. However, if we restrict our region of interest to around the focal spot and solve equation (5.6.5) using standard techniques in this region only, the increase in computer time will be minimal.

3. As explained earlier, the total radiation losses are evaluated by summing the local radiation losses over the plasma volume. This was done assuming the plasma to be optically thin to all radiation. However at high densities self-absorption of the line radiation must be taken into account in calculating the radiation loss, since this can be much smaller than in the optically thin approximation.[44]

When there is self-absorption present, the rate coefficients for the ionisation stages must be modified to take into account the processes of photoexcitation and stimulated emission between the excited states. The rate coefficient for photoexcitation is [45]

$$B'_{qp} \int_0^\infty \psi_\nu \, \rho_\nu \, d\nu \qquad (5.6.6)$$

where

$$\psi_\nu = \frac{1}{\sqrt{\pi}} (\Delta\nu_o)^{-1} \exp\left[-\left(\frac{\nu-\nu_o}{\Delta \nu_o} \right)^2 \right] \qquad (5.6.7)$$

is the Doppler spectral function, B_{qp} is the Einstein absorption coefficient, $\Delta\nu_o$ is the e^{-1} width of the Doppler broadened absorption profile for the line centred at the frequency ν_o, and ρ_ν is the radiation spectral energy density. We can evaluate the rate coefficients for the transportation of individual lines by replacing (5.6.6) by

$$\psi_{\nu_o} \, \rho_{\nu_o} \, \frac{1}{\sqrt{\pi}} (\Delta\nu_o)^{-1} \qquad (5.6.8)$$

With the above processes included, the rate at which the excited state population density n(p) changes due to radiative processes is given by

$$\frac{dn(p)}{dt} = -\left[A_{qp} + B_{qp}\frac{\rho_{\nu_o}}{\sqrt{\pi}\Delta\nu_D}\right] n(p) + \left[A_{pq} + B_{pq}\frac{\rho_{\nu_o}}{\sqrt{\pi}\Delta\nu_D}\right] n(q) \qquad (5.6.9)$$

$$+ \text{(collision terms)}$$

where A_{qp} is the stimulated emission coefficient.

APPENDICES

1. The eigenvectors for the ionisation only case
2. General expression for the a_i in the limit of no recombination
3. The eigenvectors for the recombination only case
4. General expression for the a_i in the limit of no ionisation
5. Evaluation of terms used in section 2.7
6. An alternative representation of the terms (2.7.10)
7. Partial fractions for the matrix elements in section 2.9
8. Numerical details for the exact solutions of figs. 2.4.2 and 2.6.2.
9. Simple checks for the equations developed in section 2.8

APPENDIX 1

TABLE A1 The Eigenvectors for Ionisation only Case

1	0	0	0	0	0
$\frac{\lambda_0}{\lambda_1-\lambda_0}$	1	0	0	0	0
$\frac{\lambda_0\lambda_1}{(\lambda_1-\lambda_0)(\lambda_2-\lambda_0)}$	$\frac{\lambda_1}{\lambda_2-\lambda_1}$	1	0	0	0
$\frac{\lambda_0\lambda_1\lambda_2}{(\lambda_1-\lambda_0)(\lambda_2-\lambda_0)(\lambda_3-\lambda_0)}$	$\frac{\lambda_1\lambda_2}{(\lambda_2-\lambda_1)(\lambda_3-\lambda_1)}$	$\frac{\lambda_2}{\lambda_3-\lambda_2}$	1	0	0
$\frac{\lambda_0\lambda_1\lambda_2\lambda_3}{(\lambda_1-\lambda_0)(\lambda_2-\lambda_0)(\lambda_3-\lambda_0)(\lambda_4-\lambda_0)}$	$\frac{\lambda_1\lambda_2\lambda_3}{(\lambda_2-\lambda_1)(\lambda_3-\lambda_1)(\lambda_4-\lambda_1)}$	$\frac{\lambda_2\lambda_3}{(\lambda_3-\lambda_2)(\lambda_4-\lambda_2)}$	$\frac{\lambda_3}{(\lambda_4-\lambda_3)}$	1	0
$\frac{\lambda_0\lambda_1\lambda_2\lambda_3\lambda_4}{(\lambda_1-\lambda_0)(\lambda_2-\lambda_0)(\lambda_3-\lambda_0)(\lambda_4-\lambda_0)(\lambda_5-\lambda_0)}$	$\frac{\lambda_1\lambda_2\lambda_3\lambda_4}{(\lambda_2-\lambda_1)(\lambda_3-\lambda_1)(\lambda_4-\lambda_1)(\lambda_5-\lambda_1)}$	$\frac{\lambda_2\lambda_3\lambda_4}{(\lambda_3-\lambda_2)(\lambda_4-\lambda_2)(\lambda_5-\lambda_2)}$	$\frac{\lambda_3\lambda_4}{(\lambda_4-\lambda_3)(\lambda_5-\lambda_3)}$	$\frac{\lambda_4}{\lambda_5-\lambda_4}$	1

APPENDIX 2

General expression for a_i in the limit of no recombination:-

Consider expression (2.4.1) at time zero, i.e.

$$\underline{f}^{(0)} = \sum_{i=0}^{z-1} a_i \underline{X}_i \qquad (A.2.1)$$

where $\underline{f}^{(0)}$ is the ionisation stage vector $\underline{f}$ at time zero. Using the eigenvectors of appendix 1 we can expand (A.2.1) as

$$\begin{bmatrix} f_0^{(0)} \\ f_1^{(0)} \\ f_2^{(0)} \\ \vdots \\ \vdots \end{bmatrix} \simeq a_0 \begin{bmatrix} 1 \\ \frac{\lambda_0}{\lambda_1-\lambda_2} \\ \frac{\lambda_0\lambda_1}{(\lambda_1-\lambda_0)(\lambda_2-\lambda_0)} \\ \vdots \\ \vdots \end{bmatrix} + a_1 \begin{bmatrix} 0 \\ 1 \\ \frac{\lambda_1}{\lambda_2-\lambda_1} \\ \vdots \\ \vdots \end{bmatrix} + a_2 \begin{bmatrix} 0 \\ 0 \\ 1 \\ \vdots \\ \vdots \end{bmatrix} + a_3 \begin{bmatrix} 0 \\ 0 \\ 0 \\ 1 \\ \vdots \end{bmatrix} \qquad (A.2.2)$$

Now evaluating each row separately we have

$$\begin{aligned} f_0^{(0)} &= a_o \\ f_1^{(0)} &= a_o \frac{\lambda_0}{(\lambda_1-\lambda_0)} + a_1 \\ f_2^{(0)} &= \frac{a_0\lambda_0\lambda_1}{(\lambda_1-\lambda_0)(\lambda_2-\lambda_0)} + \frac{a_1\lambda_1}{(\lambda_2-\lambda_1)} + a_2 \qquad (A.2.3) \\ f_3^{(0)} &= \frac{a_0\lambda_0\lambda_1\lambda_2}{(\lambda_1-\lambda_0)(\lambda_2-\lambda_0)(\lambda_3-\lambda_0)} + \frac{a_1\lambda_1\lambda_2}{(\lambda_2-\lambda_1)(\lambda_3-\lambda_1)} + \frac{a_2\lambda_2}{(\lambda_3-\lambda_2)} + a_3 \end{aligned}$$

etc., and the remaining terms can be obtained from appendix 1. By rearranging the expressions (A.2.3) we can write

$$
\begin{aligned}
a_o &= f_0^{(0)} \\
a_1 &= f_1^{(0)} - \frac{a_0\lambda_0}{(\lambda_1-\lambda_0)} \\
a_2 &= f_2^{(0)} - \frac{a_0\lambda_0\lambda_1}{(\lambda_1-\lambda_0)(\lambda_2-\lambda_0)} - \frac{a_1\lambda_1}{(\lambda_2-\lambda_1)} \\
a_3 &= f_3^{(0)} - \frac{a_0\lambda_0\lambda_1\lambda_2}{(\lambda_1-\lambda_0)(\lambda_2-\lambda_0)(\lambda_3-\lambda_0)} - \frac{a_1\lambda_1\lambda_2}{(\lambda_2-\lambda_1)(\lambda_3-\lambda_1)} - \frac{a_2\lambda_2}{(\lambda_3-\lambda_2)}
\end{aligned}
\qquad \text{(A.2.4)}
$$

and the remaining terms can be derived from the previous expressions. It is now apparent that the expressions (A.2.4) can be written more concisely in the general form

$$
a_i = f_i^{(0)} - \sum_{K=0}^{i-1} \frac{a_K\lambda_K\lambda_{K+1}\ \ldots\ldots\ \lambda_{i-1}}{(\lambda_i-\lambda_K)(\lambda_{i-1}-\lambda_K)\ \ldots\ (\lambda_{K+1}-\lambda_K)} \qquad i = 1, Z \quad \text{(A.2.5)}
$$

APPENDIX 3

A.3 The Eigenvectors for the recombination only case

1	$\frac{\lambda_2}{\lambda_1-\lambda_2}$	$\frac{\lambda_2\lambda_3}{(\lambda_1-\lambda_3)(\lambda_2-\lambda_3)}$	$\frac{\lambda_2\lambda_3\lambda_4}{(\lambda_1-\lambda_4)(\lambda_2-\lambda_4)(\lambda_3-\lambda_4)}$	$\frac{\lambda_2\lambda_3\lambda_4\lambda_5}{(\lambda_1-\lambda_5)(\lambda_2-\lambda_5)(\lambda_3-\lambda_5)(\lambda_4-\lambda_5)}$	$\frac{\lambda_2\lambda_3\lambda_4\lambda_5\lambda_6}{(\lambda_1-\lambda_6)(\lambda_2-\lambda_6)(\lambda_3-\lambda_6)(\lambda_4-\lambda_6)(\lambda_5-\lambda_6)}$
0	1	$\frac{\lambda_3}{\lambda_2-\lambda_3}$	$\frac{\lambda_3\lambda_4}{(\lambda_2-\lambda_4)(\lambda_3-\lambda_4)}$	$\frac{\lambda_3\lambda_4\lambda_5}{(\lambda_2-\lambda_5)(\lambda_3-\lambda_5)(\lambda_4-\lambda_5)}$	$\frac{\lambda_3\lambda_4\lambda_5\lambda_6}{(\lambda_2-\lambda_6)(\lambda_3-\lambda_6)(\lambda_4-\lambda_6)(\lambda_5-\lambda_6)}$
0	0	1	$\frac{\lambda_4}{(\lambda_3-\lambda_4)}$	$\frac{\lambda_4\lambda_5}{(\lambda_3-\lambda_5)(\lambda_4-\lambda_5)}$	$\frac{\lambda_4\lambda_5\lambda_6}{(\lambda_3-\lambda_6)(\lambda_4-\lambda_6)(\lambda_5-\lambda_6)}$
0	0	0	1	$\frac{\lambda_5}{\lambda_4-\lambda_5}$	$\frac{\lambda_5\lambda_6}{(\lambda_4-\lambda_5)(\lambda_5-\lambda_6)}$
0	0	0	0	1	$\frac{\lambda_6}{\lambda_5-\lambda_6}$
0	0	0	0	0	1

Appendix 4

General expression for a_i in the limit of no ionisation

Consider expression (2.6.1) at time zero, i.e.

$$\underline{f}^{(0)} = \sum_{i=1}^{z} a_i \underline{X}_i \qquad (A.4.1)$$

again where $\underline{f}^{(0)}$ is the ionisation stage vector $\underline{f}$ at time zero. Using the eigenvectors of Appendix 3 we can expand (A.4.1) as

$$\begin{bmatrix} f_1^{(0)} \\ f_2^{(0)} \\ f_3^{(0)} \\ f_4^{(0)} \end{bmatrix} = a_1 \begin{bmatrix} 1 \\ 0 \\ 0 \\ 0 \end{bmatrix} + a_2 \begin{bmatrix} \frac{\lambda_2}{(\lambda_1-\lambda_2)} \\ 1 \\ 0 \\ 0 \end{bmatrix} + a_3 \begin{bmatrix} \frac{\lambda_2\lambda_3}{(\lambda_1-\lambda_3)(\lambda_2-\lambda_3)} \\ \frac{\lambda_3}{(\lambda_2-\lambda_3)} \\ 1 \\ 0 \end{bmatrix} + a_4 \begin{bmatrix} \frac{\lambda_2\lambda_3\lambda_4}{(\lambda_1-\lambda_4)(\lambda_2-\lambda_4)(\lambda_3-\lambda_4)} \\ \frac{\lambda_3\lambda_4}{(\lambda_2-\lambda_4)(\lambda_3-\lambda_4)} \\ \frac{\lambda_4}{(\lambda_3-\lambda_4)} \\ 1 \end{bmatrix} \qquad (A.4.2)$$

Now evaluate each row separately starting at $f_6^{(0)}$ and looking at Appendix 3.

$$f_6^{(0)} = a_6$$

$$f_5^{(0)} = a_5 + a_6 \frac{\lambda_6}{(\lambda_5-\lambda_6)}$$

$$f_4^{(0)} = a_4 + a_5 \frac{\lambda_5}{(\lambda_4-\lambda_5)} + a_6 \frac{\lambda_5\lambda_6}{(\lambda_4-\lambda_6)(\lambda_5-\lambda_6)} \qquad (A.4.3)$$

$$f_3^{(0)} = a_3 + a_4 \frac{\lambda_4}{(\lambda_3-\lambda_4)} + a_5 \frac{\lambda_4\lambda_5}{(\lambda_3-\lambda_5)(\lambda_4-\lambda_5)} + a_6 \frac{\lambda_4\lambda_5\lambda_6}{(\lambda_3-\lambda_6)(\lambda_4-\lambda_6)(\lambda_5-\lambda_6)}$$

etc. and the remaining terms can be simply derived. By rearranging the expressions (A.4.3) we can write

$$
\begin{aligned}
a_6 &= f_6^{(0)} \\
a_5 &= f_5^{(0)} - a_6 \frac{\lambda_6}{(\lambda_5-\lambda_6)} \\
a_4 &= f_4^{(0)} - a_5 \frac{\lambda_5}{(\lambda_4-\lambda_5)} - a_6 \frac{\lambda_5\lambda_6}{(\lambda_4-\lambda_6)(\lambda_5-\lambda_6)} \\
a_3 &= f_3^{(0)} - a_4 \frac{4}{(\lambda_3-\lambda_4)} - a_5 \frac{\lambda_4\lambda_5}{(\lambda_3-\lambda_5)(\lambda_4-\lambda_5)} - a_6 \frac{\lambda_4\lambda_5\lambda_6}{(\lambda_3-\lambda_6)(\lambda_4-\lambda_6)(\lambda_5-\lambda_6)}
\end{aligned}
\qquad \text{(A.4.4)}
$$

and the remaining terms can be derived from the previous expressions.

We can now express the relations (A.4.4) more concisely in the general form

$$
a_i = f_i^{(0)} - \sum_{k=i+1}^{z_{max}} \frac{a_K \lambda_K \lambda_{K-1} \cdots \lambda_{i+1}}{(\lambda_i-\lambda_K)(\lambda_{i+1}-\lambda_K) \cdots (\lambda_{K-1}-\lambda_K)} \quad i = z_{max}-1, \ldots 0
\qquad \text{(A.4.5)}
$$

APPENDIX 5

Evaluation of the terms used in section 2.7

Consider the matrix $\underline{\underline{A}} = n_e \begin{bmatrix} -S_{z-1} & 0 \\ (S_{z-1}-R_{z+1}) & -(S_z+R_z+R_{z+1}) \end{bmatrix}$ (A.5.1)

by inspection, one can see immediately that the eigenvalues and eigenvectors of this matrix are given by

$$\lambda_1 = -n_e S_{z-1} \qquad \lambda_2 = -n_e(S_z+R_z+R_{z+1})$$

$$\underline{X}_1 = \begin{bmatrix} 1 \\ \dfrac{S_{z-1}-R_{z+1}}{\lambda_1'-\lambda_2'} \end{bmatrix} \qquad \underline{X}_2 = \begin{bmatrix} 0 \\ 1 \end{bmatrix} \tag{A.5.2}$$

where $\lambda' = \lambda/n_e$

It can also be shown quite simply that

$$\underline{\underline{A}}^{-1} = \frac{1}{n_e} \begin{bmatrix} -1/S_{z-1} & 0 \\ \dfrac{-(S_{z-1}-R_{z+1})}{\lambda_1'\lambda_2'} & \dfrac{-1}{S_z+R_z+R_{z+1}} \end{bmatrix} \tag{A.5.3}$$

Since $\begin{bmatrix} \dfrac{-1}{S_{z-1}} & 0 \\ \dfrac{-(S_{z-1}-R_{z+1})}{\lambda_1'\lambda_2'} & \dfrac{-1}{S_z+R_z+R_{z+1}} \end{bmatrix} \begin{bmatrix} -S_{z-1} & 0 \\ S_{z-1}-R_{z+1} & -(S_z+R_z+R_{z+1}) \end{bmatrix}$

$$= \underline{\underline{A}}^{-1}\underline{\underline{A}} = \begin{bmatrix} 1 & 0 \\ 0 & 1 \end{bmatrix} \tag{A.5.4}$$

as expected. And so $\underline{\underline{A}}^{-1}\underline{g}$ is given by

$$\begin{bmatrix} \frac{-1}{S_{z-1}} & 0 \\ \frac{-(S_{z-1}-R_{z+1})}{\lambda_1'\lambda_2'} & \frac{-1}{S_z+R_z+R_{z+1}} \end{bmatrix} \begin{bmatrix} R_z f'_z \\ R_{z+1} \end{bmatrix} = \begin{bmatrix} \frac{R_z f_z}{\lambda_1'} \\ \frac{1}{\lambda_2'}\left(R_{z+1} - \frac{R_z f_z}{\lambda_1'}(S_{z-1}-R_{z+1})\right) \end{bmatrix}$$

We now evaluate the initial value constants a_i, and these are evaluated using the equation (2.7.9), i.e.

$$\underline{f}^{(0)} = -\underline{\underline{A}}^{-1}\underline{g} + \sum_{i=1}^{2} a_i \underline{X}_i \qquad (A.5.6)$$

which written more explicitly is given by

$$\begin{bmatrix} f_{z-1}^{(0)} \\ f_z^{(0)} \end{bmatrix} = a_1 \begin{bmatrix} 1 \\ \frac{S_{z-1}-R_{z+1}}{\lambda_1'-\lambda_2'} \end{bmatrix} + a_2 \begin{bmatrix} 0 \\ 1 \end{bmatrix} - \begin{bmatrix} \frac{R_z f_z^{(0)}}{\lambda_1'} \\ \frac{1}{\lambda_2'}\left(R_{z+1}\frac{-R_z f_z^{(0)}}{\lambda_1'}(S_{z-1}-R_{z+1})\right) \end{bmatrix}$$

hence $$f_{z-1}^{(0)} = a_1 - \frac{R_z f_z^{(0)}}{\lambda_1'} \qquad (A.5.7)$$

$$f_z^{(0)} = a_1 \frac{S_{z-1}-R_{z+1}}{\lambda_1'-\lambda_2'} + a_2 - \frac{1}{\lambda_2'}\left(R_{z+1} - \frac{R_z f_z}{\lambda_1'}(S_{z-1}-R_{z+1})\right) \qquad (A.5.8)$$

or $$a_1 = f_{z-1}^{(0)} + \frac{R_z f_z^{(0)}}{\lambda_1'}$$

$$a_2 = f_z^{(0)} - a_1 \frac{S_{z-1}-R_{z+1}}{\lambda_1'-\lambda_2'} + \frac{1}{\lambda_2'}\left(R_{z+1} - \frac{R_z f_z}{\lambda_1'}(S_{z-1}-R_{z+1})\right)$$

APPENDIX 6

An alternative representation of the terms (2.7.10)

Consider the equations (2.7.1)

$$\frac{\partial f_{z-1}}{\partial t} = -S_{z-1}f_{z-1} + R_z f_z$$

$$\frac{\partial f_z}{\partial t} = +S_{z-1}f_{z-1} - (S_z+R_z)f_z + R_{z+1}f_{z+1} \qquad \text{(A.6.1)}$$

$$\frac{\partial f_{z+1}}{\partial t} = +S_z f_z - R_{z+1}f_{z+1}$$

in section 2.7 we substituted for the term $R_{z+1}f_{z+1}$ in the equation for f_z using the constant $f_z = 1$. In this section we will alternatively substitute for $S_{z-1}f_{z-1}$ in the same equation

$$\text{i.e.} \quad S_{z-1}f_{z-1} = S_{z-1}(1 - f_z - f_{z+1}) \qquad \text{(A.6.2)}$$

and so the equations (A.6.1) may be written as

$$\frac{\partial f_{z-1}}{\partial t} = -S_{z-1}f_{z-1} + R_z f_z$$

$$\frac{\partial f_z}{\partial t} = +S_{z-1} - (S_{z-1}+S_z+R_z)f_z + (R_{z+1}-S_{z-1})f_{z+1} \qquad \text{(A.6.3)}$$

$$\frac{\partial f_{z+1}}{\partial t} = +S_z f_z - R_{z+1}f_{z+1}$$

Now using the constraint (2.7.2) we need solve only two of the equations (A.6.3). In this case we choose to solve for f_z and f_{z+1} and we rewrite the equations in the following form

$$\frac{\partial \underline{f}}{\partial t} = \underline{\underline{A}}\underline{f} + \underline{g}$$

and $\qquad \text{(A.6.4)}$

$$f_{z-1} = 1 - f_z - f_{z+1}$$

where

$$\underline{f} = \begin{bmatrix} f_z \\ f_{z+1} \end{bmatrix} \quad \underline{\underline{A}} = n_e \begin{bmatrix} -(S_{z-1}+S_z+R_z) + (R_{z+1}-S_{z-1}) & \\ 0 & -R_{z+1} \end{bmatrix} \quad \underline{g} = n_e \begin{bmatrix} S_{z-1} \\ S_z f_z \end{bmatrix} \tag{A.6.5}$$

We now assume that the term $S_z f_z$ in the vector g is constant or unimportant, over the timestep we are considering, such that g is now constant. As in section 2.7 the solution to the matrix equation in (A.6.4) is given by

$$\underline{f} = -\underline{\underline{A}}^{-1}\underline{g} + \sum_{i=2}^{2} a_i \underline{X}_i e^{\lambda_i t} \tag{A.6.6}$$

where the a_i are constants depending on the initial conditions, i.e.

$$\underline{f}^{(0)} = -\underline{\underline{A}}^{-1}\underline{g} + \sum_{i=2}^{3} a_i \underline{X}_i \tag{A.6.7}$$

The terms in (A.6.6) can be written as

$$\lambda_1 = -n_e(S_{z-1}+S_z+R_z) \qquad \lambda_2 = -n_e R_{z+1}$$

$$\underline{X}_1 = \begin{bmatrix} 1 \\ 0 \end{bmatrix} \qquad \underline{X}_2 = \begin{bmatrix} \frac{S_{z-1}-R_{z+1}}{\lambda_1'-\lambda_2'} \\ 1 \end{bmatrix}$$

$$a_1 = f_z^{(0)} - a_2\left(\frac{S_{z-1}-R_{z+1}}{\lambda_1'-\lambda_2'}\right) + \frac{1}{\lambda_1'}\left(S_{z-1} - \frac{(R_{z+1}-S_{z-1})}{\lambda_2'} S_z f_z^{(0)}\right)$$

$$a_2 = f_{z+1}^{(0)} + \frac{S_z f_z^{(0)}}{\lambda_2'}$$

$$\underline{\underline{A}}^{-1}\underline{g} = \begin{bmatrix} \frac{1}{\lambda_1'}\left(S_{z-1} - \frac{(R_{z+1}-S_{z-1})}{\lambda_2'} S_z f_z^{(0)}\right) \\ \frac{S_z f_z^{(0)}}{\lambda_2'} \end{bmatrix} \tag{A.6.8}$$

These results will now be checked for three very simple cases

Check 1 Neglect the recombination coefficients

This can only be done for very early times (such that $f_z^{(0)} = 0$) since we divide by λ_2' (zero in this case) in some of the terms. The expressions of (A.6.8) in this case reduce to

$$\lambda_1 = -n_e(S_{z-1}+S_z) \qquad \lambda_2 = 0$$

$$\underline{X}_1 = \begin{bmatrix} 1 \\ 0 \end{bmatrix} \qquad \underline{X}_2 = \begin{bmatrix} \frac{S_{z-1}}{\lambda_1'} \\ 1 \end{bmatrix}$$

$$a_1 = \frac{S_{z-1}}{\lambda_1'} \qquad a_2 = 0 \text{ since } \underline{f}^{(0)} = \begin{bmatrix} 0 \\ 0 \end{bmatrix}$$

$$\underline{\underline{A}}^{-1}\underline{g} = \begin{bmatrix} \frac{S_{z-1}}{\lambda_1'} \\ 0 \end{bmatrix} \qquad \text{(A.6.9)}$$

and so

$$\begin{bmatrix} f_z \\ f_{z+1} \end{bmatrix} = \frac{S_{z-1}}{\lambda_1'} \begin{bmatrix} 1 \\ 0 \end{bmatrix} e^{-n_e(S_{z-1}+S_z)t} - \begin{bmatrix} \frac{S_z}{\lambda_1'} \\ 0 \end{bmatrix} \qquad \text{(A.6.10)}$$

for small times $\exp(St) \sim 1 + St$ hence

$$f_z = \frac{S_{z-1}}{\lambda_1'}\left(1 - n_e(S_{z-1}+S_z)t\right) - \frac{S_z}{\lambda_1'}$$

or $f_z = n_e S_{z-1} t$

$f_{z+1} = 0$

which is as expected, and in agreement with the results of section 2.5.

Check 2 Neglect the ionisation coefficients

This is a trivial check since $a_1 = a_2 = 0$ in this case and $\underline{\underline{A}}^{-1}\underline{g} = \underline{0}$ and so the vector $\underline{f} = \begin{bmatrix} f_z \\ f_{z+1} \end{bmatrix}$ remains unchanged again as expected.

Check 3 The full solution for early times

The terms (A.6.8) in this case reduce to

$$\lambda_1 = -n_e(S_{z-1}+S_z+R_z) \qquad \lambda_2 = -n_e R_{z+1}$$

$$\underline{X}_1 = \begin{bmatrix} 1 \\ 0 \end{bmatrix} \qquad \underline{X}_2 = \begin{bmatrix} \frac{S_{z-1}-R_{z+1}}{\lambda_1'-\lambda_2'} \\ 1 \end{bmatrix}$$

$$a_1 = \frac{S_{z-1}}{\lambda_1'} \qquad a_2 = 0 \quad \text{since } \underline{f}^{(0)} = \begin{bmatrix} 0 \\ 0 \end{bmatrix}$$

$$\underline{\underline{A}}^{-1}\underline{g} = \begin{bmatrix} \frac{S_{z-1}}{\lambda_1'} \\ 0 \end{bmatrix} \qquad \text{(A.6.11)}$$

and the solution is given by

$$\begin{bmatrix} f_z \\ f_{z+1} \end{bmatrix} = \frac{S_{z-1}}{\lambda_1'} \cdot \begin{bmatrix} 1 \\ 0 \end{bmatrix} e^{\lambda_1 t} - \begin{bmatrix} \frac{S_{z-1}}{\lambda_1'} \\ 0 \end{bmatrix} \qquad \text{(A.6.12)}$$

which for small times such that $\exp(St) \sim 1+St$ gives

$$f_z = n_e S_{z-1}\, t$$

$$f_{z+1} = 0 \qquad \text{(A.6.13)}$$

as expected.

APPENDIX 7

Partial fractions for the matrix elements in section 2.9

First, the matrix $(p\underline{\underline{I}}-\underline{\underline{L}})^{-1}$ must be evaluated:-

$(p\underline{\underline{I}}-\underline{\underline{L}})$ can be written as

$$(p\underline{\underline{I}}-\underline{\underline{L}}) = \begin{bmatrix} p+S_{z-1} & & \\ -S_{z-1} & p+S_z+R_z & \\ & -S_z & p+R_{z+1} \end{bmatrix} \qquad (A.7.1)$$

and since $\mathrm{DET}(p\underline{\underline{I}}-\underline{\underline{L}}) = \prod_i \lambda_i$ we have

$$\mathrm{DET}(p\underline{\underline{I}}-\underline{\underline{L}}) = (p+S_{z-1})(p+S_z+R_z)(p+R_{z+1}) \qquad (A.7.2)$$

and by definition

$$(p\underline{\underline{I}}-\underline{\underline{L}})^{-1} = \frac{1}{\mathrm{DET}(p\underline{\underline{I}}-\underline{\underline{L}})} (p\underline{\underline{I}}-\underline{\underline{L}})^{T}_{Co} \qquad (A.7.3)$$

where $(p\underline{\underline{I}}-\underline{\underline{L}})^{T}_{CO}$ is the transposed matrix whose elements are the cofactors of $(p\underline{\underline{I}}-\underline{\underline{L}})$

hence $(p\underline{\underline{I}}-\underline{\underline{L}})^{-1}$ is given by

$$(p\underline{\underline{I}}-\underline{\underline{L}})^{-1} = \begin{bmatrix} \frac{1}{p+S_{z-1}} & 0 & 0 \\ \frac{S_{z-1}}{(p+S_{x-1})(p+S_z+R_z)} & \frac{1}{p+S_z+R_z} & 0 \\ \frac{S_{z-1}S_z}{(p+S_{z-1})(p+S_z+R_z)(p+R_{z+1})} & \frac{S_z}{(p+S_z+R_z)(p+R_{z+1})} & \frac{1}{p+R_{z+1}} \end{bmatrix}$$

(A.7.4)

We are now required to find the inverse Laplace transform of each of the elements in the above matrix. The inverse transforms of the diagonal elements are simply

$$e^{-S_{z-1}t}, \qquad e^{-(S_z+R_z)t}, \qquad e^{-R_{z+1}t}$$

To find the inverse transforms of the remaining elements we must first of all find their partial fractions. We do the calculation for one element only and quote the results for the remaining elements. Consider

$$y(p) = \frac{G(p)}{H(p)} = \frac{S_{z-1}}{(p+S_{z-1})(p+S_z+R_z)} \qquad (A.7.5)$$

the denominator has two distinct linear factors $(p+S_{z-1})$ and $(p+S_z+R_z)$ corresponding to the roots

$$p_1 = -S_{z-1}, \qquad p_2 = -(S_z+R_z)$$

and from the theory of partial fractions

$$y(p) = \frac{A_1}{p+S_{z-1}} + \frac{A_2}{p+S_z+R_z} \qquad (A.7.6)$$

where $A_1 = \dfrac{G(-S_{z-1})}{H'(-S_{z-1})} = (S_z+R_z-S_{z-1})^{-1}$

and $A_2 = \dfrac{G(-(S_z+R_z))}{H'(-(S_z+R_z))} = (S_{z-1}-S_z-R_z)^{-1}$

hence $$\frac{S_{z-1}}{(p+S_{z-1})(p+S_z+R_z)} = \frac{S_{z-1}(S_z+R_z-S_{z-1})^{-1}}{p+S_{z-1}} - \frac{S_{z-1}(S_z+R_z-S_{z-1})^{-1}}{p+S_z+R_z}$$

and similarly

$$\frac{S_z}{(p+S_z+R_z)(p+R_{z+1})} = -\frac{S_z(S_z+R_z-R_{z+1})^{-1}}{(p+S_z+R_z)} + \frac{S_z(S_z+R_z-R_{z+1})^{-1}}{(p+R_{z+1})} \qquad (A.7.8)$$

$$\frac{S_{z-1}S_z}{(p+S_{z-1})(p+S_z+R_z)(p+R_{z+1})} = S_{z-1}S_z \frac{(S_{z-1}-S_z-R_z)^{-1}(S_{z-1}-R_{z+1})^{-1}}{(p+S_{z-1})}$$

$$+ \frac{(S_z+R_z-S_{z-1})^{-1}(S_z+R_z+R_{z+1})^{-1}}{(p+S_z+R_z)} + \frac{(R_{z+1}-S_{z-1})^{-1}(R_{z+1}-S_z-R_z)^{-1}}{(p+R_{z+1})}$$

(A.7.9)

APPENDIX 8

Numerical details for the exact solutions of figs. 2.4.2 and 2.6.2

In this section we give the numerical details for the evaluation of the ionisation fractions in an ionising and recombining plasma, under the assumptions of constant density and temperature. The results are shown in figs. 2.4.2 and 2.6.2.

In fig. 2.4.2 we assume the temperature to rise instantaneously to 5×10^5K and we hold the electron density constant at 10^{21} cm^{-3}. Using the initial condition $f^{(0)} = (0, 1, 0, 0, 0, 0)$ we follow the burn through of the ionisation stage the steady state value $f_4 \simeq 1.0$. The actual numerical details are shown in Table A.8.1.

In fig. 2.6.2 we allow the plasma to undergo rapid recombination from the starting condition $\underline{f}^{(0)} = (0, 0, 0, 0, 0, 1)$. The temperature and density are held fixed at 10^4K and 10^{21} cm^{-3} respectively and the numerical details are shown in Table A.8.2.

TABLE A.8.1 The numerical details for the exact solution shown in fig. 2.4.2 for $T = 5\times10^5$ K and $n_e = 10^{21}$ cm^{-3}.

$$\begin{bmatrix} f_1 \\ f_2 \\ f_3 \\ f_4 \\ f_5 \end{bmatrix} = 1.00 \begin{bmatrix} 1.00 \\ -1.21 \\ 2.24 \times 10^{-1} \\ -1.17 \times 10^{-2} \\ 1.75 \times 10^{-8} \end{bmatrix} e^{-(1.46\times10^{13}t)} + 1.21 \begin{bmatrix} 0 \\ 1.00 \\ -1.43 \\ 4.27 \times 10^{-1} \\ -3.65 \times 10^{-6} \end{bmatrix} e^{-(2.6\times10^{12}t)} + 1.00 \begin{bmatrix} 0 \\ 0 \\ 0 \\ 1.00 \\ -1.04 \end{bmatrix} e^{-(2.2\times10^{7}t)} + 1.04 \begin{bmatrix} 0 \\ 0 \\ 0 \\ 0 \\ 1.00 \end{bmatrix} e^{-(7.7\times10^{5}t)}$$

This calculation was based on taking $\underline{f}^{(0)} = (0, 1, 0, 0, 0, 0)$ and in the above results we have omitted the evaluation of f_6.

TABLE A.8.2 The numerical details for the exact solution shown in fig. 2.6.2 with $T = 10^4 K$ and $n_e = 10^{21}\ cm^{-3}$

$$
\begin{bmatrix} f_1 \\ f_2 \\ f_3 \\ f_4 \\ f_5 \\ f_6 \end{bmatrix} = 1.08 \begin{bmatrix} 1.00 \\ 0 \\ 0 \\ 0 \\ 0 \\ 0 \end{bmatrix} e^{-(3.97\times10^{9}t)} + 0.833 \begin{bmatrix} -1.01 \\ 1.00 \\ 0 \\ 0 \\ 0 \\ 0 \end{bmatrix} e^{-(3.58\times10^{11}t)} + (-3.93\times10^{-2}) \begin{bmatrix} 0.431 \\ -1.43 \\ 1.00 \\ 0 \\ 0 \\ 0 \end{bmatrix} e^{-(1.19\times10^{12}t)} + (3.31\times10^{-2}) \begin{bmatrix} 2.57 \\ -6.10 \\ 2.55 \\ 1.00 \\ 0 \\ 0 \end{bmatrix} e^{-(8.55\times10^{11}t)} + 11.1 \begin{bmatrix} -2.08 \\ 0.708 \\ 0.138 \\ 0.172 \\ 1.00 \\ 0 \end{bmatrix} e^{-(1.26\times10^{11}t)} + 1.00 \begin{bmatrix} 22.9 \\ -8.57 \\ -1.58 \\ -1.95 \\ -11.1 \\ 1.00 \end{bmatrix} e^{-(1.38x}
$$

This calculation was based on taking $\underline{f}^{(0)} = (0, 0, 0, 0, 0, 1)$ and the evaluation of f_o has been emitted

APPENDIX 9

Simple checks for the equations developed in section 2.8

By analogy with the checks made in section 2.7 the equations developed can be checked in the following three regimes.

a. Ionisation dominates recombination

In this case we can put all the recombination terms in the matrix $\underline{\underline{A}}$ of (2.8.2) to zero. From the analysis carried out in section 2.8, the eigenvalues etc. can be written down as

$$\lambda_1 = -n_e S_{z-1} \qquad \lambda_2 = -n_e S_z$$

$$\underline{X}_1 = \begin{bmatrix} 1 \\ \dfrac{S_{z-1}}{S_z - S_{z-1}} \end{bmatrix} \qquad \underline{X}_2 = \begin{bmatrix} 0 \\ 1 \end{bmatrix}$$

$$\underline{\underline{A}}^{-1}\underline{g} = \underline{0}$$

$$a_1 = 1 \qquad a_2 = \frac{-S_{z-1}}{S_z - S_{z-1}} \quad (\text{since } f_2^0 = f_3^0 = 0 \text{ and } f_1^0 = 1) \qquad \text{(A.9.1)}$$

and from these quantities we can construct the solution vector as

$$\begin{bmatrix} f_1 \\ f_2 \end{bmatrix} = \begin{bmatrix} 1 \\ \dfrac{S_{z-1}}{S_z + S_{z-1}} \end{bmatrix} e^{-n_e S_{z-1} t} \quad \frac{S_{z-1}}{S_z - S_{z-1}} \begin{bmatrix} 0 \\ 1 \end{bmatrix} e^{-n_e S_z t} \qquad \text{(A.9.2)}$$

which agrees with (2.7.12).

b. Recombination dominates Ionisation

Here we put all the ionisation terms in the matrix $\underline{\underline{A}}$ of (2.8.2) to zero. Again we can write down the eigenvalues which are obtained from expression (2.8.7) quite simply as

$$\lambda_1 = -n_e R_z \qquad \lambda_2 = -n_e R_{z+1}$$

and from these we can construct the eigenvectors etc. as

$$\underline{X}_1 = \begin{bmatrix} 1 \\ \\ -1 \end{bmatrix} \qquad \underline{X}_2 = \begin{bmatrix} \frac{-R_z}{R_{z+1}} \\ \\ 1 \end{bmatrix}$$

$$\underline{\underline{A}}^{-1}\underline{g} = \begin{bmatrix} -1 \\ \\ 0 \end{bmatrix}$$

$$a_1 = \frac{R_{z+1}}{R_z - R_{z+1}} \qquad a_2 = \frac{+R_{z+1}}{R_z - R_{z+1}} \qquad \left(\text{since } f_1^0 = f_2^0 = 0 \right) \quad f_3^0 = 1 \qquad \text{(A.9.3)}$$

and again we can construct the solution vector as

$$\begin{bmatrix} f_1 \\ \\ f_2 \end{bmatrix} = \frac{R_{z+1}}{R_z - R_{z+1}} \begin{bmatrix} 1 \\ \\ -1 \end{bmatrix} e^{-n_e R_z t} + \frac{R_{z+1}}{R_z - R_{z+1}} \begin{bmatrix} \frac{-R_z}{R_{z+1}} \\ \\ 1 \end{bmatrix} e^{-n_e R_{z+1} t}$$

$$+ \begin{bmatrix} 1 \\ \\ 0 \end{bmatrix} \qquad \text{(A.9.4)}$$

For small Δt we can expand the exponential terms in (A.9.4) and retain only the terms up to first order in Δt. The terms independent of Δt cancel since

$$\frac{R_{z+1}}{R_z - R_{z+1}} + \frac{R_{z+1}}{R_z - R_{z+1}} \cdot - \frac{R_z}{R_{z+1}} = -1$$

$$\text{and} \qquad \frac{R_{z+1}}{R_z - R_{z+1}} + \frac{R_{z+1}}{R_z - R_{z+1}} = 0 \qquad \text{(A.9.5)}$$

thus

$$f_1 = \frac{R_{z+1}}{R_z - R_{z+1}} \cdot -n_e R_z \Delta t + \frac{R_{z+1}}{R_z - R_{z+1}} \cdot - \frac{-R_z}{R_{z+1}} \quad -n_e R_{z+1} \Delta t = 0$$

and

$$f_2 = -\frac{R_{z+1}}{R_z - R_{z+1}} \cdot -n_e R_2 \Delta t + \frac{R_{z+1}}{R_z - R_{z+1}} \cdot - n_e R_{z+1} \Delta t = n_e R_{z+1} \Delta t \qquad \text{(A.9.6.)}$$

which is the expected result.

c. The case where $S_{z-1} = R_{z+1}$

This is a special case which reduced the matrix $\underline{\underline{A}}$ of (2.8.2) to upper triangular form and so the eigenvalues are just the diagonal elements of $\underline{\underline{A}}$, hence

$$\lambda_1 = -n_e S_{z-1} \qquad \lambda_2 = -n_e (S_z + R_z + R_{z+1})$$

$$\underline{X}_1 = \begin{bmatrix} 1 \\ 0 \end{bmatrix} \qquad \underline{X}_2 = \begin{bmatrix} \frac{-R_z}{S_z + R_z} \\ 1 \end{bmatrix}$$

$$\underline{\underline{A}}^{-1} \underline{g} = -\frac{1}{\lambda_2} \begin{bmatrix} R_z \\ S_{z-1} \end{bmatrix}$$

$$a_2 = \frac{R_{z+1}}{-(S_z + R_z + R_{z+1})} \qquad a_1 = \frac{S_z}{S_z + R_z} \left(\begin{array}{l} \text{since } f_2^{(0)} = f_3^{(0)} = 0 \\ \text{\& } f_1^{(0)} = 1 \end{array} \right) \text{(A.9.7)}$$

Thus we can now construct the solution vector as follows

$$\begin{bmatrix} f_1 \\ f_2 \end{bmatrix} = \frac{S_z}{S_z + R_z} \cdot \begin{bmatrix} 1 \\ 0 \end{bmatrix} e^{-n_e S_{z-1} t} - \frac{R_{z+1}}{S_z + R_z + R_{z+1}} \cdot \begin{bmatrix} \frac{-R_z}{S_z + R_z} \\ 1 \end{bmatrix} e^{-n_e (S_z + R_z + R_{z+1}) t}$$

$$+ \frac{1}{(S_z + R_z + R_{z+1})} \cdot \begin{bmatrix} R_z \\ S_{z-1} \end{bmatrix} \qquad \text{(A.9.8)}$$

Now expanding $e^{A\Delta t} \sim 1 + A\Delta t$ we see that the terms independent of Δt cancel (remembering that $S_{z-1} = R_{z+1}$) and for the Δt terms we have

$$f_1 = \frac{S_z}{S_z+R_z} \cdot -n_e S_{z-1} \Delta t + \frac{R_{z+1} R_z}{(S_z+R_z+R_{z+1})(S_z+R_z)} \cdot -n_e (S_z+R_z+R_{z+1}) \Delta t + 1$$

or

$$f_1 = 1 - n_e S_{z-1} \Delta t$$

and similarly

$$f_2 = +n_e S_{z-1} \Delta t \qquad \text{(A.9.9)}$$

which are the expected results.

References

1. D. Potter, Computational Physics, John Wiley and Sons 1973.

2. R.D. Richtmyer and K.W. Morton, Difference Methods for Initial Value Problems (1967) Second edition, New York/London, Interscience.

3. K.V. Roberts and D.E. Potter, Magneto hydrodynamic Calculations: Methods in Computational Physics, Vol. 9, Academic Press, New York, 1970.

4. Kreider et al, An Introduction to Linear Analysis, Addison-Wesley Inc., (1966).

5. E. Kreyszig, Advanced Engineering Mathematics, Second Edition, Wiley International Edition.

6. R. Courant and D. Hilbert, Methods of Mathematical Physics Vol. 1, New York/London, Interscience Publishers (1953).

7. J.M. Dawson, On the Production of Plasma by Giant Pulse Lasers, Physics of Fluids, Vol. 7, No. 7 (1964).

8. A.F. Haught and D.H. Polk, High Temperature Plasmas Produced by Laser Beam Irradiation of Single Solid Particles, Physics of Fluids, Vol. 9, No. 10 (1966).

9. A. Caruso and R. Gratton, Some Properties of the Plasmas Produced by Irradiating light solids by Laser Pulses, Plasma Physics, Vol. 10, pp 867-877 (1968).

10. J.P. Christiansen, N.K. Winsor and J. Magill, Castor - a two dimensional Eulerian laser-target code, to be published.

11. Laser-Fusion Program semi-annual report; July - December 1971, Report No. UCRL - 50021 - 71 Rev. 1.

12. J. Nuckolls et al; Laser Implosion of DT to Densities > 1000 gm/cm^3, Optimum Pulse Shape; Fusion Yield vs Laser Energy, UCRL - 74116 Preprint.

13. P. Mulser, R. Sigel and S. Witkowski, Plasma Production by Laser, Physics Reports (Section C of Physics Letters) 6, No. 3, (1973) 187-239.

14. F.E. Irons, R.W.P. McWhirter and N.J. Peacock, The ion and velocity structure in a laser produced plasma, J. Phys. B., Atom. Molec. Phys., Vol. 5, (1972).

15. R.W.P. McWhirter and T.F. Stratton in "Plasma Diagnostic Techniques" (R.H. Huddlestone and S.L. Leonard, Eds.), Academic Press, New York, 1965.

16. H.P. Summers, The Ionisation Equilibrium of Hydrogen-like to Argon-like Ions of Elements, Mon. Not. R. astr. Soc. (1974), 169, 663-680.

17. F.E. Irons, and N.J. Peacock, A spectroscopic study of the recombination of C^{6+} to C^{5+} in an expanding laser-produced plasma, J. Phys. B., Atom. Molec. Phys., Vol. 7, No. 15, (1974).

18./

18. A.C. Kolb and R.W.P. McWhirter, Ionisation Rates and Power Loss from θ-pinches by impurity radiation, Physics of Fluids 7, No.4, (1974).

19. R.W.P. McWhirter, Atomic collision processes in low density plasma, Atomic energy research establishment, Harwell, Report No. AERE - R2980 (1959).

20. D.R. Bates, A.E. Kingston, and R.W.P. McWhirter, Recombination between electrons and atomic ions I.Optically thin plasmas, Proc. Roy. Soc. A., Vol. 267, No. 1330, pp 297-312.

21. D. Mosher, The coronal equilibrium of high atomic number plasmas, NRL Memorandum Report 2563 (1973).

22. H.A. Hyman, Degree of ionisation of a high temperature plasma, Applied Physics Letters, Vol. 25, No. 10, (1974).

23. G.J. Pert, Calculations of ionisation and recombination in laser produced plasmas, Presented at Joint Spring Meeting on Computational Plasma Physics at Imperial College London, March (1974).

24. J.P. Christiansen and K.V. Roberts, Numerical treatment of Rapid Equipartition Rates, Journal of Computational Physics, Vol. 17, No. 3, March 1975.

25. J.H. Wilkinson, The Algebraic Eigenvalue problem, Oxford, Clarendon P, 1965.

26. J.H. Wilkinson and C. Reinsch, Linear Algebra, Ed. F.L. Bauer, Berlin, Springer, 1971.

27. R. Bellman, Perturbation Techniques in Mathematics, Physics, and Engineering, Holt, Rinehart and Winston, Inc., London.

28. D.L. Book, Plasma Formulary, Naval Research Laboratory, Report No. CR74 126.

29. J.P. Christiansen, D.E.T.F. Ashby and K.V. Roberts, MEDUSA, A one dimensional laser fusion code, Computer Physics Communications 7, (1974), 271-287, North-Holland Publishing Company.

30. H.R. Griem, Plasma Spectroscopy, McGraw-Hill, New York, 1964.

31. S. Glasstone and R.H. Lovberg, Controlled Thermonuclear Reactions, D. Van Nostrand Company, Inc., London.

32. K.V. Roberts, An introduction to the Olympus system, Computer Physics Communications 7 (1974) 237-243.

33. J.P. Christiansen and K.V. Roberts, Olympus - a standard control and utility package for initial value fortran programs, Culham Laboratory Preprint CLM - P373.

34. P. Lorrain and D. Corson, Electromagnetic Fields and Waves, 2nd Edition, W.H. Freeman and Company, San Francisco.

35. S.I. Braginskii, in Reviews of Plasma Physics, ed. M.A. Leontovich, Consultants Bureau, New York 1965, Vol. 1, 205-311.

36./

36. J.P. Boris and D.L. Book, Flux-Corrected Transport, 1, Shasta, A Fluid Transport Algorithm that works, Journal of Computational Physics 11, 38-69 (1973).

37. A.R. Mitchell, Computational Methods in Partial Differential Equations, London, John Wiley and Sons Ltd.

38. J. Magill and J.P. Christiansen, A Time Dependant Atomic Physics Model Applied to Laser Produced Plasmas, Paper presented at Third National Computational Physics Conference, TRANSCRIPTA BOOKS (1976) To be Published.

39. L. Spitzer, Physics of Fully Ionised Gases, Interscience Publishers Ltd., London.

40. M. Galanti and N.J. Peacock, Quantitative X-Ray Spectroscopy of the Light Absorption Region at the Surface of Laser - Irradiated Polyethylene, Culham Laboratory Report CLM - P401 (1974).

41. R.J. Dewhurst, D. Jacoby, G.J. Pert and S.A. Ramsden, Ionisation - Recombination and Population Inversion in Laser Produced Plasmas, Presented at the 7th European Conference on Plasma Production by High Power Lasers at Garching (1974).

42. S. Slutz et al, X-Ray Lasers, Necessary Conditions and some Possible Approaches, Lawrence Livermore Laboratory Report No. UCID 16290.

43. G.J. Pert and S.A. Ramsden, Population Inversion in Plasmas Produced by Picosecond Laser Pulses, Optics Communications Vol. 11, No. 3 (1974).

44. K.G. Whitney and J. Davis, Hot-Spot Model of K-Line Emission from laser-heated Plasmas, Journal of Applied Physics, Vol. 45, No. 12 (1974).

45. N.K. Winsor, Private Communication (1974).